OPERATION OF GASPERS FOR REDUCING AIRBORNE DISEASE TRANSMISSION IN COMMERCIAL AIRLINERS WITH PERSONALIZED DISPLACEMENT VENTILATION

HOU YUNGE

PhD

The Hong Kong Polytechnic University

2025

The Hong Kong Polytechnic University
Department of Building Environment and Energy Engineering

Operation of Gaspers for Reducing Airborne Disease Transmission in Commercial Airliners with Personalized Displacement Ventilation

Hou Yunge

A thesis submitted in partial fulfilment
of the requirements for the degree of
Doctor of Philosophy

August 2025

CERTIFICATE OF ORIGINALITY

I hereby declare that this thesis is my own work and that, to the best of my knowledge and belief, it reproduces no material previously published or written, nor material that has been accepted for the award of any other degree or diploma, except where due acknowledgement has been made in the text.

_____(Signed)

HOU Yunge (Name of student)

Department of Building Environment and Energy Engineering
The Hong Kong Polytechnic University
Hong Kong, China
August 2025

ABSTRACT

Abstract of the thesis entitled:

Operation of Gaspers for Reducing Airborne Disease Transmission in Commercial Airliners with Personalized Displacement Ventilation

Submitted by HOU Yunge

For the Degree of: Doctor of Philosophy

at The Hong Kong Polytechnic University in August 2025

By 2024, the number of air passengers had reached nearly 5 billion, which is approximately 2.5 times the level observed in 2004. As air travel gets increasingly popular, the flying public is paying more attention to the cabin environment. The air distribution system plays a critical role in creating a comfortable and healthy cabin environment. Personalized displacement ventilation systems have been developed to control contaminant transmission more effectively compared to the prevalent mixing ventilation systems and conventional displacement ventilation systems. Additionally, overhead gaspers are also available in most commercial airliners for individual ventilation and thermal regulation. However, the impact of gaspers on airborne disease transmission remains unclear. Furthermore, practical instructions for passengers on the control of airborne disease transmission in cabins are still not available. Therefore, this study aims to investigate the operation of gaspers for reducing airborne disease transmission in commercial airliners with personalized displacement ventilation system.

This study first conducted experimental measurements in a simplified cabin mock-up to validate the computational fluid dynamics (CFD) method. A full-scale mockup of a three-row, single-aisle aircraft cabin with personalized displacement ventilation system was built. A gasper was mounted between the source passenger and the receptor passenger on the ceiling. The distributions of air velocity and contaminant concentration were measured on a plane

located 0.05 m in front of the mouth of the second-row passengers. For each measurement point, the sampling duration was 8 minutes. Then, the measured data was used to evaluate the performance of CFD method for calculating air distribution and airborne disease transmission with the RANS SST k-ω model and the Eulerian method. The results showed that the complex interaction of the main flow, gasper-induced jet flow, and thermal plume can be accurately predicted by the CFD model. The overall normalized root mean square errors (NRMSE) of the measurement points was 0.24. Additionally, the CFD method can reliably predict the spatial distribution of contaminants.

The above validated CFD method was then used to systematically investigate the impact of source and receptor passengers' gaspers on airborne disease transmission in aircraft cabins with personalized displacement ventilation. Numerical calculations were conducted in a seven-row, single-aisle, fully occupied, economy-class aircraft cabin with. This study first investigated the impact of source gasper direction and flow rate on the airborne transmission near the contaminant source. Then, the protective effect of the receptor's gasper was investigated. For a source passenger's gasper, the direction and flow rate of the gasper flow either increased or decreased the air contaminant transmission to other passengers. Directing the source gasper to the abdomen with a medium flow rate performed best by reducing the receptors' mean exposure index by at least 45%, as this approach minimized the contaminant circulation in the cabin. Turning on a receptor passenger's gasper could be an effective strategy to protect the receptor, and the working mechanism was revealed. The gasper-induced jet flow entrained the surrounding air into the jet region, and the protective effect was related to the contaminant concentration at ceiling level. With a suitable gasper direction and flow rate, the gasper jet formed a virtual barrier between the source passenger and the receptor. When the contaminants were transported upwards to a receptor's breathing zone, turning on the receptor's gasper reduced the contaminant concentration, since the downward gasper jet altered the airflow pattern in front of the receptor.

The above study only focused on the impact of a single gasper, while the remaining gaspers in the cabin were assumed to be closed. However, the real situation involves concurrent operation of gaspers by passengers. The interaction between the main airflow and the multiple gasper-induced jet flows inevitably increases the complexity of the contaminant transmission in the cabin. To identify an executable gasper operation strategy by which passengers can control the transmission of airborne diseases, this study performed CFD simulation in a seven-row section

of a single-aisle, fully occupied, economy-class aircraft cabin with a personalized displacement ventilation system. First, a seat-type-dependent gasper operation strategy based on the working mechanism of a single gasper was proposed. Next, random gasper operation under realistic conditions was used as the benchmark to evaluate the performance of the proposed gasper operation strategy. The results showed that the effectiveness was sensitive to the seat type of the source and the locations of the passengers. Specifically, when the source passenger was in the window seat or middle seat, the proposed strategy increased the exposure risk for the passengers in front of the source, and on the same side of the aisle as the source passenger. Meanwhile, for passengers in other seats, opening the gaspers in accordance with the proposed operation strategy was effective in controlling the contaminant transmission. When the source passenger was in the aisle seat, there was no significant difference between the proposed strategy and random operation in controlling the transmission.

The above findings suggest that it is challenging for passengers to manually adjust their gaspers to effectively mitigate infection risk. Therefore, the key question should be answered: is there a centralized control mode of the gasper system feasible for mitigating airborne contaminant transmission? Moreover, since the gasper system is originally designed to improve individual comfort, the performance of the centralized control mode of the gasper system in maintaining passengers' individual comfort preference should also be considered. To address the above gaps, this study used CFD simulations to evaluate the centralized control mode of the gasper system in a seven-row section of a single-aisle, fully occupied, economy-class aircraft cabin with personalized displacement ventilation. Two centralized control modes were proposed, full control of engaged gaspers, and partial control of engaged gaspers. The no-control mode was used as the benchmark case. The results show that under full control of engaged gaspers, the number of relatively high-risk passengers was effectively reduced by 83%, 79% and 97% when the source passenger was in the window, middle, and aisle seat, respectively, compared with the number of cases under the no-control mode. However, the gasper open ratio and flow direction distributions significantly differed from those under the no-control mode. Under partial control of engaged gaspers, the number of relatively high-risk passengers was effectively reduced by 81%, 66% and 88% for each source location. Meanwhile, individual comfort preference was maintained for the majority of passengers. These findings demonstrate the feasibility of partial-control mode to achieve both airborne infection mitigation and comfort preferences in realistic cabin environments.

Overall, this thesis systematically investigated the operation of gaspers for reducing airborne disease transmission in commercial airliners with personalized displacement ventilation system. Firstly, experimental measurements of both airflow and contaminant concentration distributions were conducted in a mock-up of an aircraft cabin to validate the CFD simulation results. Secondly, the validated CFD method was used to numerically investigate the influence of gasper direction and flow rate on the contaminant transport near the source and receptor passengers. Thirdly, a seat-type-dependent gasper operation strategy was proposed based on the working mechanism of a single gasper to provide practical guidance for passengers. Fourthly, since the gasper system is originally designed to improve individual comfort, this study proposed and evaluated a centralized control mode that could achieve both airborne infection mitigation and individual comfort preference in realistic cabin environments. The achievements of this thesis are expected to be implemented in actual aircraft cabins through automation control devices to execute the optimal gasper operations, thereby improving the cabin environment.

LIST OF PUBLICATIONS

Peer Reviewed Journal Papers

- **Y. Hou**, R. You, Investigating the impact of gaspers on airborne disease transmission in an economy-class aircraft cabin with personalized displacement ventilation, *Building and Environment*. 245 (2023) 110963. https://doi.org/10.1016/j.buildenv.2023.110963.

- **Y. Hou**, R. You, A practical concurrent gasper-operation strategy for controlling airborne disease transmission in an economy-class aircraft cabin with personalized displacement ventilation, *Building and Environment*. 285 (2025) 113636. https://doi.org/10.1016/j.buildenv.2025.113636.

- **Y. Hou**, W. Wang, Y. Zhou, R. You, Evaluating different control modes of the gasper system in an economy-class aircraft cabin with personalized displacement ventilation, Submitted to *Aerospace Science and Technology*, under review.

- **Y. Hou**, J. Xie, L. N. Jin, R. You, X. Li, Identifying emission sources of airborne antibiotic resistance genes in wastewater treatment plants using CFD simulation, *ACS ES&T Air*. 2 (11) (2025) 2692-2703. https://doi.org/10.1021/acsestair.5c00285.

Conference Papers

- **Y. Hou**, R. You, Investigating the protection effect of gaspers in an aircraft cabin with personalized displacement ventilation. 18th Conference of the International Society of Indoor Air Quality and Climate Indoor Air 2024 (IA2024), July 7-11, Honolulu, Hawaii, USA.

- **Y. Hou**, R. You, Evaluating the concurrent operation of gaspers for controlling the airborne disease transmission in an economy-class aircraft cabin. Healthy Buildings Europe 2025 (HB2025), June 8-11, Reykjavík, Iceland.

ACKNOWLEDGEMENTS

To begin with, I would like to extend my sincere appreciation to my supervisor, Prof. You Ruoyu, for her insightful guidance, patience, and constant encouragement throughout my doctoral studies. Her high standards of scholarship and dedication to research have profoundly influenced me, not only in shaping my academic pursuits but also in fostering my personal growth.

I am also deeply grateful to my friends. I would like to express my sincere appreciation to Dr. Jianong Li for her support in both academic and personal life. My heartfelt thanks go to Dr. Jue Wang, whose insightful suggestions always inspired me whenever I encountered difficulties, and whose kind invitations to her home provided many joyful and memorable weekends. I am indebted to Dr. Yiding Zhou for his generous help with algorithmic work, and to Wei Wang for his invaluable assistance and support during the experiments. Appreciation is also extended to Houzhi Wang, Rui Zhao, Xuan Feng, and Jie Liang, whose companionship has made our research group a warm and supportive family, rendering this journey more meaningful and fulfilling. I would also like to thank all my friends from office ZS869, who always shared snacks and souvenirs from around the world, bringing warmth and joy to my daily life.

My deepest gratitude goes to my family. I am profoundly thankful to my parents and my younger sister, whose unwavering love and steady support have sustained me in countless ways. Their confidence in me has been a quiet yet powerful force, helping me to withstand moments of uncertainty and reminding me of the strength that comes from family. I would also like to express my heartfelt appreciation to my beloved, Shaojie Liu, my partner in both life and learning. From our first days together as undergraduates at Jilin University, to pursuing separate master's degrees at Zhejiang University and Tongji University, and finally reuniting as doctoral candidates at The Hong Kong Polytechnic University, our paths have always been intertwined. At every stage, we have supported, motivated, and inspired each other. Looking ahead, I cherish the prospect of continuing this journey hand in hand, building together whatever the future may hold.

Finally, I would like to acknowledge myself. Thank you for enduring the countless moments of doubt, for choosing perseverance over surrender, and for carrying this endeavor through to the very end. The PhD journey has been more than an academic pursuit, it has been a profound exercise in resilience, patience, and self-discovery. I am proud of the person I have become through this process, and I will treasure this transformation as one of the most meaningful rewards of my life.

TABLE OF CONTENTS

LIST OF TABLES

LIST OF FIGURES

CHAPTER 1 INTRODUCTION

1.1 Background and Significance

According to the International Air Transport Association (IATA), nearly 5 billion passengers travelled by air in 2024, which is approximately 2.5 times the level observed in 2004 [1]. As air travel gets increasingly popular, the flying public is paying more attention to the cabin environment. However, the current environment is often unsatisfactory, being either too hot or too cold [2, 3] and containing contaminants [4, 5]. More importantly, aircraft cabins can also facilitate the transmission of airborne infectious diseases [6-13] such as tuberculosis (TB) [14], severe acute respiratory syndrome (SARS) [7], and coronavirus disease 2019 (COVID-19) [13] due to the high occupant density and long exposure time. For instance, during a 3-hour flight from Hong Kong to Beijing in 2003, 22 passengers were infected by one single patient [7]. Similar thing also occurred during a 10-hour flight from London to Hanoi in 2020, 12 persons in whom severe acute respiratory syndrome coronavirus 2 (SARS-CoV-2) infection were passengers seated in business class along with the only symptomatic person [10]. It is crucial, therefore, to improve the air quality along with thermal comfort in aircraft cabins for the health of the general public.

The air distribution system plays a major role in controlling air quality and thermal comfort in aircraft cabins [15-18]. Currently, mixing ventilation systems are commonly utilized in commercial airliners to provide a suitable cabin environment. A mixing ventilation system supplies fresh air to the cabin at ceiling and/or shoulder level and removes the cabin air through the side walls at floor level. The large-scale circulations in the cabin result in a well-mixed cabin air, and heat accumulation in the occupied zones [19]. Therefore, mixing ventilation is not efficient in removing heat and controlling contaminant transport [19-22]. Displacement ventilation systems have been found more effective than mixing ventilation systems in removing contaminants and improving cabin air quality [19, 21-23]. The reason is that the displacement ventilation system supplies fresh air at floor level and removes the cabin air at ceiling level; thus, the airflow pattern is consistent with the thermal plumes created by passengers. However, the displacement ventilation could lead to poor thermal comfort due to the temperature stratification [19]. Moreover, personalized ventilation systems have been developed to further improve the cabin environment [24]. Individual diffusers are installed

under the seats to supply clean air directly to the breathing zones of the passengers behind. This configuration provides a more uniform temperature distribution and a lower infection risk in cabins [16, 21, 22, 24-27].

However, the performance of the personalized displacement ventilation system has not been thoroughly assessed. This is because, in addition to the main ventilation system, a system of gaspers is also available in most commercial airliners for individual ventilation and thermal regulation as the cabin environment is not necessarily satisfactory for all passengers. Gaspers are a system of small, circular, adjustable vents installed above the seat for each passenger. Gasper-induced jet flow is directed downwards, as gaspers are mounted on the ceiling, while the main flow and thermal plume generated by passengers travel upwards in a cabin with a personalized displacement ventilation system. The interaction of the flows from different directions and the impact of this interaction on contaminant transport have not been well explored. In other words, it is unknown whether the personalized ventilation system is still effective in controlling the airborne disease transmission when gaspers are in use. Although the previous studies have provided great insight into gasper-induced jet flow and its influence on air quality [28-36], there is a lack of systematic studies of the impact of gaspers as the real situation involves concurrent operation of gaspers. Specifically, each passenger can adjust both the flow rate and direction of his/her gasper according to their preference without external control [3, 37, 38]. The multiple gasper-induced jet flows inevitably increase the complexity of the contaminant transmission in the cabin. Therefore, it is crucial to comprehensively investigate the operation of gaspers for reducing airborne disease transmission in commercial airliners with personalized displacement ventilation system.

1.2 Outline of This Thesis

This thesis research focuses on investigating the operation of gaspers for reducing airborne disease transmission in commercial airliners with personalized displacement ventilation system. The outline of this thesis is shown as follows.

Chapter 2 reviews existing experimental and numerical studies on air distribution and contaminant transport in aircraft cabins with gaspers on. The review summarized gasper-

induced jet flow characteristic and its influence on air quality. Finally, major problems of the existing studies were identified, which will be addressed in the following chapters.

Chapter 3 presents experimental and numerical study of airflow patterns and contaminant concentration distributions in a three-row, single-aisle aircraft cabin mock-up equipped with personalized displacement ventilation system and a gasper on. The measured data were then used to evaluate the performance of the CFD method in predicting air distribution and contaminant transport in cabins with personalized displacement ventilation and the gasper system.

Chapter 4 investigates the impact of gasper direction and flow rate on the airborne transmission near the source passenger and the protective effect of the receptor's gasper. CFD simulation method, validated in chapter 3, was used to conduct numerical studies in a seven-row section of a single-aisle, fully occupied, economy-class aircraft cabin with personalized displacement ventilation. The summarized working mechanism of an individual gasper provides a theoretical basis for subsequent chapters.

Chapter 5 proposes a seat-type-dependent gasper operation strategy based on the working mechanism of an individual gasper obtained in chapter 4. To evaluate the performance of the proposed gasper operation strategy, random gasper operation under realistic conditions was used as the benchmark. The two operation strategies were then applied to a seven-row section of a single-aisle, fully occupied, economy-class aircraft cabin with a personalized displacement ventilation system. This chapter evaluates the effectiveness of concurrent gasper operation and identifies an executable gasper operation strategy by which passengers might control airborne disease transmission.

Chapter 6 evaluates a centralized control mode of the gasper system in a single-aisle, fully occupied, economy-class aircraft cabin with personalized displacement ventilation using CFD simulations. Two centralized control modes were proposed: full control of engaged gaspers and partial control of engaged gaspers, where engaged gaspers refer to those originally turned on by passengers under no-control mode. The no-control mode, representing real-life situation in which all passengers freely adjusted the flow rate and flow direction of their gaspers, was used as the benchmark. This chapter demonstrates the feasibility of partial centralized control

mode to achieve both airborne infection mitigation and comfort preference in realistic cabin environments.

Chapter 7 summarizes the conclusion and discusses the potential future work.

CHAPTER 2 LITERATURE REVIEW

This chapter first reviews existing studies on gasper-induced jet flow characteristic and its influence on air quality in order to identify the research gasps. Then the research methods for investigating air distribution and contaminant transport in aircraft cabins are reviewed to determine the research method. Finally, four tasks to be addressed are proposed to achieve the research objective.

2.1 Main Ventilation Systems

The air distribution system plays a major role in controlling air quality in aircraft cabins [15-19, 21, 39-41], most previous studies, therefore, have focused on the impact of the air distribution systems on the transmission of airborne diseases in aircraft cabins. Currently, commercial airliners prevalently use a mixing air distribution system. A mixing ventilation (MV) supplies fresh air to the cabin at shoulder and/or ceiling level and then exhausts cabin air through the side walls at floor level, as shown in Figure 2.1(a). Zhang et al. [20] measured the air velocity, temperature, and contaminant concentration in a section of a full-sized, half-occupied, twin-aisle cabin mock-up with a mixing ventilation system. They found that the contaminant concentration in the four-row cabin was rather uniform due to the well-mixing airflow pattern and the end-wall blockage in the longitudinal direction. Zhang et al. [19] conducted experimental research to obtain the local mean age of air, temperature and velocity distribution in a seven-row cabin mockup built with the same dimensions as the Boeing 737-200 in full-scale with three different mixing ventilations. They found that mixing ventilation can cause heat accumulation in the cabin due to the role of large-scale, low-speed circulation. Additionally, You et al. [21] employed the Wells-Riley method integrated with CFD to evaluate the SARS infection risk in aircraft cabins with mixing ventilation, conventional displacement ventilation, and personalized displacement ventilation system. The results showed that the infection risk of passengers was the highest with the mixing ventilation system. The above studies indicated that the mixing ventilation creates a homogeneous air distribution with uniform temperature and contaminant concentration distributions. Therefore, this air distribution system is not efficient in controlling contaminant transmission.

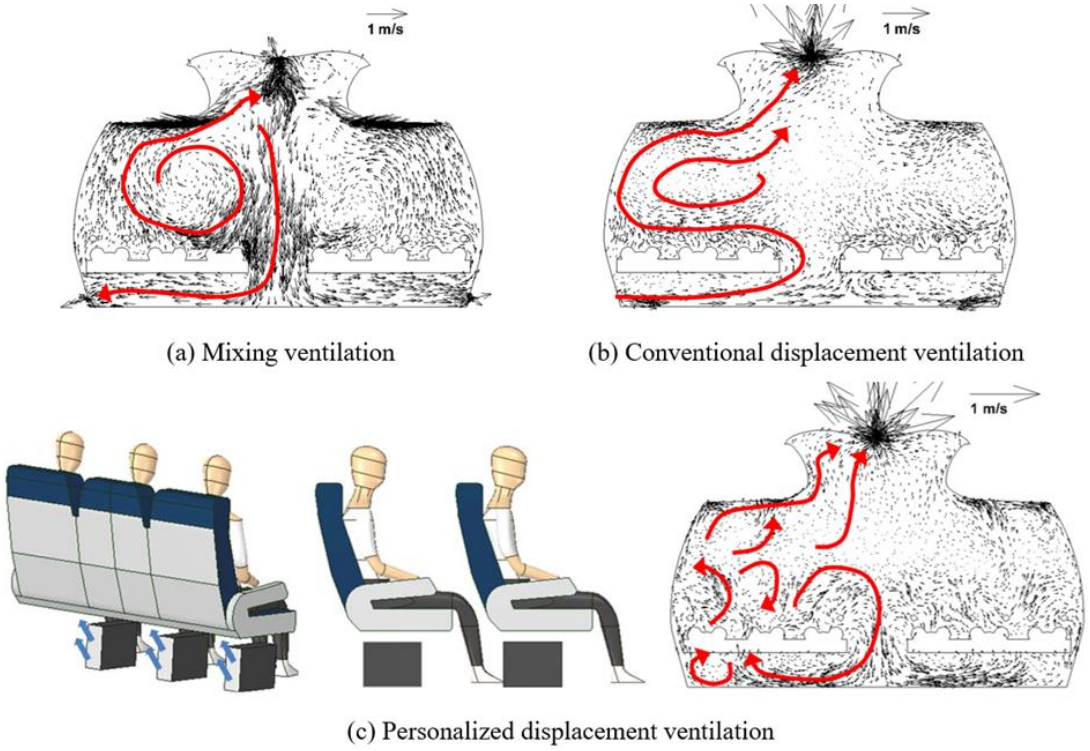

Figure 2.1. Cross-sectional air distribution with (a) mixing ventilation, (b) conventional displacement ventilation, and (c) personalized displacement ventilation by You et al. [21].

In order to overcome the potential deficiencies of mixing ventilation system, alternative main ventilation systems were studied. Widely used in buildings, displacement ventilation (DV), is an alternative ventilation concept, which has been found to provide thermal comfort and good indoor air quality [19, 21-23, 25, 42-48]. The reason is that, in a displacement ventilation system, fresh air is provided through side diffusers near the floor, and the cabin air is discharged at ceiling level, as shown in Figure 2.1(b), thus the airflow structure is in accordance with human generated thermal plumes. Bosbach et al. [49] were the first to test displacement ventilation under flight conditions in an A320 aircraft cabin. They found that the fresh air raised only in the vicinity of the heat loads and leaved the cabin through the ceiling outlets. Recently, Liu et al. [22] evaluated contaminant transmission and thermal comfort performance under mixing ventilation and displacement ventilation in terms of comfort and health. The results showed that during the initial outbreak of the epidemic, passengers posed a lower infection risk under displacement ventilation compared to mixing ventilation. However, wearing a mask can effectively reduce the infection risk under mixing ventilation to a level comparable to that under displacement ventilation. Additionally, the thermal comfort under displacement ventilation was relatively poor due to an excessively high vertical temperature difference. Maier et al. [50] experimentally analysed thermal comfort of displacement ventilation in an aircraft passenger

cabin. The results indicated that although the known disadvantages, vertical temperature difference and lower temperature around the feet, were confirmed, these did not influence the passengers' satisfaction ratings very much. In addition, the heat removal efficiency was significantly higher under displacement ventilation in comparison to mixing ventilation system.

To further improve thermal comfort and air quality in the cabin, personalized ventilation (PV) systems have been developed by supplying fresh air directly to the breathing zone of the passengers [16, 21, 22, 25-27, 38, 51, 52]. For example, Gao and Niu [16] proposed a personalized ventilation system that supplies fresh air through a flexible "goose-neck" duct embedded in chair armrests. They found that this system can shield up to 60% of the user's exposure. Zhang and Chen [25] proposed an innovative system, in underfloor air distribution served the background ventilation and armrest-embedded air terminals provided personal ventilation by supplying fresh air directly to the breathing zone of passengers. They found the system is robust to prevent contaminants released at any height from entering passengers' breathing zone. You et al. [24] further proposed an innovative personalized displacement ventilation system that combined displacement and personalized ventilation systems to improve the cabin environment. In this system, individual diffusers installed on the floor under the seat supply clean air to the passengers in the row behind, and the cabin air is exhausted at ceiling level, as shown in Figure 2.1(c). The personalized displacement ventilation system was found to reduce the average exposure in the cabin by more than 50% compared with conventional mixing and displacement ventilation systems [21, 24], indicating its potential to improve contaminant control. The advantages and disadvantages of the above main ventilation systems have been summarized in Table 2.1.

Table 2.1. Comparison of different main ventilation systems.

Main ventilation systems	Advantages	Disadvantages
Mixing ventilation	Uniform temperature distribution	Inefficient at removing contaminants due to well-mixed cabin air
Displacement ventilation	Remove contaminants effectively	Temperature stratification
Personalized displacement ventilation	Remove contaminants effectively Uniform temperature distribution	/

2.2 Gasper System

However, the performance of the above innovative personalized displacement ventilation system has not been thoroughly assessed. This is because, in addition to the main ventilation system, a system of gaspers is also available in most commercial airliners for individual ventilation and thermal regulation as the cabin environment is not necessarily satisfactory for all passengers. Gaspers are a system of small, circular, adjustable vents installed above the seat for each passenger, as shown in Figure 2.2. Passengers can adjust both the direction and flow rate of gaspers to help achieve their preferred cabin environment [3, 37, 38].

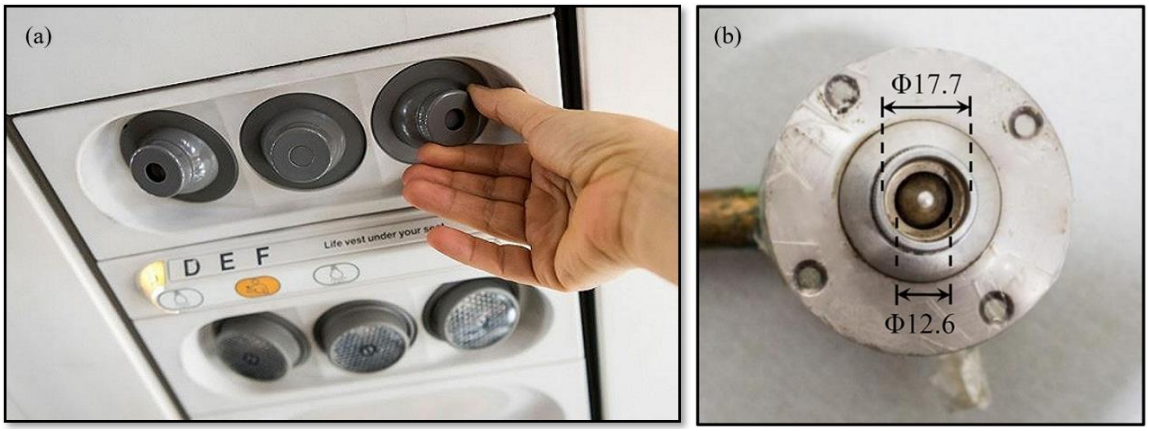

Figure 2.2. (a) Photography of the gasper system in an actual aircraft cabin from [53] and detailed geometry of the gasper (unit: mm) [28].

Studies on the impact of gaspers on airflow and contaminant transport have been summarized in Table 2.2. Previous studies have proved that the gasper-induced flow alters the air distribution and thus affects the contaminant transport in the cabin [28-33, 35, 36, 54]. For example, Dai et al. [28] conducted experiments in a simplified aircraft cabin without main ventilation system in order to study the characteristics of a gasper jet. They found that the airflow induced by the gasper was complicated near the nozzle, but the axial mean velocity decay along the centerline and radial profiles could be simplified when fully developed. Meanwhile, Shi et al. [29] investigated the impact of the gasper jet on air quality in a passenger's breathing zone using the computational fluid dynamics (CFD) method. According to the results, more than 90% of the air in a passenger's breathing zone was entrained from the surroundings, which means that the gasper had only a minor impact on the air quality in a passenger's breathing zone even though gaspers provide fresh air aiming at passengers. Note

that the main ventilation system was still not considered in that study. In fact, the practical application environment of gaspers in an aircraft cabin is one with mixed airflow from diffusers and gaspers. Therefore, You et al. [32] built a full-scale mock-up of half of a one-row, single-aisle aircraft cabin for measuring airflow distribution above the passenger of the cabin mock-up with a gasper on. They found that in the region near the gasper outlet, it was possible to regard the gasper-induced jet as a fully developed round jet. When the distance increased, the gasper-induced jet was influenced by both the main airflow and the thermal plume generated by the human simulator. Additionally, Li et al. [30] investigated the interactions between the gasper jet and the mixing ventilation. They used particle image velocimetry (PIV) system to measure the air distribution under different operation conditions and flow rates. The results showed that the decay of the gasper jet was accelerated by the mixing ventilation, and a gasper with a medium or high flow rate decreased the air velocity around the adjacent passenger.

Table 2.2. Overview of studies on the impact of gaspers on airflow and contaminant transport.

#	Author (year)	Ref.	Main ventilation system	Number of gaspers	Gasper operation
1	Dai et al. (2015)	[28]	No main ventilation	Single	Adjustable
2	Shi et al. (2016)	[29]	No main ventilation	Single	Adjustable
3	You et al. (2016)	[32]	Mixing ventilation	Single	Fixed
4	You et al. (2016)	[33]	Mixing ventilation	Single	Fixed
5	Li et al. (2016)	[31]	Mixing ventilation	Multiple	Fixed
6	Tang et al. (2017)	[36]	No main ventilation	Single	Fixed
7	You et al. (2017)	[34]	Mixing ventilation	Multiple	Fixed
8	Li et al. (2018)	[30]	Mixing ventilation	Single	Adjustable
9	Liu et al. (2021)	[35]	Mixing ventilation	Two	Adjustable

Note that the above studies have provided great insight into gasper-induced jet flow and its impact on air quality, they only focused on a single gasper. However, according to experimental investigations [37, 55], more than 60% of passengers open their gaspers during flights, which means that the real situation involves concurrent operation of gaspers. Therefore, it is crucial to investigate the impact of concurrent gasper operation on airborne disease transmission in the cabin. Li et al. [31] measured the distributions of air velocity, air temperature, and contaminant concentration in a five-row section of an aircraft cabin with mixing ventilation, with two-fifths of the gaspers open. When these gaspers were open, the air velocity was higher, and the air temperature was more uniform; however, the air quality in this scenario was not better than when gaspers were closed. You et al. [34] employed a CFD simulation to investigate the impact of the gasper open/closed distribution on the exposure risk for passengers, considering five different gasper utilization rates. The results showed that the overall effect of opening a passenger's gasper on his/her mean exposure risk was neutral. Note that the above findings on the impact of concurrent gasper operation on air quality were based on a mixing ventilation system. In cabins with personalized displacement ventilation, the conclusions may be quite different. The reason is that the downward gasper-induced jet flow is not in accordance with the direction of the main airflow and human-generated thermal plumes. Additionally, practical instructions for passengers on the control of airborne disease transmission in cabins are still not available. Therefore, further efforts should be made to evaluate the effectiveness of concurrent gasper operation in a cabin with personalized displacement ventilation and to provide practical guidance for passengers.

2.3 Research Method

According to reviews of the state-of-the-art methods for investigating air distributions in commercial airliner cabins [18, 56, 57], two main methods are available: experimental measurements and numerical simulations.

2.3.1 Experimental Measurements

It is ideal to use an actual aircraft cabin for obtaining reliable and high-quality experimental data. However, very few experimental studies of air distribution in airliner cabins were conducted in actual airplanes. For example, Mo et al. [58] used the particle image velocimetry

(PIV) technique to measure the velocity and turbulence intensity profiles of the airflow in a section of a narrow body (737) aircraft cabin. The cabin section, cut from a salvage aircraft, had 18 seats distributed in three rows and a thermal manikin to simulate a human body. The measured data was used for validation of the computational fluid dynamics (CFD) models. Liu et al. [59] used hot-sphere anemometers (HSA) combined with ultrasonic anemometers (UA) to measure high-resolution flow field in the first-class cabin of a functional MD-82 commercial airliner. Significant longitudinal flow was found during the experiment but the airplane was designed to have minimal longitudinal flow. This is because, although the airplane was functional, the thermo-fluid boundary conditions were difficult to control, which led to uneven airflow rate and velocity of diffusers along the longitudinal direction. Note that the above test cabin did not include heated manikins, thus the flow characteristics may differ from those in a real cabin. However, the measured data provided high-quality boundary conditions for validating CFD models. Meanwhile, Li et al. [31] measured the distributions of air velocity, air temperature, and contaminant concentrations in five rows of the economy-class section of an MD-82 commercial airliner with two of five gaspers on. The measured section was fully occupied with heated manikins. This study aimed to investigate the impact of gasper airflow on the air quality in a cabin, and the results showed that although the gaspers directed clean air toward the passengers, the air quality in the breathing zone was not improved in this case.

Although experimental measurements in actual cabins were more reliable but thermo-fluid boundary conditions were difficult to control and the cabin interior settings were difficult to change. Accordingly, full-scale cabin mock-up experiments have become the most popular alternative method for studying air distributions in airliner cabins [24, 32, 60-66]. For instance, You et al. [32] conducted experimental measurements of airflow distribution in a mock-up of half of a full-scale, one-row, single-aisle aircraft cabin with a gasper on. The measured airflow field data was then used to identify suitable turbulence model for simulating air distribution in cabins with gasper-induced flow. Meanwhile, You et al. [24] measured the air velocity, air temperature, and contaminant distribution in a seven-row, single-aisle, fully occupied aircraft cabin mock-up equipped with an innovative personalized displacement ventilation system proposed in their previous study. The experimental data was used to validate CFD method, and then the validated CFD method was used to study the performance of different configurations of the new ventilation system. Additionally, Wang et al. [60] measured thermo-fluid boundary conditions, airflow and temperature distributions in a full-scale, seven-row, single-aisle aircraft cabin mock-up. The measurement error and uncertainty were quantified in detail to evaluate

measurement accuracy. This investigation aimed to provide accurate and favorable boundary conditions for CFD simulation. The above studies indicated that most experimental measurement data were used to validate the CFD model, as the experimental measurements is expensive and time consuming. In contrast, CFD simulation is cheaper and can effectively provide more detailed information [56].

2.3.2 Numerical Simulations

2.3.2.1 Airflow Simulation

The CFD method was the most popular for predicting air distribution as it can provide informative and accurate air distribution results in aircraft cabins [56]. For example, Yan et al. [67] used the standard k–ε model to calculate a steady airflow field in a Boeing 767-300 aircraft cabin, and the airflow patterns were similar to those observed in the experiment. Zhang et al. [20] employed the re-normalization group (RNG) k–ε model [68] to calculated the air distribution in a four-row, twin-aisle aircraft cabin mockup, and the discrepancies between the simulated and measured airflow patterns were significant. This may be due to the fact that it was difficult to obtain accurate flow boundary conditions of the air supply diffusers. Since different turbulence models have been used in previous studies, it is necessary to identify a suitable turbulence model for predicting the air distribution in aircraft cabins. Lin et al. [69] found that the Reynolds-average Navier-Stokes (RANS) simulation substantially underpredicted the turbulence intensity in commercial aircraft cabins, especially in and around the breathing zone, while the LES-predicted turbulence level had a good agreement with the test data. Additionally, Liu et al. [70] evaluated the RNG k–ε model, large eddy simulation (LES) [71, 72], and detached eddy simulation (DES) [73, 74] for their ability to predict the airflow in the first-class cabin of a functional MD-82 commercial airliner. The results showed that for the mixed convection in the fully-occupied cabin, the simulated results by both LES and DES were acceptable, while the RNG k–ε model failed to accurately predict the air distribution in some areas.

Note that the above studies mainly focus on the turbulence models for simulating the main flow or the interaction of the main flow and the thermal plume generated by passengers rather than gasper-induced flow. Gasper-induced flow is a jet flow with high gradients of pressure and velocity. Recently, considerable efforts have been made to seek more reliable and accurate

turbulence models for simulating complex flows with gasper-induced flow [32, 34, 75]. For instance, Shi et al [75] systematically evaluated the performances of most prevalent models in simulating stratified flows, including six RANS models and one LES model. They found that the shear stress transport (SST) *k–ω* model [76] was the best for the strongly stratified jet. Meanwhile, You et al. [32] used measured data to evaluate the performance of the RNG *k–ε* model and the SST *k–ω* model for predicting air distribution in cabins with gasper on, and the SST *k–ω* model was found to be more accurate in gasper-induced jet dominant region. Therefore, this study used the SST *k–ω* model to simulate the air distribution in aircraft cabins with gasper on.

2.3.2.2 Contaminant Transport Simulation

For contaminant transport modelling, the Eulerian and Lagrangian models are the most popular methods. The Eulerian model assumes the particle phase as a continuum and solves the following scalar transport equation [77]:

$$\frac{\partial(u_j C)}{\partial x_j} = \frac{\partial}{\partial x_j} \cdot \left(\frac{\nu_t}{\sigma_C}\frac{\partial \mathrm{C}}{\partial x_j}\right) + S_C \tag{2.1}$$

where u_j is the average air velocity, ν_t is the turbulent kinetic viscosity, σ_C is the turbulent Schimidt number, and S_C is the particle source term. A User-Defined Function (UDF) can be used to realize the Eulerian model in ANSYS Fluent.

You et al. [24] employed the Eulerian method to simulate the contaminant distributions in an aircraft cabin with an innovative personalized displacement ventilation system. The calculated contaminant distributions were compared with measured data for validation. The results showed that the Eulerian model was capable of predicting the general trends of the contaminant distribution in aircraft cabins. Then, You et al. [21] applied the validated Eulerian method to simulate the contaminant transport in aircraft cabins to evaluate the performance of different air distribution systems. Additionally, Liu et al. [78] used the Eulerian method to evaluate the infection risk for susceptible people in a large office building under different ventilation strategies. The above studies indicated that the Eulerian method has been widely used for predicting airborne disease transmission in enclosed environments.

On the other hand, the Lagrangian model [79, 80] calculates the trajectory of each individual particle by solving the following equation in accordance with Newton's law [77]:

$$\frac{d\vec{u}_p}{dt} = F_D\left(\vec{u}_a - \vec{u}_p\right) + \frac{\vec{g}\left(\rho_p - \rho_a\right)}{\rho_p} + \vec{F}_a \tag{2.2}$$

where $\vec{u}_p$ is the particle velocity, $\vec{u}_a$ is the air velocity, $\vec{g}$ is the gravitational acceleration, ρ_p and ρ_a is the density of particle and air, $\vec{F}_a$ is Brownian motion force, and $F_D\left(\vec{u}_a - \vec{u}_p\right)$ is the drag force, which can be calculated by:

$$F_D\left(\vec{u}_a - \vec{u}_p\right) = \frac{18\mu_a}{\rho_p d_p^2}\frac{C_D Re}{24}\left(\vec{u}_a - \vec{u}_p\right) \tag{2.3}$$

where μ_a is the molecular viscosity of the air, d_p is the diameter of particle, C_D is the drag coefficient, R_e is the Reynolds number, which is defined as

$$Re \equiv \frac{\rho_a\left|\vec{u}_p - \vec{u}_a\right|}{\mu_a} \tag{2.4}$$

Recent studies attempted to use CFD simulations with the Lagrangian model to predict the infection risk [39-41, 81-83]. For example, Ren et al. [39] used the Lagrangian model to simulate the particle trajectories of respiratory droplets and aerosols from the coughing process in prefabricated COVID-19 ward under three different ventilation strategies. Moreover, Wang et al. [84] evaluated the performance of five airflow models, including a RANS model, a Unsteady-RANS (URANS) model, a LES model, and two DES models, with the Eulerian and Lagrangian methods in predicting particle concentration distributions in enclosed environments. For steady-state condition, the RANS model with the Eulerian method is recommended due to their reasonable accuracy and low computing cost. As this study mainly focused on steady-state airflow condition, the Eulerian method will be used to simulate the contaminant transport in aircraft cabins.

Overall, CFD simulations offer a more cost-effective and information-rich approach compared to experimental measurements. However, these numerical models incorporate various approximations and simplifications when modeling the airflow and contaminant distributions, which introduces uncertainties in the simulation results. Therefore, to ensure reliability, this thesis first used the experimental data with similar airflow characteristics to validate the CFD method. The validated CFD method was then used to investigate air distribution and contaminant transport under a more realistic condition [58, 85].

2.4 Research Gaps

Currently, there is a lack of reliable and high-quality experimental data in the literature characterizing the interaction between personalized displacement ventilation, gasper-induced jet flow, and thermal plumes generated by passengers in cabin environments. Additionally, the validation of CFD simulation for calculating this complex flow configuration is also not available. Therefore, an aircraft cabin mock-up replicating the airflows needs to be built and experimental measurements should be conducted. Accordingly, obtained experimental data should be used to validate the CFD tool.

Secondly, previous studies have provided great insight into gasper-induced jet flow and its influence on air quality. For example, Li et al. [31] reported that the contaminant was pushed down to the lower part of the cabin when the gaspers were on. This indicates that turning on gaspers may increase the exposure risk for other passengers, especially in a cabin with a personalized displacement ventilation system. The reason is that gasper-induced jet flow is directed downwards, as gaspers are mounted on the ceiling, while the main flow and thermal plume generated by passengers travel upwards. In other words, it is unknown whether the personalized ventilation system is still effective in controlling the airborne disease transmission when gaspers are in use. Therefore, further investigation is needed to explore the interaction of the flows from different directions and the impact of this interaction on contaminant transport in aircraft cabins with personalized ventilation system.

Thirdly, gaspers' usage behavior is quite complex, as passengers can adjust both the direction and flow rate of gaspers to help achieve their preferred cabin environment [3, 37, 38]. Li et al. [30] built a 1:1, large-scale, 2D-PIV experimental platform of an aircraft cabin environment to

investigate the interactions between gasper-induced flow and main ventilation. They found that both the flow rate and direction of gaspers altered the air distribution and thus had a substantial impact on contaminant transport in the cabin. Therefore, it is crucial to systematically investigate the impact of gasper settings, including the flow rate and flow direction, on airborne disease transmission in aircraft cabins with personalized ventilation system.

Fourthly, in practice, multiple gaspers are operated simultaneously by passengers, and their interaction with the main airflow significantly complicates the contaminant transport in the cabin. Therefore, it is crucial to investigate the impact of concurrent gasper operation on airborne disease transmission. Moreover, current literature lacks actionable guidelines for passengers on how to operate gaspers effectively to mitigate disease transmission.

Finally, the existing studies have primarily focused on the impact of gasper operation on airborne contaminant transmission, without considering passengers' comfort preferences. However, in actual cabin environments, both factors are critical and should be addressed concurrently given that the gasper system is originally designed to improve individual thermal comfort. In addition, field survey [33] found that over 60% of passengers utilize the gasper system during cruise. Therefore, the key question arises: is there a feasible control mode that can simultaneously mitigate infection risk and maintain passengers' individual comfort preferences?

2.5 Proposed Tasks

According to the literature review conducted in this chapter, the following tasks are proposed in this thesis to investigate the operation of gaspers for reducing airborne disease transmission in commercial airliners with personalized displacement ventilation system:

(1) Conduct experimental measurements to obtain high-quality data and use the measured data to validate the performance of CFD method;

(2) Investigate systematically the impact of source and receptor gaspers on airborne disease transmission in aircraft cabins with personalized displacement ventilation;

(3) Identify and evaluate an executable concurrent gasper-operation strategy for controlling airborne diseases transmission in aircraft cabins with personalized displacement ventilation;

(4) Propose and evaluate the feasibility of a centralized control mode for simultaneously mitigating infection risk and maintaining passengers' comfort preferences.

CHAPTER 3 MODEL VALIDATION OF AIRFLOW AND CONTAMINANT TRANSPORT IN AN AIRCRAFT CABIN MOCK-UP

This chapter first carried out experimental measurements in a simplified three-row, single-aisle aircraft cabin mock-up with personalized displacement ventilation and a single gasper. Then, the measured distributions of air velocity and contaminant concentration were analysed. Finally, the obtained experimental data were compared with simulated results for CFD model validation.

3.1 Experimental Measurements

3.1.1 Experimental Setup

To obtain reliable and high-quality data, a simplified single-aisle aircraft cabin mock-up with personalized displacement ventilation was built for experimental measurements, as shown in Figure 3.1(a). The cabin dimensions were 3.56 m in width (x) and 2.30 m in depth (y), with ceiling heights ranging from 1.61 m at the lowest to 2.21 m at the highest. The cabin mockup contained three rows with 18 passenger seats, four of which were occupied by heated manikins (human simulators) simulating seated passengers, as shown in Figure 3.1(a). Among them, manikins 2a and 2b served as target passengers, representing the source passenger and receptor passenger, respectively. Manikins 1a and 1b were positioned ahead of the target passengers to minimize the influence of the front surface on the airflow patterns in front of the target passengers. The heat load of each manikin was 112.5 W. The main airflow was provided by individual diffusers installed on the floor, each delivering approximately 7.5 L/s [24]. Additional air was supplied through the gasper located above the manikins in the second row, with a flow rate of 0.66 L/s [31]. The total airflow rate in the cabin mock-up was 135.66 L/s, corresponding to an air change rate of 32.7 ACH. The cabin air was exhausted through the slot at the ceiling center. A tracer gas, the mixture of 1% sulfur hexafluoride (SF_6) and 99% N_2, was used to simulate a gaseous contaminant, which was released continuously from a porous rubber bulb in front of the source passenger's mouth, as shown in Figure 3.1(d). The total volume flow rate of the gas mixture released from the bulb was only 0.9 L/min [31], at which rate there is no observable air movement on the bulb surface. The tracer-gas source can be

considered as zero-momentum source. The cabin mockup was placed in an air-conditioned room maintained at 23℃, with non-insulated wall surfaces. Although the cabin mock-up differed slightly from an actual aircraft cabin, the experiments remained meaningful because the airflow characteristics were similar to those in a cabin with personalized displacement ventilation.

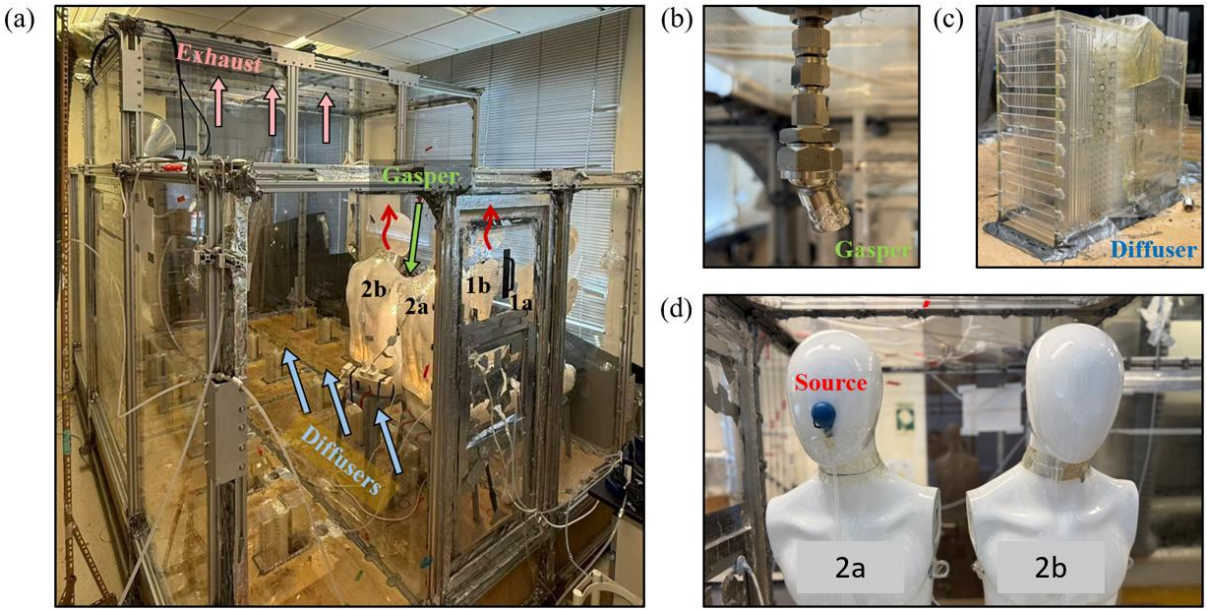

Figure 3.1. The aircraft cabin mockup: (a) field view of the mockup interior, and detailed view of (b) gasper, (c) diffusers, and (d) manikins.

The airflow field in front of the human simulator was the most complex, since the main airflow, the gasper-induced jet, and the thermal plume generated by the human simulator interacted in this region. Therefore, the distributions of air velocity and contaminant concentration were measured on the plane located 5 cm in front of the target passenger's mouth. The measurement locations for air velocity are shown in Figure 3.2(a). The air velocity was measured using a hot wire anemometer (Testo 440) with an accuracy of 0.03 m/s and an error of ±4%. Since only one anemometer was available, it was manually moved from one location to another in order to capture the air velocity field. At each location, velocity was recorded for 8 minutes at a sampling frequency of 1 Hz. After relocating the anemometer, a stabilization period of approximately 2 minutes was allowed before recording to avoid disturbances caused by sensor movement. Given the high air exchange rate in the cabin, a 2-min waiting time was sufficient to minimize such effects. The measurement locations for contaminant concentration are shown

in Figure 3.2(b), with a total of 135 measurement points. An INNOVA 1312 photoacoustic multi-gas monitor was used to measure the SF_6 concentrations.

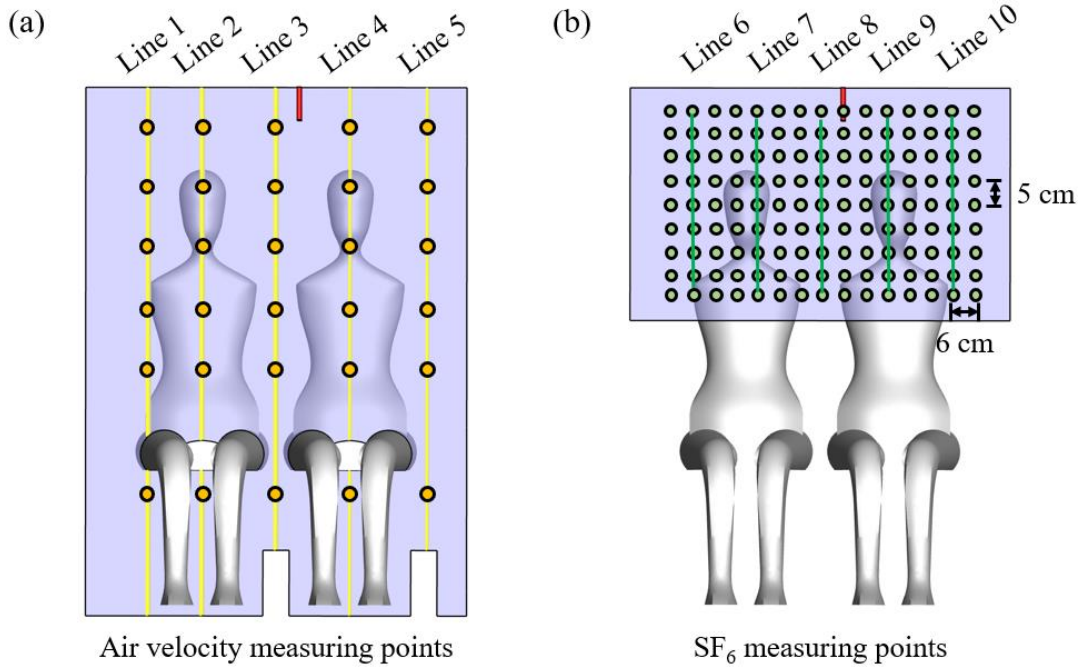

Figure 3.2. Setup for experimental measurements: (a) measurement area for airflow field and measurement locations for air velocity, (b) measurement locations for contaminant field.

3.1.2 Experimental Procedure

Before the experiment, the environmental control system of the cabin was operated for approximately two hours to ensure stable airflow and temperature distributions. An infrared camera was used to measure the surface temperatures of the manikins, which were divided into five sections: head, chest, abdomen, thighs, and calves. Since the cabin walls were non-insulated, surface temperatures were also measured with thermocouples at the ceiling, sidewalls, floor, and the front and back walls. Although the surface temperatures were not perfectly uniform, the averaged surface temperature values provided a reasonable representation of the thermal conditions for each surface. Table 3.1 summarizes the averaged surface temperatures measured in this study, which were subsequently used as input parameters for the CFD simulations. To determine the boundary conditions of each diffuser, a tracer-gas technique [24] was used to measure the flow rates, and an ultrasonic anemometer was used to measure the flow directions of each diffuser.

Table 3.1. Measured temperatures in the cabin mock-up.

	Temperature (°C)
Supply air	23.0
Ceiling	23.0
Side wall near the manikins	23.5
Side wall far from the manikins	22.0
Floor	22.5
Front wall	23.0
Back wall	22.4
Manikins	27.5

3.2 Numerical Approach

The CFD method was adopted in this study for calculating air distribution and airborne disease transmission. A commercial CFD code, ANSYS Fluent, was employed [77]. The SST *k*-*ω* model [76] was used for predicting the steady-state air distribution in aircraft cabins with gaspers on, considering that this model performs best for a jet flow [29, 32, 33, 75]. In the SST *k*-*ω* model, the turbulence kinetic energy (*k*) and the specific dissipation rate (*ω*) are obtained from the following transport equations [77]:

$$\frac{\partial}{\partial t}(\rho k) + \frac{\partial}{\partial x_i}(\rho k U_i) = \frac{\partial}{\partial x_j}\left[\left(\mu + \frac{\mu_t}{\sigma_k}\right)\frac{\partial k}{\partial x_j}\right] + G_k - Y_k \tag{3.1}$$

$$\frac{\partial}{\partial t}(\rho \omega) + \frac{\partial}{\partial x_i}(\rho \omega U_i) = \frac{\partial}{\partial x_j}\left[\left(\mu + \frac{\mu_t}{\sigma_\omega}\right)\frac{\partial \omega}{\partial x_j}\right] + G_\omega - Y_\omega + D_\omega \tag{3.2}$$

where σ_k and σ_ω are the turbulent Prandtl number for k and ω, respectively. Meanwhile, G_k represents the generation of k due to mean velocity gradients; G_ω represents the generation of ω; Y_k and Y_ω represent the dissipation of k and ω, respectively, due to turbulence; and D_ω is the cross-diffusion term.

The exhaled air contaminant was assumed to be in the form of fine particles with dispersion characteristics similar to those of gaseous contaminants [86]. Therefore, the Eulerian method

[87] was used to simulate contaminant transport in aircraft cabins, as this method has been widely used in previous studies on airborne disease transmission [12, 88-90]:

$$\frac{\partial \rho \phi}{\partial t} + \frac{\partial}{\partial x_i}\left(\rho \phi U_i - \Gamma_\phi \frac{\partial \phi}{\partial x_i}\right) = S_\phi \tag{3.3}$$

where ϕ is contaminant concentration, t is time, ρ is density, U_i is air velocity, Γ_ϕ is the diffusion coefficient, and S_ϕ is the mass flow rate of contaminant source per unit volume. This study used User-Defined Scalar (UDS) to simulate the contaminant, and a scalar transport equation was activated in ANSYS Fluent.

The Boussinesq approximation was adopted to consider the buoyancy effect [91]. The SIMPLE algorithm [92] was employed for coupling pressure-velocity equations. The PRESTO! scheme was used for discretizing pressure, and the second-order scheme was used for all the other variables. This investigation assumed that the calculation reached convergence with velocity residuals at 10^{-4}, turbulence residuals at 10^{-5}, and the energy residual at 10^{-6}.

3.3 Results

The measured air velocity and contaminant concentration distributions were first presented and analysed. Subsequently, the obtained experimental data were compared with simulated results for CFD model validation.

3.3.1 Experimental Results

This study measured the air velocity field under two conditions: gasper off and gasper on to the abdomen of the receptor passenger (manikin 2b). The velocity profiles along lines 1-5 are shown in Figure 3.3. When the gasper was closed, line 3 exhibited the highest velocity values because it was located directly in front of the diffuser. This area was dominated by the main flow of the diffusers, and a velocity peak was observed at a height of about 1.0 m, corresponding to the breathing zone. Lower velocities were recorded along lines 1, 2, 4, and 5. When the gasper was open to the abdomen of the receptor passenger, noticeable velocity increases occurred along Lines 3 and 4, reflecting the influence of the additional gasper-

induced jet flow. In contrast, velocities along Lines 1, 2, and 5 remained unchanged, indicating that the effect of the gasper-induced jet flow was localized around the region near the receptor. The above results confirmed that the gasper-induced flow altered the surrounding airflow patterns while having minimal influence further away.

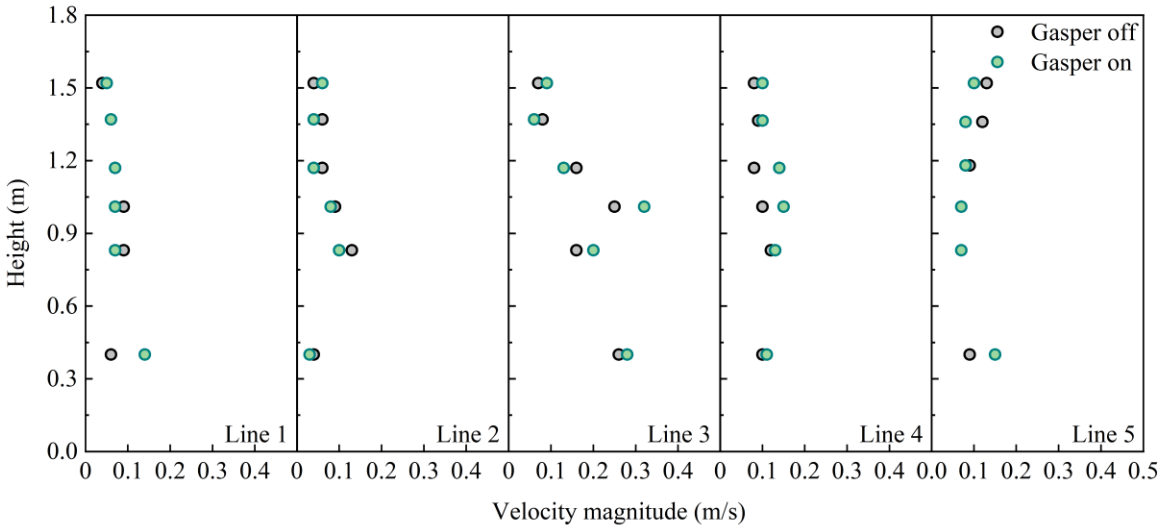

Figure 3.3. The measured air velocity profiles along Lines 1-5 with gasper off and on to the abdomen of the receptor.

Figure 3.4(a) and (b) present the measured dimensionless SF_6 concentration C^* (normalized by the concentration of return air) distributions with gasper off and on towards the receptor. When the gasper was off, the SF_6 released from the source accumulated primarily in the upper region above the source passenger, as the contaminant was transported upward by thermal plumes generated from the manikins. In this case, the receptor's breathing zone contained relatively lower concentrations, since the upward buoyant flow carried the contaminant away from the receptor. In contrast, when the gasper was directed toward the receptor, the gasper jet altered the transport pathway of SF_6. The gasper-induced jet flow pushed part of the contaminant from the source region toward the receptor passenger, leading to visibly higher concentrations in the receptor's breathing zone. These observations indicate that while the gasper supplied additional fresh air, it can also entrain and alter the transport path of contaminants, thereby may increase the exposure risk of nearby passengers.

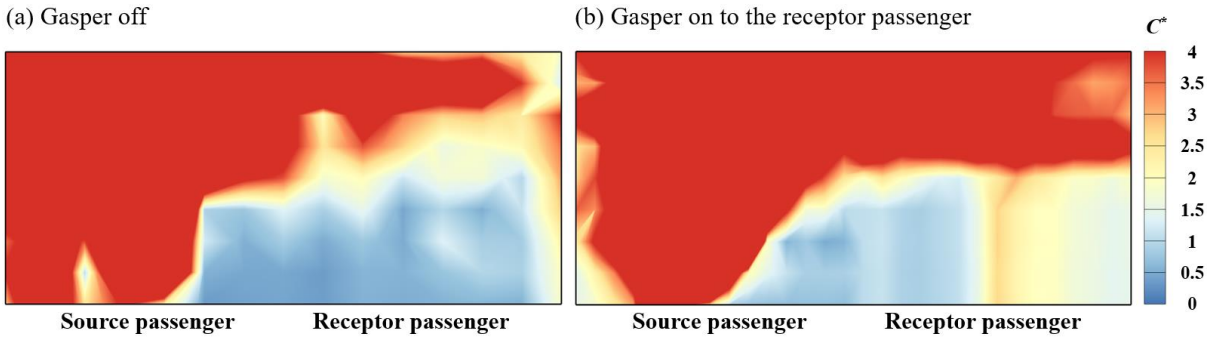

Figure 3.4. The measured dimensionless SF_6 concentration fields in the measurement area: (a) gasper off, (b) gasper on to the abdomen of the receptor.

3.3.2 Model Validation

Figure 3.5 compares the measured and simulated velocity profiles along lines 1-5 when the gasper was directed toward the receptor gasper. Overall, the CFD simulation results showed good agreement with the experimental data, particularly along lines 1-2 and lines 4-5. The consistency at lines 2 and 4 is of particular importance, as these lines represent the airflow patterns in front of the manikins. This agreement indicated that the predicted airflow field in front of the passenger was reliable. However, some discrepancies remained along line 3, where the predicted peak velocity occurred at a lower height than in the experimental measurements. This deviation likely arises from the challenge of determining accurate diffuser boundary conditions in the experiment.

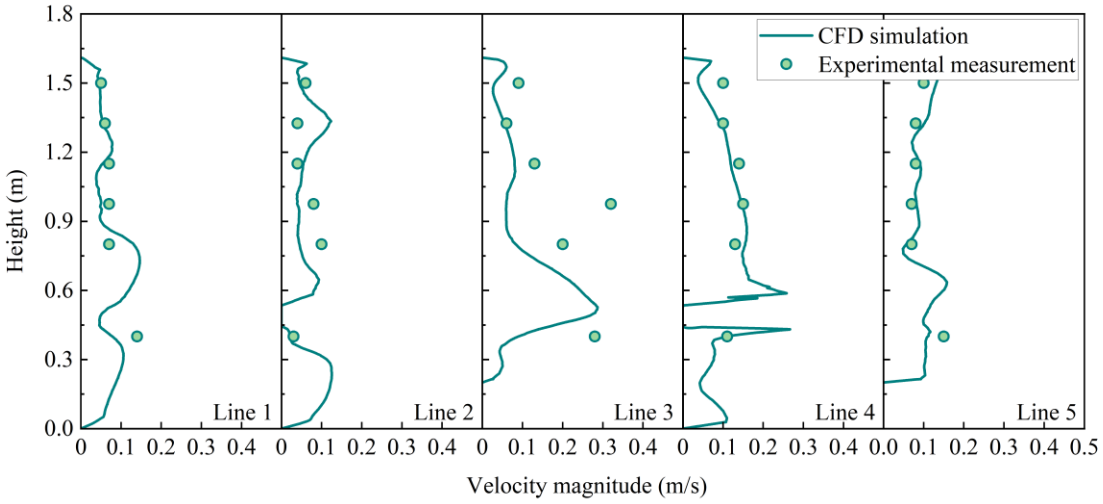

Figure 3.5. Comparison of the simulated and measured velocity magnitude along Lines 1-5.

To quantitatively compare the accuracy of the models, the normalized root mean square errors (NRMSE) between the predicted and measured data were calculated by:

$$NRMSE = \frac{\sqrt{\left[\sum_{i=1}^{n}\left(\emptyset_{exp,i} - \emptyset_{sim,i}\right)^2\right]/n}}{\emptyset_{exp,max} - \emptyset_{exp,min}} \tag{3.4}$$

where $\emptyset_{exp,i}$ is a data point from the experimental data, $\emptyset_{sim,i}$ is the corresponding data point from CFD simulations. $\emptyset_{exp,max}$ and $\emptyset_{exp,min}$ are the maximum and minimum values, respectively, of the experimental data. The overall NRMSE of the measurement points was 0.24. The comparison results demonstrate that the SST *k-ω* turbulence model can accurately capturing the main airflow features induced by the interaction of the diffuser flow, thermal plumes and the gasper flow.

Figure 3.6 presents the predicted distributions of the dimensionless contaminant concentration C^* (normalized by the concentration of return air) on the plane 5 cm in front of the receptor passenger's mouth. The green rectangles represent the measurement areas during the experiments shown in Figure 3.2(b). The CFD simulation reproduced similar concentration distributions with those observed in the experiments. Specifically, when the gasper was off (Figure 3.6(a)), contaminants released from the source passenger were transported upward by the thermal plumes and subsequently exhausted along the ceiling. In contrast, when the gasper was directed toward the receptor passenger (Figure 3.6(b)), part of the contaminants that originally accumulated above the source passenger was entrained by the gasper jet and transported into the receptor passenger's breathing zone, resulting a higher concentration in front of the receptor passenger. The above results demonstrate that the CFD model can reliably predict the spatial distribution of contaminants, highlighting its effectiveness as a tool for analyzing airflow patterns and contaminant transport in aircraft cabins.

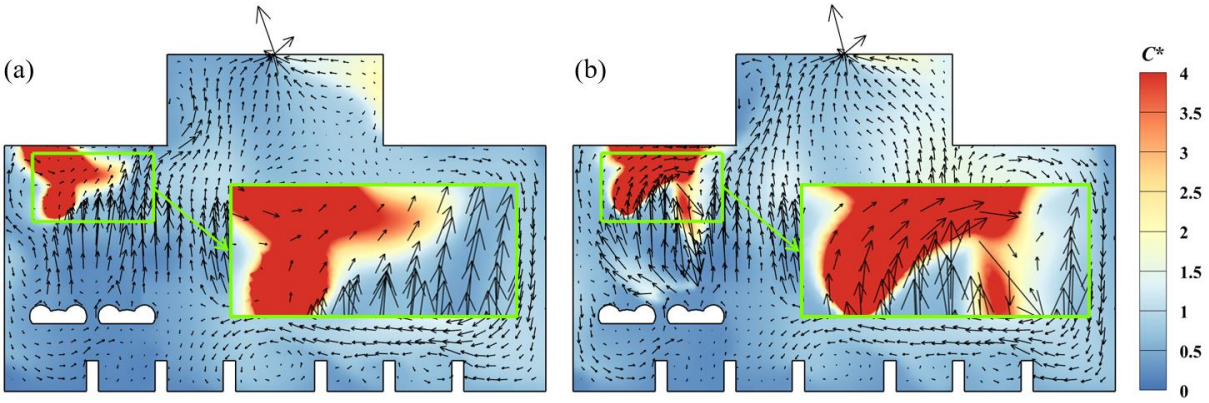

Figure 3.6. The simulated dimensionless SF_6 concentration distributions in the measurement area: (a) gasper off, (b) gasper on to the abdomen of the receptor passenger.

3.4 Summary

This study first conducted experimental measurements in a simplified three-row, single-aisle aircraft cabin mock-up with personalized displacement ventilation and a single gasper. Then, the measured distributions of air velocity and contaminant concentration with gasper off and on were analysed. Finally, the obtained experimental data were compared with simulated results for CFD model validation. Within the scope of this study, the following conclusions can be made:

- The gasper-induced flow altered the cabin airflow field and consequently influenced the transport of airborne contaminants.

- The CFD model accurately predicted the distributions of air velocity and contaminant concentration.

CHAPTER 4 INVESTIGATING THE IMPACT OF SOURCE AND RECEPTOR GASPERS ON AIRBORNE DISEASE TRANSMISSION

This chapter first investigated the impact of source gasper direction and flow rate on airborne disease transmission near the source in a seven-row, single-aisle, fully occupied, economy-class aircraft cabin with the CFD method. Next, the protective effect of the receptor's gasper was evaluated. Finally, the most effective gasper settings for source passengers and the working mechanism of the receptor's gasper were identified.

4.1 Case Setup

A seven-row, single-aisle, fully occupied, economy-class aircraft cabin with a personalized displacement ventilation system is illustrated in Figure 4.1(a). In this system, 42 individual diffusers (300 mm in height and 80 mm in width) were installed, one diffuser under each seat, to provide clean air directed towards the breathing zone of the passengers in the row behind the seats. A system of gaspers was installed on the ceiling. The total flow rate of supply air was 320.46 L/s [24], corresponding to an air change rate of 39.7 ACH. The cabin air was exhausted through two slots with a width of 4 mm at the ceiling center. The turbulence intensity at the diffusers and gaspers was assumed to be 10%, and the turbulence length scale was set as the opening width [21]. The temperature of the supply air was 19.3 ℃ [21]. The surface temperatures of the floor, sidewalls, ceiling, and passengers were 23.8 ℃, 24.5 ℃, 25.0 ℃, and 31.0 ℃, respectively [21]. In some aircraft types such as Boeing 737 or Airbus A320, a separate class is outfitted with 25 rows of seats [93]. Therefore, a 25-row section model with wall boundaries for the front and rear surfaces closely resembles a real-life scenario. Accordingly, we also simulated the air distribution in a 25-row section of an aircraft cabin to provide momentum and thermal data for the front and rear surfaces of the seven-row section model. The breathing flow rate caused by constantly exhaling or constantly inhaling was not considered in this study. Contaminants were released continuously with zero momentum from a cube (100 mm in side length) in front of the mouth of the source passenger. For a specific receptor, we used the exposure index [94] to quantify the relative intake of contaminants exhaled by the source passenger, as this index has been widely adopted in previous studies [24,

95-97]. The exposure index ε was defined as the ratio of the contaminant concentration in a receptor's breathing zone to the contaminant concentration in the return air [94]. The breathing zone was assumed to be a hemisphere in front of the shoulders, centered on the mouth and nose, with a radius of 20 cm [98], as shown in Figure 4.1(b).

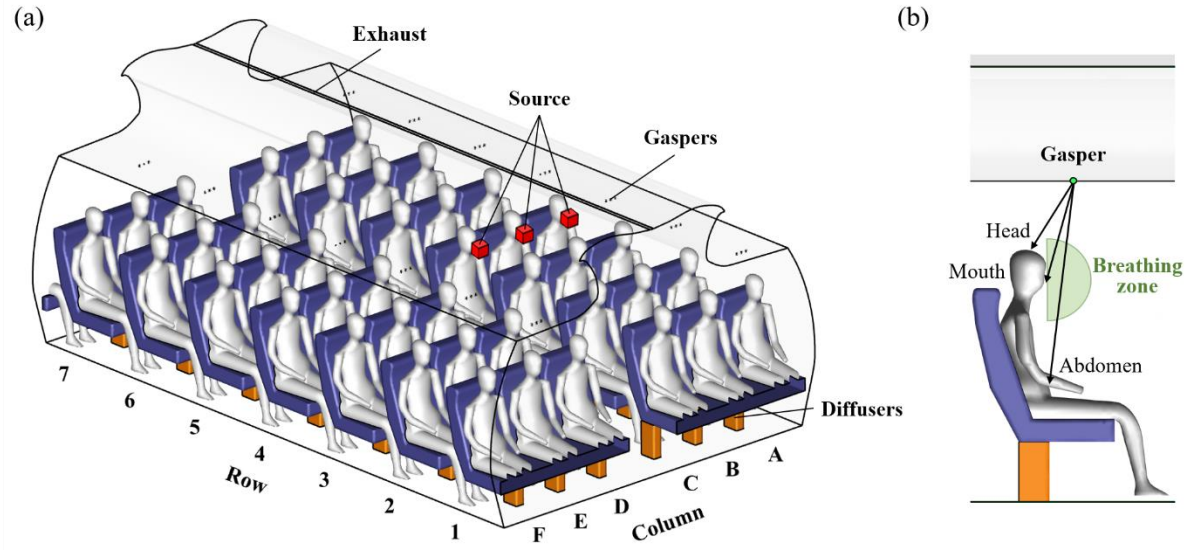

Figure 4.1. (a) Schematic of a seven-row section of the single-aisle, fully occupied, economy-class aircraft cabin and (b) the breathing zone and gasper directions in the side view.

To investigate the impact of gaspers on near-source transmission, we considered three source locations according to symmetry: the source passenger seated at 4A (window seat), 4B (middle seat), and 4C (aisle seat). The other passengers' gaspers were assumed to be closed. For the source passenger's gasper, the flow rates of 0.66 L/s (half-open) [31] and 1.32 L/s (fully open) were considered, and turning the gasper off was used as a benchmark. In a previous study, Fang et al. [37] experimentally found that more than 68% of participants adjusted the gaspers to target their bodies above waist level. Therefore, in the present study, three directions were considered (see Figure 4.1(b)) for the source passenger's gasper direction: to the head (H), to the mouth (M), and to the abdomen (A). A total of 21 cases were calculated. To investigate the impact of the receptor's gasper, we focused on the three most at-risk receptors with the highest exposure for each seat type, and the gaspers of other receptors were assumed to be closed. Another 18 cases were calculated, and the total number of cases in this study was 39.

A grid-independence test was conducted in a one-row section of the cabin with three grid resolutions, a coarse grid of 0.48 million, a moderate grid of 1.20 million, and a fine grid of

3.24 million. As shown in Figure 4.2(a), we compared the air velocity along the vertical centreline of the aisle (Line 1) and the gasper-induced jet flow direction (Line 2). The results in Figure 4.2(b)-(c) clearly showed that the moderate grid was adequate to capture the main flow and jet flow in the cabin.

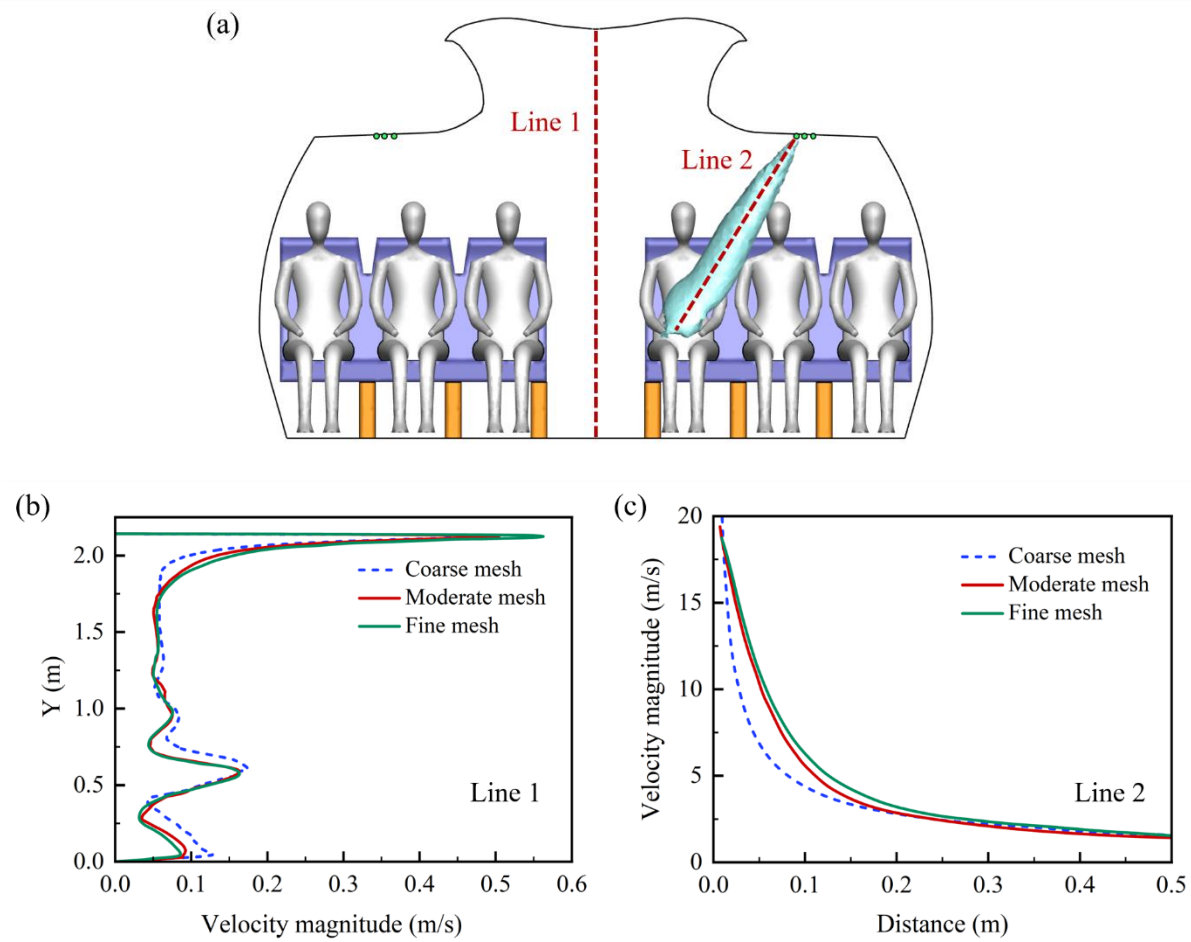

Figure 4.2. (a) The one-row section of aircraft cabin for grid independence test, and comparison of the velocity profiles at (b) Line 1 and (c) Line 2.

With the above moderate grid resolution, the grid distribution employed in this study is shown in Figure 4.3. The smallest meshes used around the exhaust and gaspers were 1 mm (labeled as ①) and 1.4 mm (labeled as ②), respectively. The size of the mesh on the passenger surfaces was 25 mm to depict the complex geometry. In other areas, the mesh size increased gradually by a factor of 1.2 to a maximum size of 60 mm. This led to a total grid number of 8.36 million for the seven-row section model.

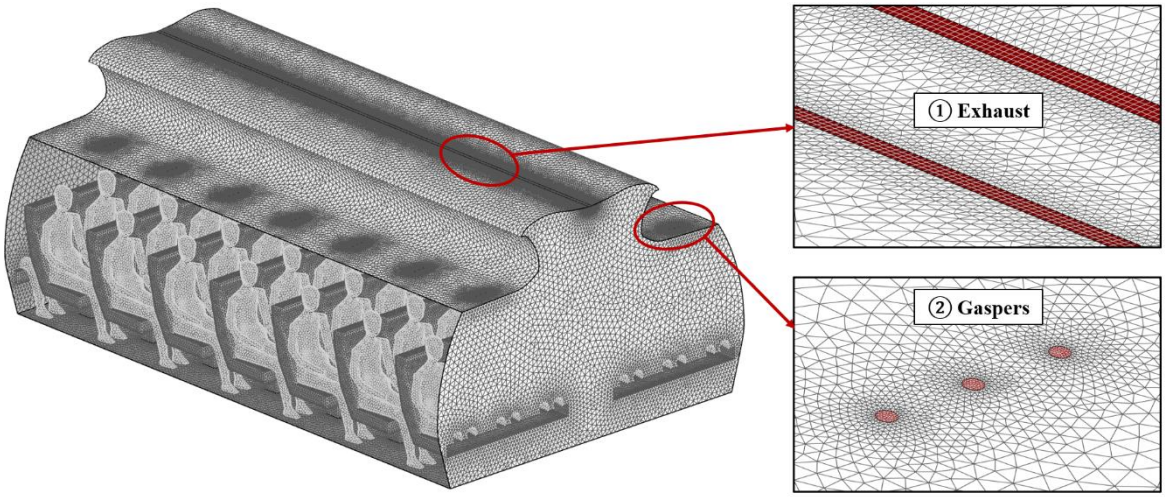

Figure 4.3. Grid distribution for the seven-row section of aircraft cabin.

4.2 Impact of Source Gasper on Near-source Transmission

To investigate the impact of gaspers on near-source transmission, we first analysed the airflow pattern and exposure index of the receptors when the source passenger was in different seat locations with all gaspers off as the benchmark. We then compared the exposure index under different source gasper settings, including directions and flow rates. Finally, we assessed the performance of different gasper settings in reducing overall exposure to obtain the optimal gasper setting for source passengers.

4.2.1 Gaspers off

When all gaspers were turned off, the air distribution in the cabin was dominated by the main flow and thermal plume. The airflow pattern in the cross section located 0.05 m in front of the mouth of the passengers in the fourth row (CS4) is shown in Figure 4.4(a). The red arrows represent the general airflow structure. At breathing level, the air at the window seat moved towards the sidewall, while the air at the aisle seat moved towards the aisle. The air at the middle seat moved upwards due to the thermal plume. At ceiling level, the air ascended to the exhaust in the ceiling center. In the lower part of the aisle, the air descended to the floor and then moved to the region under the seats on both sides. The airflow pattern in the horizontal section at breathing level (HS) is shown in Figure 4.4(b). It can be seen that the airflow at breathing level was forward.

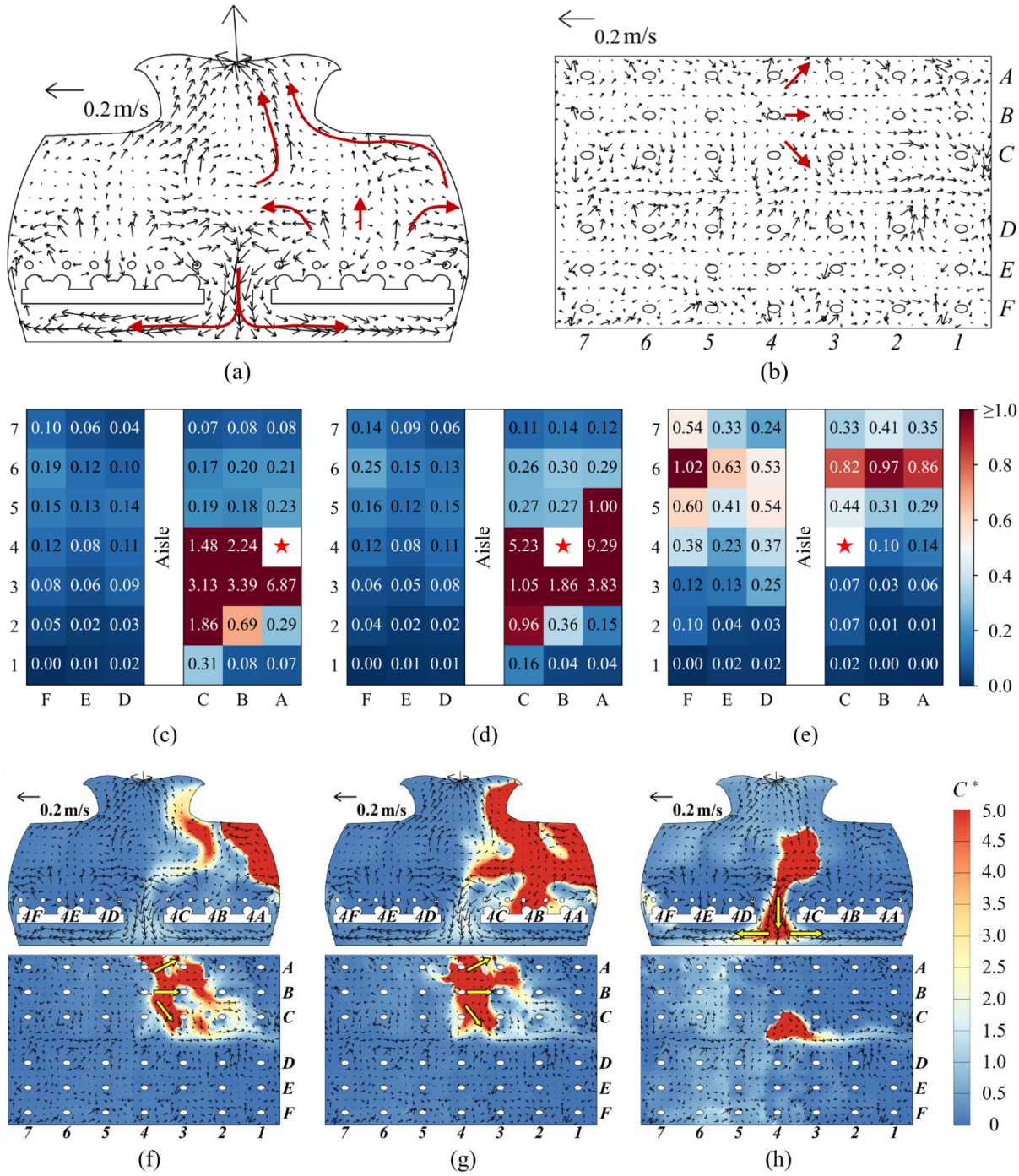

Figure 4.4. The airflow patterns at (a) CS4 and (b) HS, (c-e) the exposure index, and (f-h) the *C** distributions at CS4 and HS with source passenger in the window seat, middle seat, and aisle seat.

The exposure index of the receptors with source passenger in different seat locations are shown in Figure 4.4(c)-(e). The red star represents the source location. When the source passenger was in the window or middle seat (see Figure 4.4(c) and (d)), passengers with higher exposure

index were clustered in the few rows directly in front of the source passenger. However, when the source passenger was in the aisle seat (see Figure 4.4(e)), passengers behind the source passenger had higher exposure risk.

To analyse the contaminant transmission route, we also compared the dimensionless contaminant concentration C^* (normalized by the contaminant concentration of return air) distributions at CS4 and HS with different source locations, as shown in Figure 4.4(f)-(h). When the source passenger was in the window or middle seat, the contaminants moved forward due to the forward airflow at breathing level (see Figure 4.4(f) and (g)). When the source passenger was in the aisle seat, a considerable amount of the exhaled contaminants was transported downwards to the aisle floor (see Figure 4.4(h)), moved to both sides, and finally entered the breathing zone of the passengers in the back rows. Therefore, the passengers behind the source passenger were exposed to a higher concentration of contaminants.

4.2.2 Source Gasper on

The relative positions of the source passenger and his/her gasper were different for each source location, as shown inFigure 4.5. The green arrows represent the general direction of the gasper-induced jet flow. When the source passenger was seated in the window seat, the source gasper was in front of the right side of the source passenger, and the gasper flow thus moved backwards and left towards the sidewall. In contrast, when the source passenger was seated in the middle or aisle seat, the gasper of the source passenger was in front of the left side of the source passenger. Therefore, the gasper flow moved backwards and right towards the aisle.

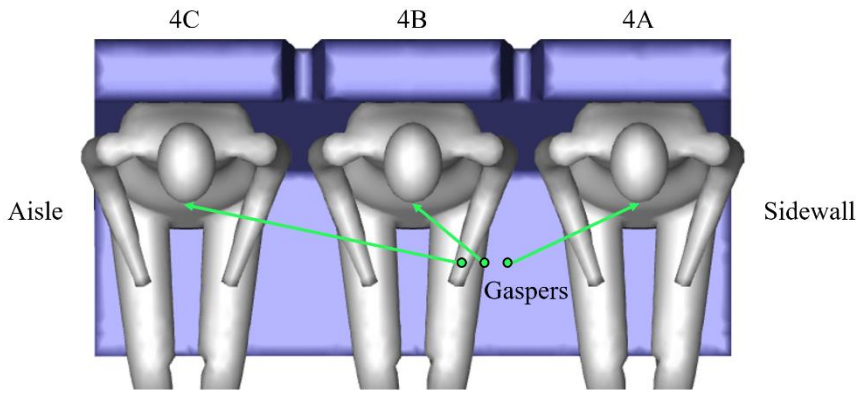

Figure 4.5. Relative positions of source passengers and gaspers in the top view.

4.2.2.1 Window Seat

When the source passenger was in the window seat 4A, three directions (see Figure 4.1(b)) and two flow rates of the source gasper were considered. We compared the exposure index under different source gasper settings, as shown in Figure 4.6(a)-(c). To keep the chapter concise, only the results for some of the cases are presented, and the remaining results can be found in Appendix A. The results show that opening the source gasper increased the exposure index of receptors behind the source passenger, particularly when the flow rate was high. For instance, when the source gasper was fully open towards the mouth (see Figure 4.6(b)), the exposure index of five of the receptors behind the source passenger was above 1, in contrast with the benchmark case, where the exposure index of all receptors behind the source passenger was less than 1 (see Figure 4.4(c)).

To clarify the influence mechanism of the gasper, we further analysed the airflow pattern and C^* distribution at CS4, HS, and the longitudinal section for passengers in column A (LSA), as shown in Figure 4.6(d)-(f). When the source gasper was open, as the gasper-induced flow was towards the sidewall (see Figure 4.5), the jet flow entrained the contaminants backwards to the sidewall. With a higher flow rate, the gasper jet flow gained more momentum and transported the contaminants further towards the rear rows. Simultaneously, a portion of the contaminants was transported to the floor and then entered the breathing zone of rear receptors by upwards flow from the diffusers, as shown in Figure 4.6(e). However, when the gasper was half-open to the abdomen, the jet flow was blocked by the body of the source passenger, as depicted in Figure 4.6(f), preventing the backward transmission of contaminants. Therefore, the exposure index of rear receptors was not notably increased (see Figure 4.6(c)).

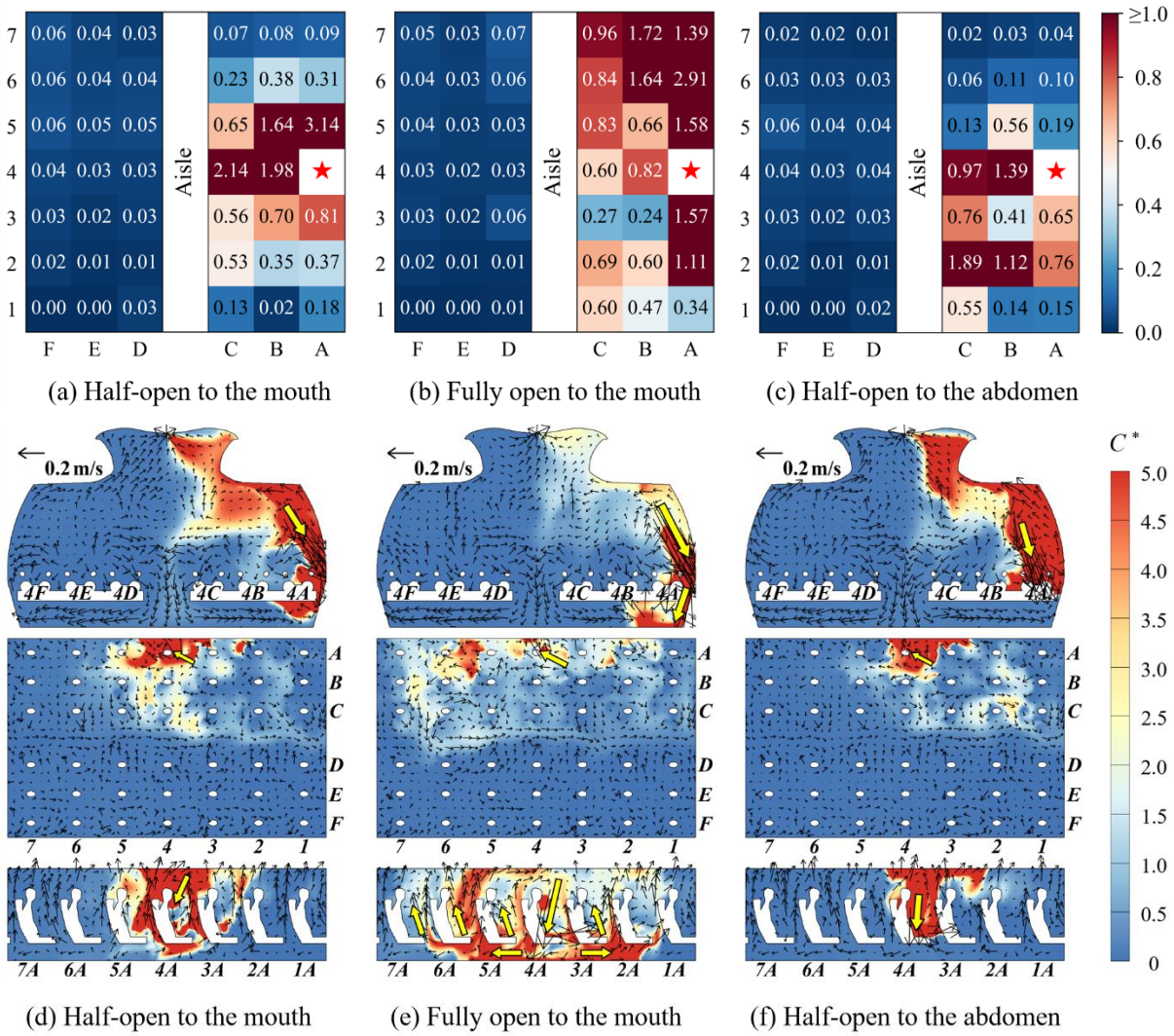

Figure 4.6. (a-c) Exposure index, and (d-f) the airflow patterns and C^* distributions at CS4, HS, and LSA under different gasper settings with source passenger in the window seat 4A.

4.2.2.2 Middle Seat

When the source passenger was in the middle seat 4B, three directions (see Figure 4.1(b)) and two flow rates of the source gasper were considered. The exposure index under different source gasper settings are shown in Figure 4.7(a)-(c). The results indicate that when the source gasper was open, the exposure index of receptors behind the source passenger even on the opposite side of the aisle was increased, while the exposure index of receptors in front of the source passenger was decreased. To explain this phenomenon, we analysed the airflow patterns and C^* distributions at CS4, HS, and the longitudinal section for passengers in column B (LSB), as shown in Figure 4.7(d)-(f). When the source gasper was open, as the gasper-induced flow was towards the aisle, the jet flow entrained the contaminants backwards to the aisle (see Figure

4.5). If the gasper was open at a high flow rate, the gasper-induced flow gained more momentum, and entrained the contaminants further backwards even across the aisle (Figure 4.7 (e)). However, with a lower flow rate, the momentum of gasper-induced flow was insufficient to transport the contaminants across the aisle (see Figure 4.7(d) and (f)). Instead, the contaminants were transported to the aisle, carried by the main flow to the aisle floor, and finally moved to the receptors in the rear rows.

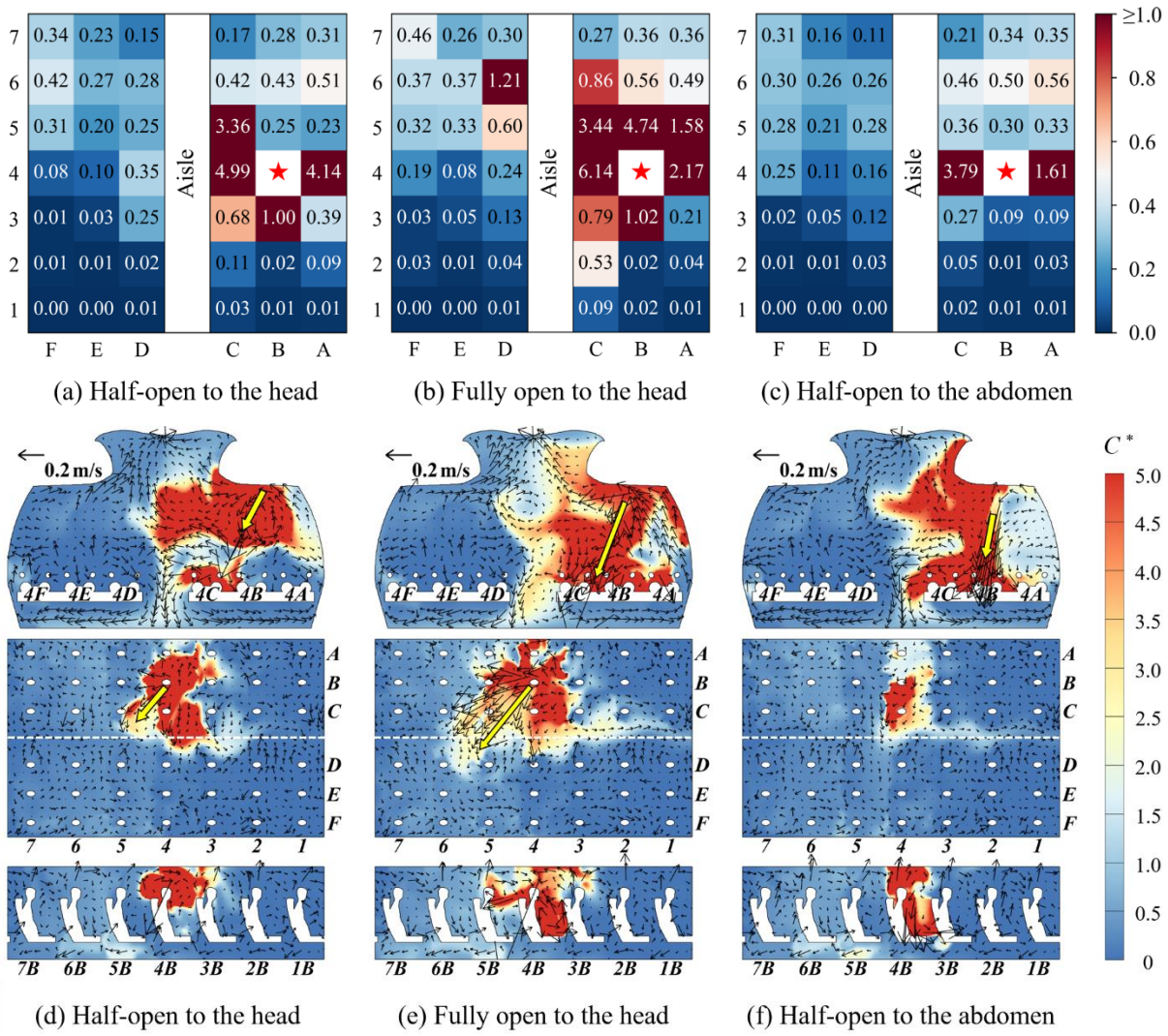

(a) Half-open to the head (b) Fully open to the head (c) Half-open to the abdomen

(d) Half-open to the head (e) Fully open to the head (f) Half-open to the abdomen

Figure 4.7. (a-c) Exposure index, and (d-f) the airflow patterns and C^* distributions at CS4, HS, and LSB under different gasper settings with source passenger in the middle seat 4B.

4.2.2.3 Aisle Seat

When the source passenger was in the aisle seat 4C, three directions (see Figure 4.1(b)) and two flow rates of the source gasper were considered. We compared the exposure index under

different source gasper settings, as shown in Figure 4.8(a)-(c). It can be seen that when the source gasper was half-open to the abdomen, the exposure index of almost all receptors was reduced (see Figure 4.8(b)). As for other source gasper settings, the exposure of receptors behind the source passenger even on the opposite side of the aisle was increased, while the exposure of receptors in front of the source passengers was decreased, which was similar to the situation when the source passenger was in the middle seat with the gasper on.

Next, we analysed the airflow pattern and *C** distribution at CS4, HS, and the longitudinal section for passengers in column C (LSC), as shown in Figure 4.8(d)-(f). The results indicate that the airborne transmission routes varied under different source gasper settings. For example, when the source gasper was half-open to the head, as illustrated in Figure 4.8(d), some of the exhaled contaminants were entrained by the gasper-induced jet flow and directly entered the breathing zone of the receptors on the opposite of the aisle. Meanwhile, the other portion of contaminants were transported downwards to the aisle floor and then entered the breathing zone of the receptors in the rear rows. When the source gasper was fully open to the abdomen, as shown in Figure 4.8(f), the gasper-induced flow entrained a considerable amount of the exhaled contaminants across the aisle to the floor. The contaminants were then transported to the breathing zone of the receptors in the rear rows. However, when the source gasper was half-open to the abdomen, the contaminants were not transported across the aisle due to obstruction by the body of the source passenger. Instead, the contaminants were carried by the main flow and then exhausted directly through the ceiling center, as shown in Figure 4.8(e).

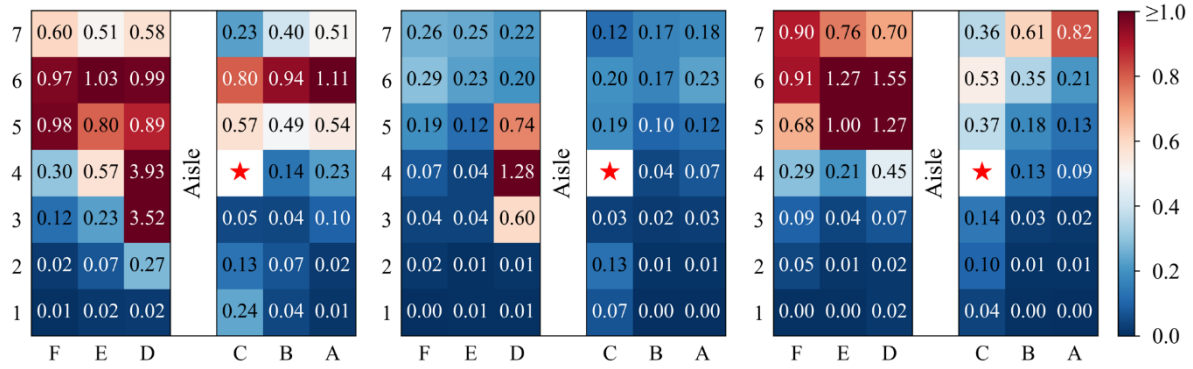

(a) Half-open to the head (b) Half-open to the abdomen (c) Fully open to the abdomen

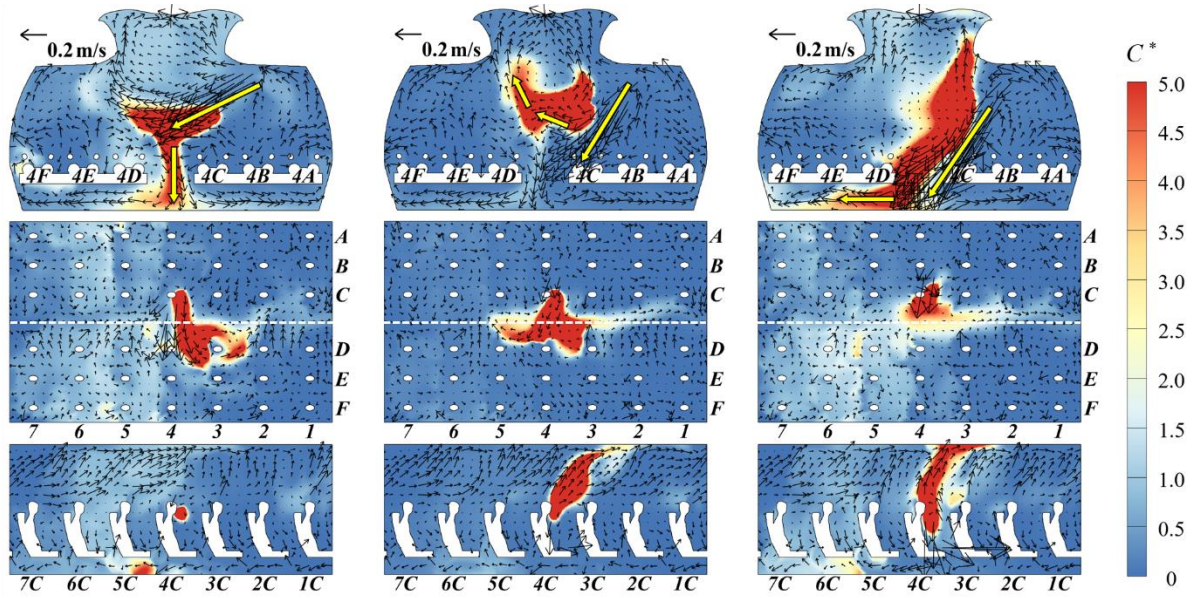

(d) Half-open to the head (e) Half-open to the abdomen (f) Fully open to the abdomen

Figure 4.8. (a-c) Exposure index, and (d-f) the airflow patterns and C^* distributions at CS4, HS, and LSC under different gasper settings with source passenger in the aisle seat 4C.

4.2.3 Assessment of Different Source Gasper Settings

For a quantitative assessment of the performance of different source gasper settings, Table 4.1 displays the mean exposure index of all receptors (ε_{mean}) and the number of receptors with an exposure index above 1 ($No_{\varepsilon>1}$) for different source gasper settings with different source locations. It can be seen that the source passenger's setting could result in either a positive or negative impact on the mean exposure index of all receptors. Taking the source passenger seated at 4C as an example, when the source gasper was half-open to the abdomen, the mean exposure of all receptors was 0.16, which was 45% lower than the benchmark (0.29). In contrast, when the source gasper was half-open to the head, the mean exposure was 0.56, almost twice the benchmark level.

Table 4.1. ε_{mean} and $No_{\varepsilon>1}$ for different gasper settings with different source locations.

Source location	Assessment indicator	Gasper off	Head half-open	Head fully open	Mouth half-open	Mouth fully open	Abdomen half-open	Abdomen fully open
4A	ε_{mean}	0.57	0.32	0.58	0.37	0.50	0.26	0.27
	$No_{\varepsilon>1}$	6	4	10	4	7	3	4
4B	ε_{mean}	0.67	0.51	0.70	0.53	0.54	0.30	0.48

4C	$No_{\varepsilon>1}$	5	3	7	2	3	2	4
	ε_{mean}	0.29	0.56	0.55	0.39	0.48	0.16	0.35
	$No_{\varepsilon>1}$	1	4	10	5	6	1	3

The number of receptors with an exposure index above 1 should also be considered in addition to the mean exposure. Taking the source passenger seated at 4A as an example, when the source gasper was fully open to the mouth, although the mean exposure (0.50) was lower than the benchmark (0.57), the value of $No_{\varepsilon>1}$ (7) was higher than the benchmark (6). Thus, more receptors were exposed to high infection risk when the source gasper was fully open to the mouth.

Among all gasper settings for each source location, keeping the gasper half-open towards the abdomen resulted in the lowest ε_{mean} and $No_{\varepsilon>1}$, and it reduced the $\varepsilon_{mean}$by at least 45%. This is because more contaminants were exhausted directly through the ceiling center, and the contaminant circulation in the cabin was reduced. Therefore, keeping the gasper half-open to the abdomen is recommended for source passengers.

4.3 Impact of Receptor's Gasper

To evaluate the effectiveness of gaspers in protecting receptors, we first identified the most at-risk receptor for each seat location as the target receptors. We then compared the exposure index of a given target receptor under different receptor gasper directions and flow rates to quantify the impact of the receptor's gasper settings. Furthermore, we analysed the airflow pattern and *C** distribution to characterize the working mechanism of the gasper.

4.3.1 Window Seat

According to the exposure index in Section 4.2, the highest exposure index among all receptors in the window seat was 9.29 (see Figure 4.4(d)). This receptor was seated at 4A, with the source passenger in 4B keeping the source gasper off, as shown in Figure 4.9(a). We considered different directions and flow rates of the receptor's gasper, and the calculated exposure index of the receptor 4A is shown in Figure 4.9(b). Turning the receptor's gasper off was used as the benchmark, with an exposure index of 9.29. When the receptor's gasper was directed to the

head or mouth, keeping the gasper fully open performed better, whereas a half-open gasper was worse than the benchmark. For example, when the receptor's gasper was half-open to the head, the receptor's exposure index was 25.40, almost three times the benchmark. In contrast, the exposure index was only 2.74 when the gasper was fully open to the head, 71% lower than the benchmark. Possible reasons are as follows. In the benchmark case, as shown in Figure 4.9(c), the air at source passenger 4B moved leftwards, rightwards, and upwards, resulting in high contaminant concentration at 4A, 4C, and ceiling level. When the receptor's gasper was open, the jet flow from the ceiling entrained the contaminants into the receptor's breathing zone, as shown in Figure 4.9(d), resulting in higher contaminant concentration compared with the benchmark. With a high flow rate, the entrained contaminants were quickly carried away to the sidewall and the back row, as shown in Figure 4.9(e).

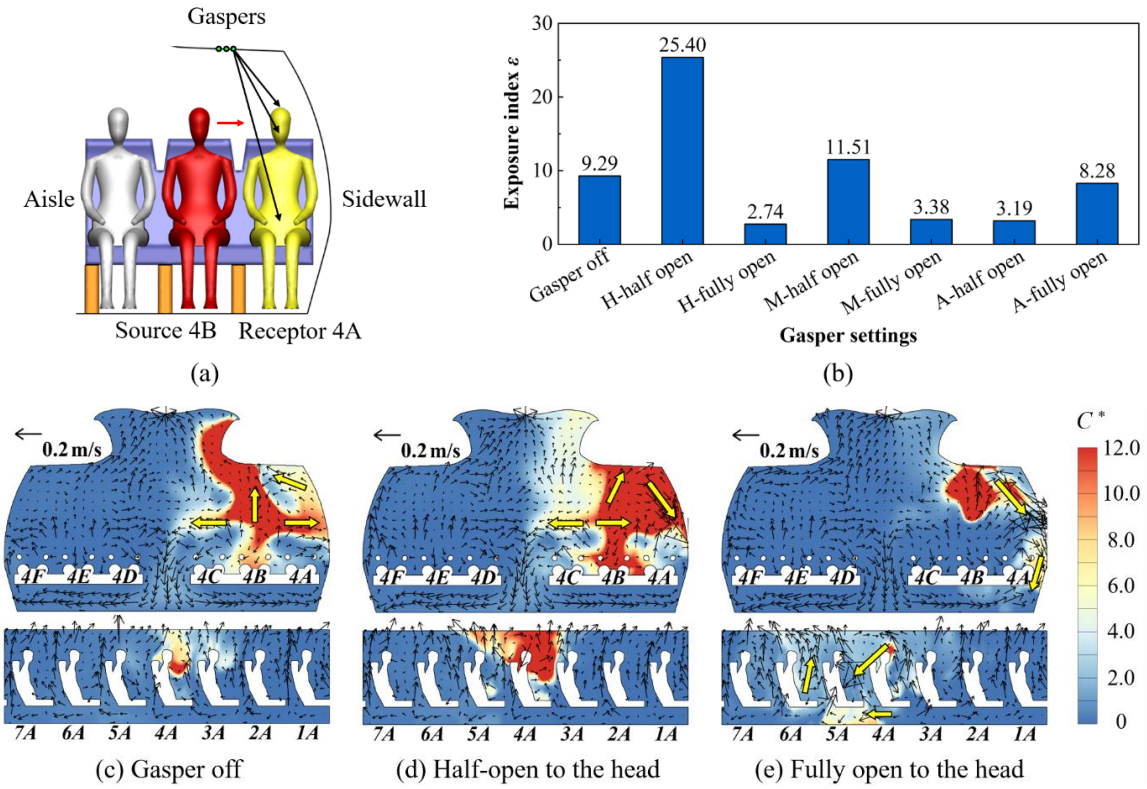

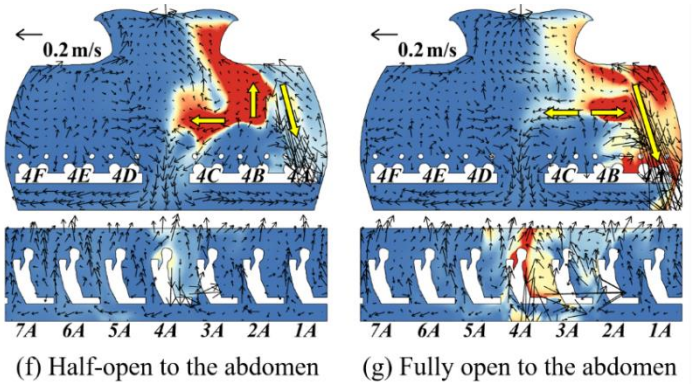

(f) Half-open to the abdomen (g) Fully open to the abdomen

Figure 4.9. (a) The relative positions of the source passenger and the receptor, (b) exposure index of the receptor 4A, and (c-g) airflow patterns and C^* distribution at CS4 and LSA under different receptor gasper settings.

Additionally, when the receptor's gasper was directed to the abdomen, opening the gasper with a medium flow rate performed much better than the benchmark. As shown in Figure 4.9(a), the gasper jet when directed to the abdomen was positioned between the source passenger and the receptor. When the gasper was half-open as in Figure 4.9(f), the gasper jet formed a virtual barrier between the source passenger and the receptor and thus reduced the contaminant concentration in the receptor's breathing zone [99]. However, with a high flow rate, as shown in Figure 4.9(g), the gasper jet from the ceiling entrained the contaminants at ceiling level, resulting in a higher contaminant concentration in the receptor's breathing zone compared with the low flow rate scenario.

4.3.2 Middle Seat

Among all receptors in the middle seats, the highest exposure index was 4.74 (see Figure 4.7(b)). This most at-risk receptor was seated at 5B, with the source passenger in 4B keeping the source gasper fully open to the head, as shown in Figure 4.10(a). The exposure index of the receptor 5B under different gasper settings is shown in Figure 4.10(b). The results indicate that opening the receptor's gasper performed better than the benchmark. The exposure index of the receptor 5B with the gasper turned on ranged from 2.19 to 3.93, all lower than the benchmark. In the benchmark case, the contaminants were transported backwards at breathing level from the source passenger to the receptor, as indicated by the yellow arrow in Figure 4.10(c), and the contaminant concentration at ceiling level above 5B was low. When the receptor's gasper was open, the jet flow from the ceiling entrained the clean air into the receptor's breathing zone,

as shown in Figure 4.10(d) and (e), resulting in a lower contaminant concentration compared with the benchmark.

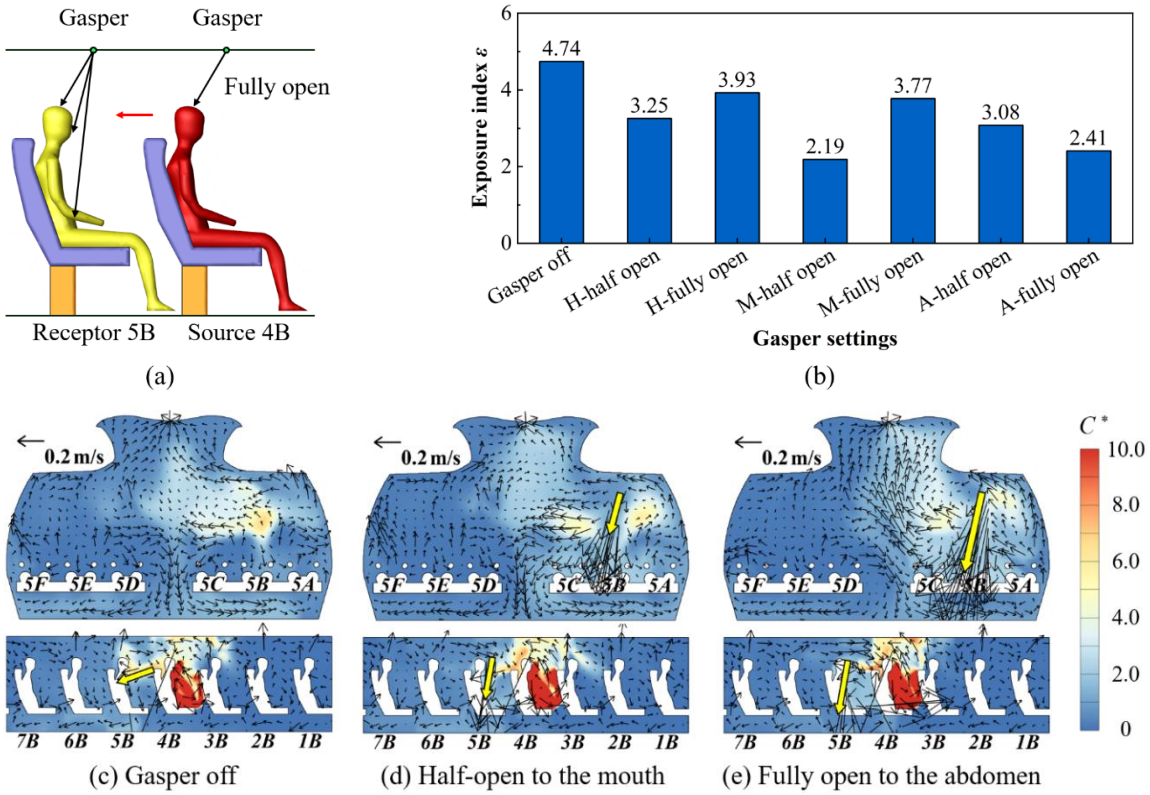

Figure 4.10. (a) The relative positions of the source passenger and the receptor, (b) exposure index of the receptor 5B, and (c-e) airflow patterns and C^* distribution at CS5 and LSB under different receptor gasper settings.

4.3.3 Aisle Seat

Among all receptors in the aisle seats, the highest exposure index was 7.98 (see Figure. A. 3(c)). This most at-risk receptor was seated at 4C, with the source passenger in 4B keeping the source gasper fully open to the abdomen, as shown in Figure 4.11(a). The exposure index of the receptor 4C under different gasper settings is shown in Figure 4.11(b). Turning the receptor's gasper off was used as the benchmark, with an exposure index of 7.98. The results showed that opening the receptor's gasper performed better than the benchmark. Possible reasons are as follows. When the receptor's gasper was turned off, the contaminants was transported to the receptor at thigh level by the jet flow of the source's gasper, and then carried by the thermal plume upwards into the receptor's breathing zone, as indicated by the yellow arrow in Figure 4.11(c). If the receptor's gasper was open, the downward gasper jet altered the air flow pattern in front of 4C. For instance, the airflow in front of 4C was downward when the gasper was

half-open to the mouth as shown in Figure 4.11(d). Thus, the jet flow could effectively decrease the contaminant concentration in the receptor's breathing zone, and a stronger gasper jet performed better (see Figure 4.11(e)).

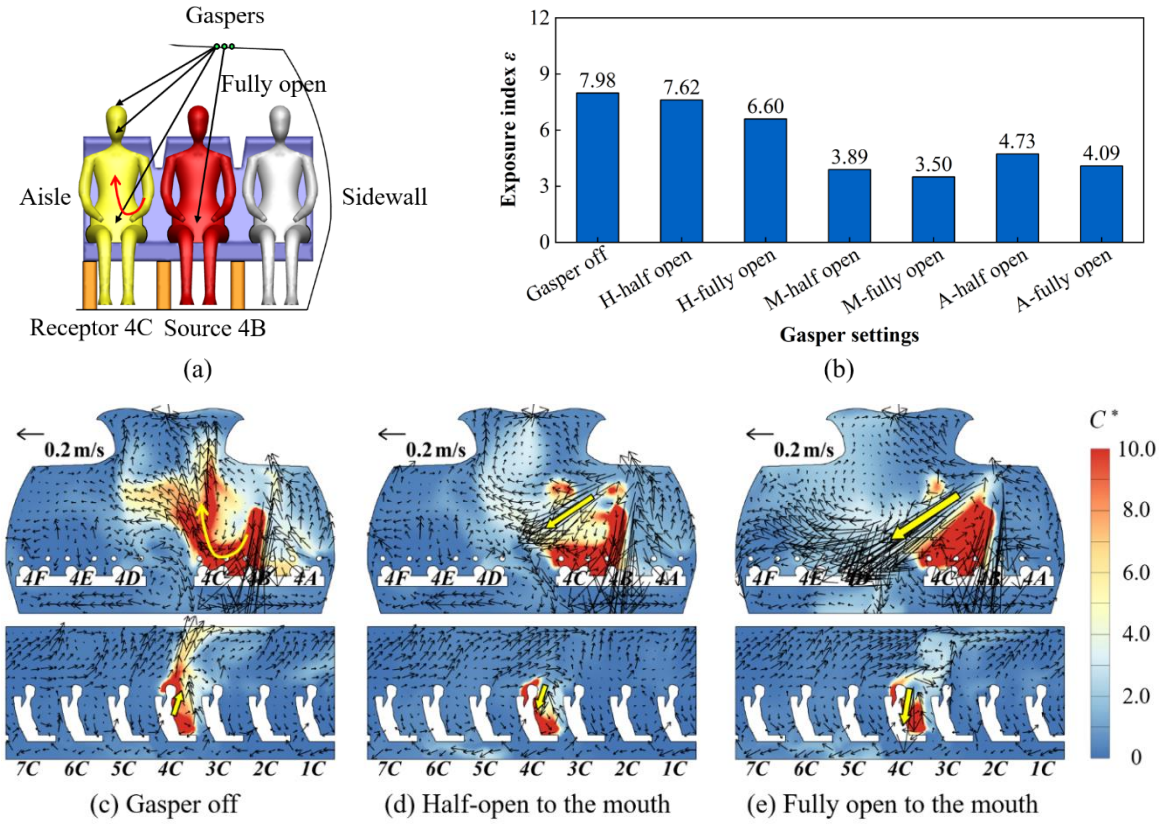

Figure 4.11. (a) The relative positions of the source passenger and the receptor, (b) exposure index of the receptor 4C, and (c-e) airflow patterns and C^* distribution at CS4 and LSC under different receptor gasper settings.

4.3.4 Protective Effect and Working Mechanism

As illustrated in previous sections, the impact of the gasper on the three most at-risk receptors varied with different gaper settings. As summarized in Table 4.2, the mean exposure index was also calculated to evaluate the overall impact of turning on the receptor's gasper. When the receptor's gasper was turned on, the overall mean exposure index of three target receptors was 5.75, 21.7% lower than the benchmark (7.34). Therefore, turning on a receptor's gasper with an appropriate setting could be an effective strategy to protect the receptor.

Table 4.2. Exposure index of the target receptor for different receptor's gasper settings.

Receptor	Gasper off	Gasper on					
		Head half-open	Head fully open	Mouth half-open	Mouth fully open	Abdomen half-open	Abdomen fully open
4A	9.29	25.40	2.74	11.51	3.38	3.19	8.28
5B	4.74	3.25	3.93	2.19	3.77	3.08	2.41
4C	7.98	7.62	6.60	3.89	3.50	4.73	4.09
Overall Mean	7.34	5.75					

Based on the analysis of the impact of the gasper on the three most at-risk receptors, the working mechanism of a receptor's gasper can be described as follows:

- The gasper-induced jet flow entrained the surrounding air to the jet region, leading to either a positive or negative impact on the receptor's exposure. Since the gaspers were mounted on the ceiling, if the contaminant concentration at ceiling level was low, the gasper flow entrained clean air to the lower part of the cabin and thus reduced the concentration in the receptor's breathing zone. If the concentration at ceiling level was high, directing the gasper with a low flow rate to the mouth or head resulted in a high contaminant concentration in the receptor's breathing zone.

- With a suitable gasper direction and flow rate, the gasper jet formed a virtual barrier between the source passenger and the receptor. This mechanism reduced the contaminant transmission to the receptor's breathing zone.

- When the contaminants were transported upwards to the receptor's breathing zone, turning on the receptor's gasper reduced the contaminant concentration, since the downward gasper jet altered the airflow pattern in front of the receptor.

4.4 Discussion

To evaluate whether the selected cases in Section 4.3 were representative, we analysed the transmission route of the contaminants for each receptor from the calculations in Section 4.2 (see Figure. A. 10Figure. A. 11Figure. A. 12Figure. A. 13). For the first typical scenario, the contaminants entered the receptor's breathing zone either from ceiling level or horizontally at

breathing level. We designated this scenario as the ceiling/breathing (C/B) scenario. For the other typical scenario, the contaminants were transported upwards to the receptor's breathing zone from floor level or from thigh level due to the thermal plume before entering the receptor's breathing zone. This scenario was designated as the floor/thigh (F/T) scenario. The calculated probability of each scenario and the exposure range of receptors for each seat type are shown in Figure 4.12. When the gasper of the source passenger was off, as depicted in Figure 4.12(a), the C/B scenario had a higher probability of occurrence. Moreover, as shown in Figure 4.12(b), receptors under the C/B scenario had higher mean and peak exposure values. Therefore, the C/B scenario was the most common and dangerous scenario when the source gasper was turned off. For the receptor in the window seat in Section 4.3.1, the source gasper was off and the contaminants were transported at breathing level into the receptor's breathing zone. Thus, it was a representative case. When the source gasper was open, as depicted in Figure 4.12(c) and (d), the C/B scenario also had a higher probability of occurrence, but with a lower mean exposure index compared with the F/T scenario. Therefore, both the C/B and F/T scenarios were typical. For the receptor in the middle seat in Section 4.3.2 and the receptor in the aisle seat in Section 4.3.3, the source gasper was open and the contaminants were transported from breathing level and thigh level, respectively. Therefore, all three of the selected cases in Section 4.3 represent typical scenarios.

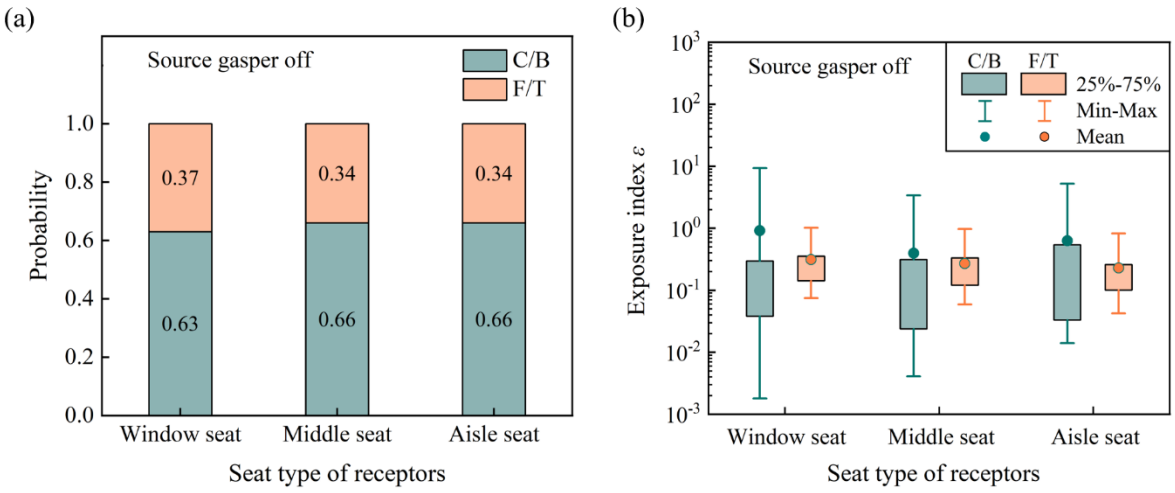

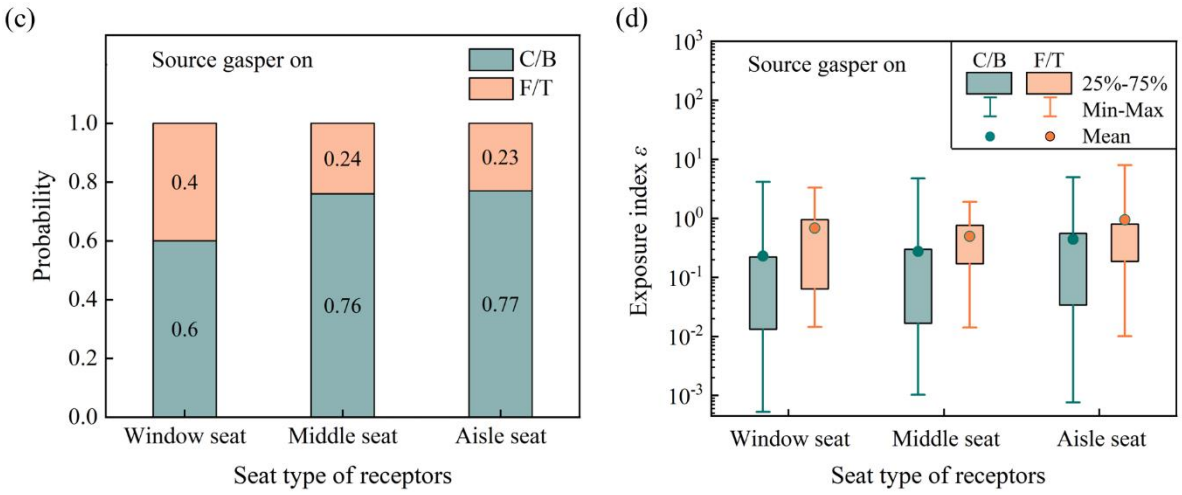

Figure 4.12. When the source gasper was turned off, (a) the probability and (b) exposure of receptors for different scenarios and receptor seat types; and when the source gasper was turned on, (c) the probability and (d) exposure of receptors for different scenarios and receptor seat types.

Figure 4.13 shows the airflow pattern at the window seat in longitudinal section LSA. In the middle section, the airflow under the seat was backward, while it was forward in the front and rear sections. This is because of the cabin's partitions at the front and the back of the cabin. The difference in airflow structure would further affect the contaminant transmission. In this study we only investigated the seven rows in the middle of the cabin. For the front or rear section of the cabin, the results and conclusions may be different. Further studies are needed to examine the effects of longitudinal flow and extend our findings to the whole cabin.

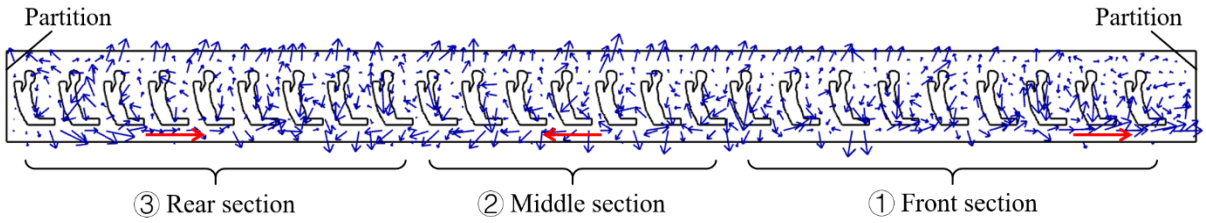

Figure 4.13. The airflow pattern at LSA in a 25-row, single-aisle, fully occupied, economy-class aircraft cabin.

This study only considered three most at-risk receptors, and the gaspers of other passengers were assumed to be closed. Note that each passenger may choose whether to turn on his/her gasper. Other possible gasper on/off distributions were not addressed in this study, and current results were not sufficient to provide recommendations for gasper settings. Moreover, as mixing ventilation is prevalently used in commercial airliners, it is worthwhile to compare the

performance of gaspers in different ventilation systems. Therefore, follow-up studies are needed for practical applications in the future.

4.5 Summary

This study aimed to investigate the impact of source and receptor gaspers on airborne disease transmission in an aircraft cabin with a personalized displacement ventilation system. We conducted numerical studies in a seven-row section of a single-aisle, fully occupied, economy-class aircraft cabin with the CFD simulation method. We first investigated the impact of source gasper direction and flow rate on the airborne transmission near the source. Next, we investigated the protective effect of the receptor's gasper. Within the scope of this study, the following conclusions can be made:

- For a source passenger's gasper, the direction and flow rate of the gasper flow either increased or decreased the air contaminant transmission to other passengers. Directing the source gasper to the abdomen with a medium flow rate significantly mitigated the overall exposure, as this approach minimized the contaminant circulation in the aircraft cabin. This setting was recommended for the source passenger, and could reduce the mean exposure index by at least 45% compared to the benchmark.

- For a receptor's gasper, turning on the gasper with an appropriate setting could be an effective strategy to protect the receptor. The working mechanism of a receptor's gasper can be summarized as follows:

  (1) The gasper-induced jet flow entrained the surrounding air into the jet region, leading to either a positive or negative impact on the receptor's exposure. The protective effect depended on the contaminant concentration at ceiling level.

  (2) With a suitable gasper direction and flow rate, the gasper jet formed a virtual barrier between the source passenger and the receptor. This mechanism reduced the contaminant transmission to the receptor's breathing zone.

  (3) When the contaminants were transported upwards to the receptor's breathing zone,

turning on the receptor's gasper reduced the contaminant concentration, since the downward gasper jet altered the airflow pattern in front of the receptor.

CHAPTER 5 A PRACTICAL CONCURRENT GASPER-OPERATION STRATEGY FOR CONTROLLING AIRBORNE DISEASE TRANSMISSION

This chapter first proposed a seat-type-dependent operation strategy for gaspers based on the working mechanism of a single gasper in our previous study. To evaluate the performance of the proposed gasper operation strategy in controlling contaminant transmission, we innovatively used random gasper operation under realistic conditions as the benchmark. Random gasper operation means that each passenger can adjust his/her gasper according to preference without external control. The proposed operation strategy and the random gasper operation were then applied to a seven-row section of a single-aisle, fully occupied, economy-class aircraft cabin with a personalized displacement ventilation system for numerical investigation. Three possible locations of the source passenger, namely, the window seat, middle seat, and aisle seat, were considered. The contaminant transport and exposure risk for passengers under the proposed gasper operation strategy were compared with the results under random gasper operation to evaluate the effectiveness of the proposed strategy.

5.1 Case Setup

Numerical investigations were conducted in a seven-row, single-aisle, fully occupied, economy-class aircraft cabin with a personalized displacement ventilation system, as shown in Figure 5.1(a). In this system, clean air was supplied through individual diffusers under the seats and through gaspers above the passengers. The temperature of the supply air was set as 19.3 ℃ [21]. The total flow rate was 320.46 L/s [24], corresponding to an air change rate of 39.7 ACH. Note that for different gasper operation strategies, the total flow rate for the aircraft cabin was kept constant at 320.46 L/s. The breathing flow rate arising from continual exhalation and inhalation was not considered in this study, as its influence on passenger exposure to gaseous contaminants is generally minor [100]. This assumption has also been adopted in relevant studies focusing on the impact of ventilation systems on the air quality in aircrafts cabin [17, 24]. The cabin air was exhausted through two slots at the ceiling centre. The surface temperatures of the floor, sidewalls, ceiling, and passengers were set as 23.8 ℃, 24.5 ℃, 25.0 ℃, and 31.0 ℃, respectively [21]. Further details of the boundary conditions can be found

in the reference [54].

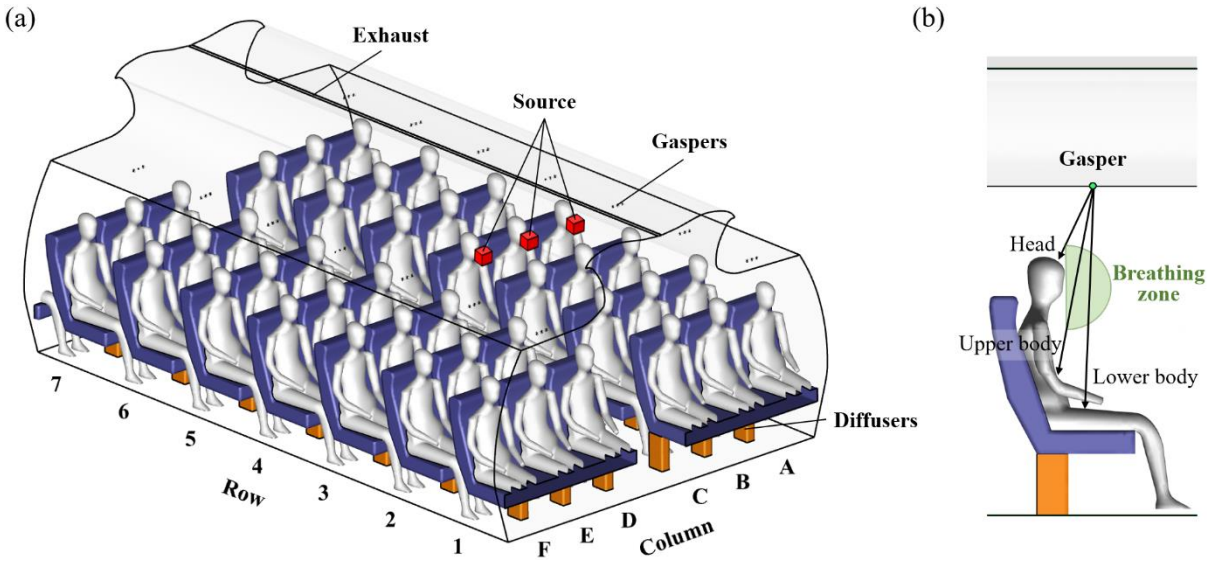

Figure 5.1. (a) Schematic of a seven-row section of a single-aisle, fully occupied, economy-class aircraft cabin and (b) side view of gasper directions and the breathing zone.

Three source locations were considered according to symmetry: the source passenger seated at 4A (window seat), at 4B (middle seat), and at 4C (aisle seat). Contaminants were released continuously with zero momentum from a cube with a side length of 100 mm in front of the mouth of the source passenger [21, 54, 101], shown as the red cube in Figure 5.1(a). We used an exposure index [94] to quantify the exposure risk; this index has been widely adopted in previous studies [24, 54, 95-97]. The exposure index ε was defined as the ratio of the contaminant concentration in a passenger's breathing zone to that in the return air [94]. The breathing zone was defined as a hemisphere with a radius of 20 cm in front of the mouth [98], as shown in Figure 5.1(b).

The total number of cells in the grid for this seven-row section of an aircraft cabin was 8.36 million, which was proved in our previous study [54] to be adequate to capture the complex airflow patterns in a cabin with gaspers open. For the detailed grid size and distribution, please refer to our previous study [54].

To identify an operation strategy that was executable by passengers, we first proposed a seat-type-dependent strategy for gaspers based on the findings in our previous study [54]. We found that opening the gasper to an appropriate setting effectively protected the passenger, and the

appropriate gasper setting depended on the transmission route of contaminants to the passenger's breathing zone [54]. Therefore, a representative transmission route was first identified for each seat type. Next, the appropriate gasper setting was determined. Accordingly, a seat-type-dependent operation strategy for the gaspers was proposed. To evaluate the performance of the proposed gasper operation strategy in controlling contaminant transmission, random gasper operation under realistic conditions was used as the benchmark. Random operation means that each passenger can adjust his/her gasper based on preference without external control. The random gasper operation and proposed gasper operation are described in Sections 5.1.1 and 5.1.2, respectively.

5.1.1 Random Gasper Operation

Random gasper operation represents the real situation in which each passenger can adjust both the flow rate and direction of his/her gasper based on preference without external control. According to a field survey on gasper usage behaviour in aircraft cabins conducted by Fang et al. [55], in summer, most passengers chose to open the gasper, with 42.4% partially open and 28.2% fully open, while only 29.4% of passengers kept their gaspers closed. As for gasper direction, passengers preferred to direct the gaspers towards their upper body (52.4%), followed by the lower body (39.0%), and finally the head (8.6%). Thus, there are billions of possible gasper setting distributions throughout the cabin. Obviously, calculating all possible scenarios would be unrealistic. Instead, the quasi-random sampling method [102] was used to determine representative gasper setting distributions, in light of the method's low discrepancy and high efficiency compared with the random sampling method. First, gaspers for passengers in seats 1A to 7F were numbered from 1 to 42. Next, 42 points in the $(0, 1)^2$ region were quasi-randomly selected from the Halton sequence using MATLAB, as shown in Figure 5.2. The horizontal axis represented the flow rate through the gasper, while the vertical axis represented the direction of the gasper. Note that a partially open gasper was assumed to be half-open, with a flow rate of 0.66 L/s [31]. Each point corresponded to a specific gasper setting by the passenger in this seat. This process constituted a single iteration of quasi-random sampling.

To define the representative gasper setting distribution cases with an acceptable tolerance of error, we needed to determine how many iterations of the quasi-random sampling process were sufficient. In this study, we calculated the mean absolute error (MAE) of the probability of each gasper setting for each passenger under different numbers of iterations by:

$$MAE = \frac{\sum_{i=1}^{n} |p_i - \bar{p}|}{n} \tag{5.1}$$

where n is the total number of passengers, p_i is the probability of a specific gasper setting for a passenger under a given number of iterations, and $\bar{p}$ is the actual probability of the specific gasper setting according to Fang et al. [55]. Taking the gasper setting "closed" as an example, $\bar{p}$ is 0.294. In this study, the tolerance of error was set as 5%. Therefore, when the calculated MAE for each gasper setting was below 5%, the generated scenarios represented typical random gasper setting distributions. Under this criterion, the number of representative scenarios was 15. The gasper setting distribution for each scenario is shown in detail in Figure 5.2. Since there were three source locations, the total number of cases was 45 for the random gasper operation condition.

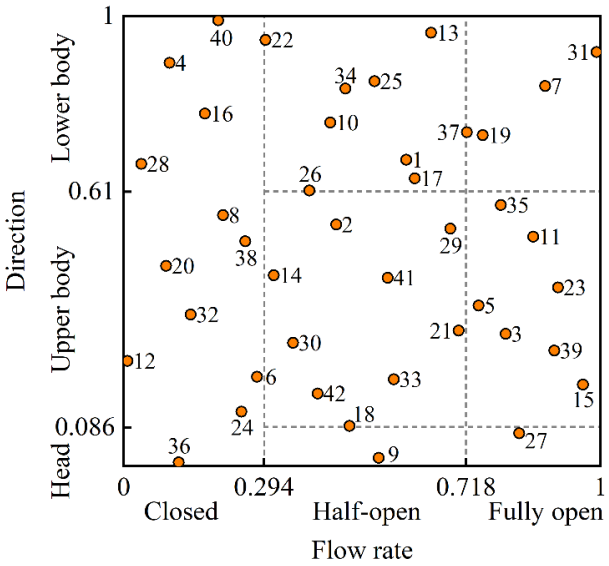

Figure 5.2. The random gasper setting distribution generated for a single iteration of quasi-random sampling.

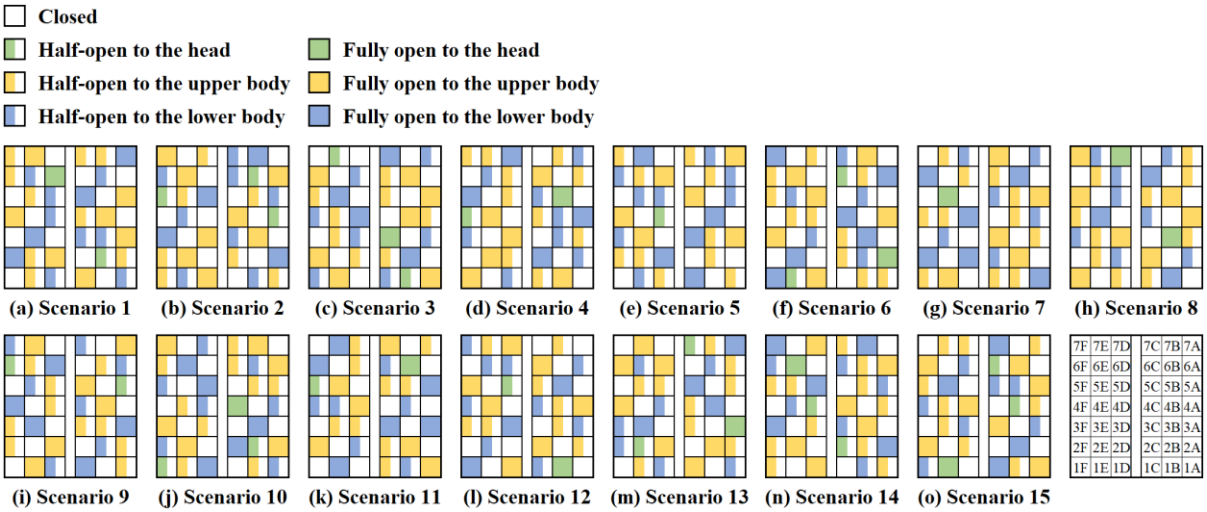

Figure 5.3. Representative gasper setting distributions for random gasper operation determined using the quasi-random sampling method.

5.1.2 Proposed Gasper Operation Considering Two Utilization Scenarios

The proposed gasper operation strategy was determined as described in our previous study [54]. We found that the appropriate gasper setting depended on the transmission route of the contaminants. Specifically, when the contaminants entered the passengers' breathing zone from floor level or thigh level, opening the gasper at a high flow rate was more effective in controlling contaminant transmission. In comparison, when the contaminants entered the passengers' breathing zone from ceiling level or breathing level, directing the gasper towards the abdomen with a medium flow rate was more effective. Therefore, we first identified the representative transmission route for passengers under each seat type. The results showed that for passengers in the window seat, contaminants tended to move upwards into the breathing zone from floor or thigh level, with a probability of 64.7%. Meanwhile, nearly 70% of passengers in the middle or aisle seat were exposed to high concentrations of contaminants that flowed from ceiling or breathing level. Based on the findings in our previous study and the results of the transmission route analysis, the following seat-dependent gasper operation strategy was proposed: for passengers in the window seat, the gasper setting was fully open towards the upper body, and for passengers in the middle or aisle seat, the gasper setting was half-open towards the upper body.

Having proposed the aforementioned gasper operation strategy, we then considered two situations for its practical application. One situation was an ideal scenario in which all

passengers opened their gaspers as instructed. We designated it as the proposed gasper operation with full utilization, and the detailed gasper setting distribution is shown in Figure 5.4(a). The other scenario was one in which passengers opened their gaspers as instructed but based on their needs. In other words, only those who preferred to open their gaspers followed the proposed operation, while other passengers kept their gaspers closed. According to field surveys [55], gasper utilization is typically 67%. With this typical utilization, 28 out of 42 gaspers are opened, and there are still billions of possible gasper open/closed distributions. The quasi-random sampling method was used to determine 9 representative gasper setting distributions under the proposed gasper operation with typical utilization, as shown in Figure 5.4(b). Since there were three source locations, the total number of cases was 30 for the proposed gasper operation.

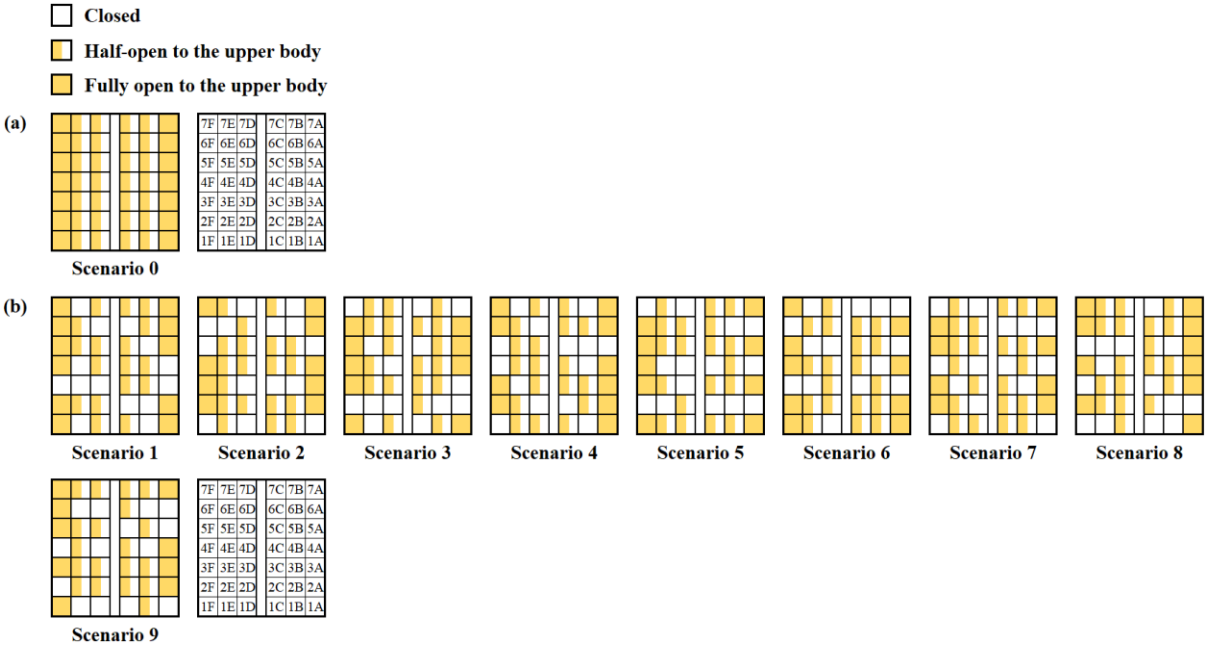

Figure 5.4. Representative gasper setting distributions for the proposed gasper operation: (a) full utilization, and (b) typical utilization.

5.2 Comparison of Gasper Operation Strategies

5.2.1 Source Passenger in the Window Seat

Three gasper operation strategies were compared in this study: random operation, the proposed operation with full utilization, and the proposed operation with typical utilization. Random operation means that there is no external control, which represents the real situation. The

proposed operation with full utilization means that all passengers opened their gaspers in accordance with the proposed operation pattern, and the proposed operation with typical utilization means that passengers opened their gaspers in accordance with the proposed pattern based on their needs. Figure 5.5 compares the exposure index for each passenger under the random operation and under the proposed operation with full utilization, when the source passenger was located in window seat 4A. The exposure index for a given passenger would vary with the gasper setting distribution. In other words, there are many exposure index data points for each passenger, corresponding to different gasper setting distribution scenarios. The symbols and the upper and lower bounds of the error bars, represent the mean, maximum, and minimum of the exposure index for each passenger. The shaded area highlights passengers located in front of the source passenger (i.e., rows 1–3 and columns A–C). A similar trend was observed in the comparison between the random operation and the proposed operation with typical utilization, as illustrated in Figure. A. 14 in the Appendix. According to the results, the performance of the proposed gasper operation was dependent on passenger location. Specifically, for passengers in front of the source passenger, i.e., passengers in rows 1-3 and columns A-C as indicated by the shaded area in Figure 5.5, the proposed gasper operation with full utilization resulted in higher mean exposure index values than the random operation. In contrast, for passengers in other seats, the proposed operation with full utilization reduced the mean exposure index by 41.6% compared to the random operation. Under the proposed operation with typical utilization, the reduction was 21.7%.

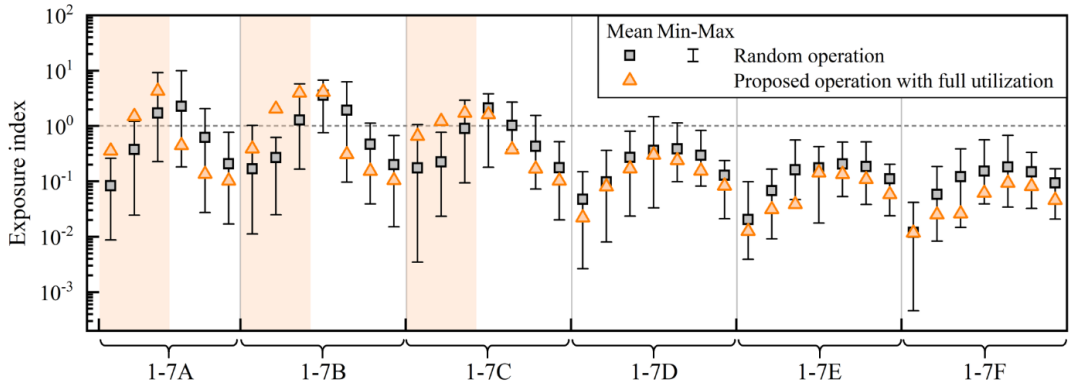

Figure 5.5. Comparison of the exposure index value for each passenger under random operation and the proposed operation with full utilization, with the source passenger located in window seat 4A.

To explain the results, we analysed the airflow patterns and the dimensionless contaminant concentration C^* (normalized by the contaminant concentration in the return air) distributions

in the cross section located 0.05 m in front of the mouth of the source passenger (CS), the horizontal section at breathing level (HS), and the longitudinal section for passengers in column A (LSA). For the sake of conciseness, the results for only some of the scenarios are presented here. The airflow patterns and C^* distributions at CS, HS and LSA under scenario 11 of the random operation and under the proposed operation with full utilization are shown in Figure 5.6(a) and (b), respectively. It can be seen that the airflow above the source passenger was in the forward direction (see the yellow arrows in Figure 5.6), resulting in high contaminant concentration at ceiling level. When the passengers in front of the source passenger all opened their gaspers in accordance with the proposed strategy, the gasper-induced jet flow entrained the contaminants downward into the passengers' breathing zone, resulting in a higher contaminant concentration at breathing level in rows 1-3 and columns A-C, as shown in the green rectangle in Figure 5.6(b). In contrast, the random operation resulted in a lower contaminant concentration at breathing level in rows 1-3 and columns A-C due to a lower gasper utilization rate, as shown in Figure 5.6(a). For passengers in other seats, the proposed operation with full utilization obviously reduced the contaminant concentration at breathing level compared with the random operation. Possible reasons are as follows. The gasper-induced jet flow entrained clean air into the passenger's breathing zone, formed a virtual barrier between the contaminants and the passenger, or altered the airflow pattern in front of the passenger in accordance with the working mechanism of an individual gasper described in our previous study [54].

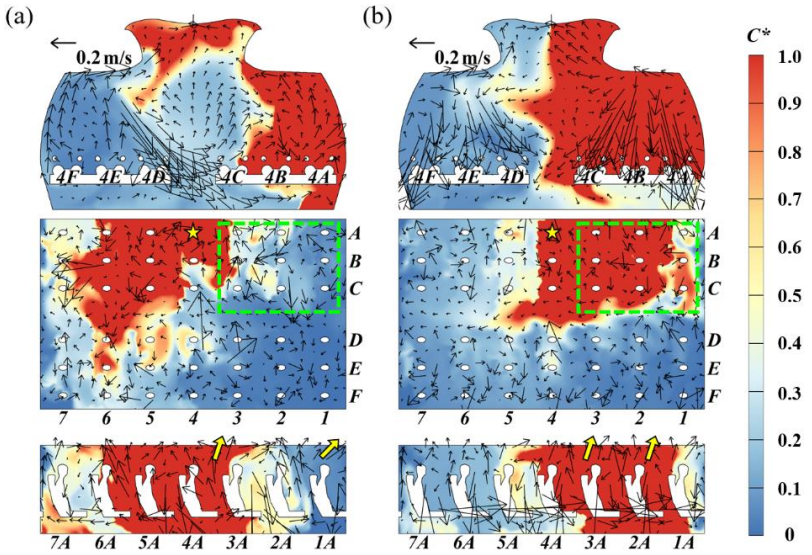

Figure 5.6. The airflow patterns and C^* distributions at CS, HS, and LSA under (a) scenario 11 of the random operation, and (b) the proposed operation with full utilization, with the source passenger located in window seat 4A.

In addition, particular attention should be given to relatively high-risk passengers when evaluating the effectiveness of the proposed operation strategy. Relatively high-risk passengers in this study refer to those with an exposure index $\varepsilon > 1$, which means that the air contaminant concentration in the passenger's breathing zone is higher than the level when the air contaminants are fully mixed throughout the cabin. Namely, this passenger would be exposed to a higher concentration of contaminants than the average. Figure 5.5 showed that under the random operation conditions, relatively high-risk passengers were mainly clustered near the source passenger, specifically occupying rows 3-5 and columns A-C. The proposed operation could not reduce the exposure index for all relatively high-risk passengers, depending on the location of the passenger. For example, for relatively high-risk passenger 3B, the proposed operation with full utilization increased the mean exposure index from 1.29 to 3.95, compared with the random operation. However, for relatively high-risk passenger 5B, the mean exposure index was reduced from 1.93 to 0.31.

5.2.2 Source Passenger in the Middle Seat

Figure 5.7 compares the exposure index for each passenger under the random operation and under the proposed operation with full utilization, when the source passenger was located in middle seat 4B. Definitions of symbols, error bars, and shaded areas in Figure 5.7 are the same as in Figure 5.5. A similar trend was observed in the comparison between the random operation and the proposed operation with typical utilization, as illustrated in Figure. A. 15 in the Appendix. The results led to exactly the same conclusions as the situation with the source passenger in window seat 4A. Specifically, for passengers in front of the source passenger, i.e., in rows 1-3 and columns A-C in the shaded areas, the proposed operation with full utilization resulted in a higher mean exposure index value than the random operation. In contrast, for passengers in other seats, the proposed operation with full utilization reduced the mean exposure index by 25.4% compared to the random operation. Under the proposed operation with typical utilization, the reduction was 5.4%.

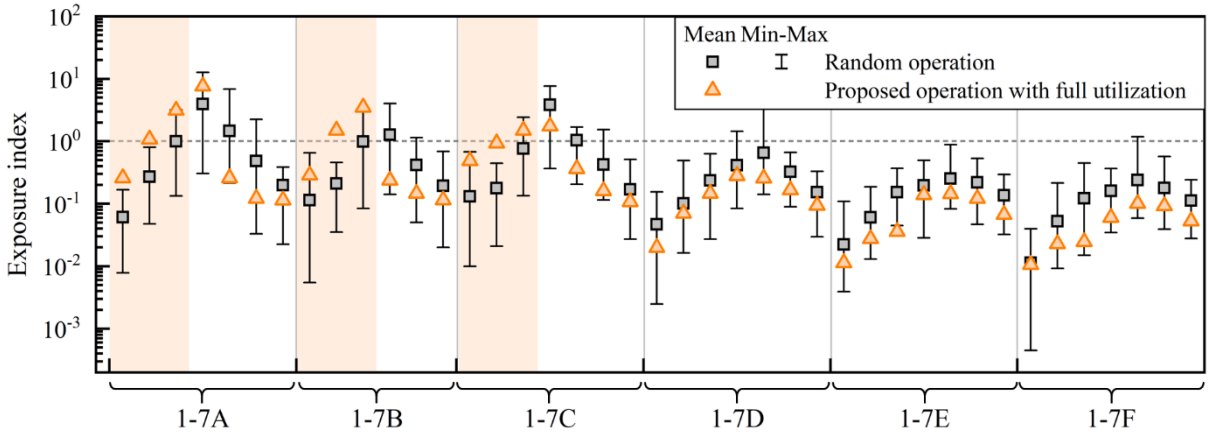

Figure 5.7. Comparison of the exposure index value for each passenger under the random operation and the proposed operation with full utilization, with the source passenger located in middle seat 4B.

Next, we analysed the airflow patterns and C^* distributions at CS, HS, and LSB under scenario 11 of the random operation and then under the proposed operation with full utilization, as shown in Figure 5.8. Similar C^* distributions were observed when the source passenger was in the middle seat and when the source passenger was in the window seat. Specifically, for those passengers located in front of the source and on the same side of the aisle as the source passenger, the contaminant concentration at ceiling level was high. Accordingly, opening the gaspers would have a negative impact, because the gasper-induced flow from the ceiling was found to entrain the contaminants into the passengers' breathing zone, as indicated by the green rectangle in Figure 5.8(b). Meanwhile, for passengers in other seats, the contaminant concentration at ceiling level was low. The impact of opening the gaspers in accordance with the proposed operation strategy was positive, as the jet flow reduced the contaminant concentration in the passengers' breathing zone by entraining the clean air, forming a virtual barrier between the source and the passengers or altering the airflow pattern in front of the passengers according to our previous study [54].

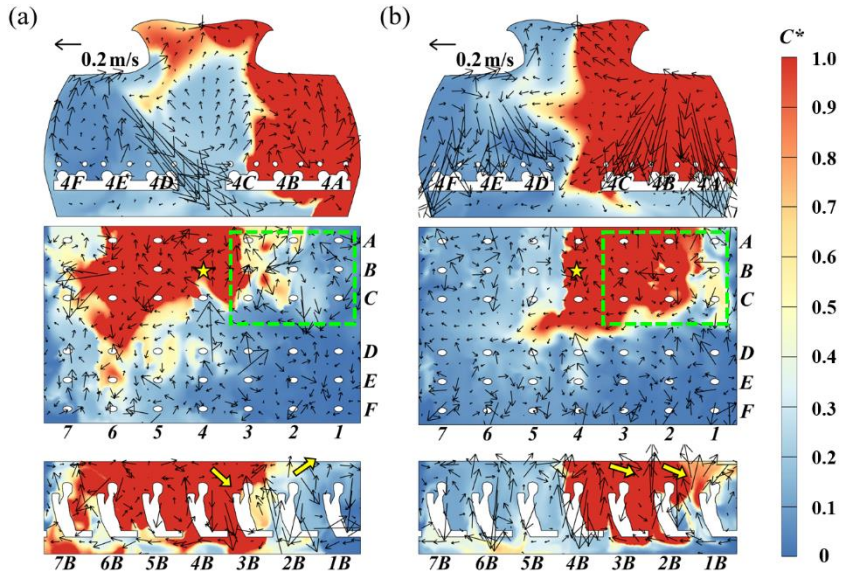

Figure 5.8. The airflow patterns and C^* distributions at CS, HS, and LSB under (a) scenario 11 of the random operation, and (b) the proposed operation with full utilization, with the source passenger located in middle seat 4B.

Additionally, under the random operation conditions, relatively high-risk passengers were mainly clustered near the source passenger, i.e., in rows 3-5 and columns A-C. Thus, the proposed operation was location-dependent, and it was not effective in reducing the exposure index value for all relatively high-risk passengers. For example, for relatively high-risk passenger 3A, the proposed operation with full utilization increased the mean exposure index value to 3.14, as compared to 1.00 with the random operation. Meanwhile, for relatively high-risk passenger 5A, the mean exposure index value was reduced to 0.26 from a value of 1.47 under the random operation.

5.2.3 Source Passenger in the Aisle Seat

Figure 5.9 compares the exposure index value for each passenger under the random operation and the proposed operation with full utilization, with the source passenger located in aisle seat 4C. The symbols and the upper and lower bounds of the error bars, represent the mean, maximum, and minimum of the exposure index for each passenger. A similar trend was observed in the comparison between the random operation and the proposed operation with typical utilization, as illustrated in Figure. A. 16 in the Appendix. When the source passenger was in aisle seat 4C, the results were quite complicated, and there was no significant difference between the proposed operation and random operation. Moreover, when the proposed operation

with full utilization was in effect, the number of passengers with reduced mean exposure index value was 21, comparable to 20 passengers with increased mean exposure index value. The results may be attributed to the fact that when the source passenger was in the aisle seat, the contaminant transmission route became substantially more complex due to the dominant influence of surrounding gaspers. Consequently, the proposed operation strategy exhibited limited effectiveness in reducing the exposure risk. Taking the real situation with random operation as an example, we analysed the airflow patterns and C^* distributions at CS, HS, and LSC under scenario 3 and scenario 5 of the random operation strategy, successively, as shown in Figure 5.10. For scenario 3, most of the contaminants exhaled by source passenger 4C were directly removed by the exhausts, as shown in CS in Figure 5.10(a). Meanwhile, a small amount of contaminant was transported to the aisle by the gasper of passenger 3C and then discharged at the centre of the ceiling, as shown in HS in Figure 5.10(a). For scenario 5, the contaminant exhaled by source passenger 4C was entrained by the downward gasper jets of passengers 3C, 4B, and 5C to the lower part of the cabin (see CS and LSC in Figure 5.10(b)), resulting in a high contaminant concentration at breathing level near the source, as shown in HS in Figure 5.10.

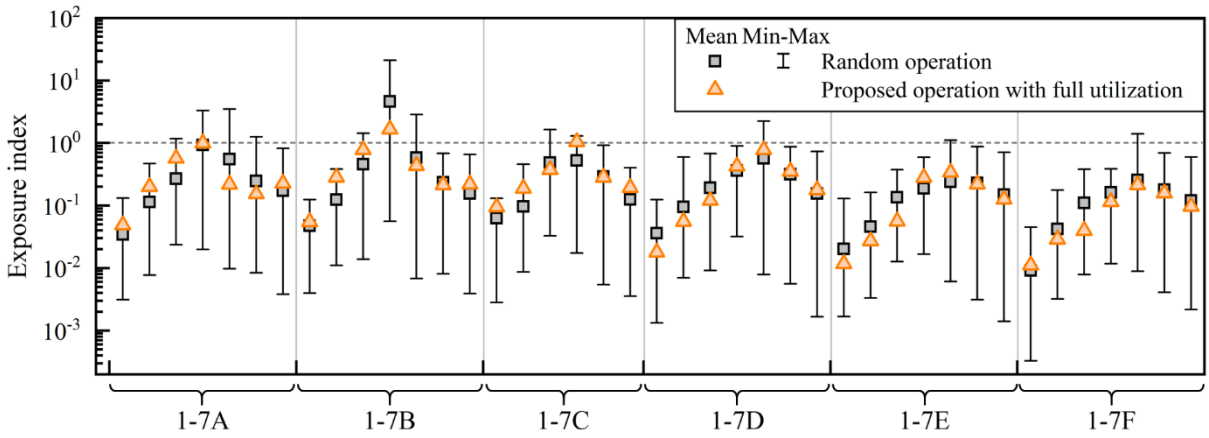

Figure 5.9. Comparison of passengers' exposure index values under random operation and the proposed operation with full utilization, with the source passenger located in aisle seat 4C.

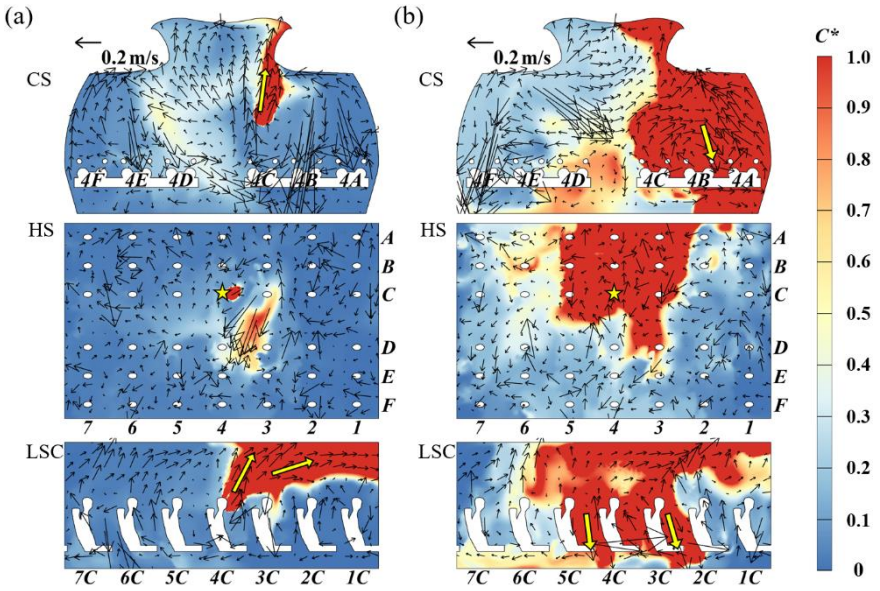

Figure 5.10. The airflow patterns and C^* distributions at CS, HS, and LSC under (a) scenario 3 of the random operation, and (b) scenario 5 of the random operation when the source passenger was in aisle seat 4C.

Additionally, the random operation resulted in only 1 relatively high-risk passenger, and the proposed operation in only 2 such passengers, significantly fewer than the minimum of 6 observed when the source passenger was in the window or middle seat. This finding indicated that the contaminant was more effectively removed from the cabin when the source passenger was in the aisle seat than when the source location was in the window or middle seat.

5.2.4 Impact of Source Passenger's Gasper Setting

Note that the proposed seat-type-dependent gasper operation in this study does not distinguish between the source passenger and receptors to improve executability. Namely, the source passenger and receptors follow the same gasper setting if the seat type is identical. However, the working mechanism of source passenger's gasper and receptor passengers' gasper are different as described in our previous study [54]. Therefore, the effectiveness of the proposed strategy for the source passenger in controlling the contaminant transmission remain uncertain. In light of this, we further investigated the impact of the source gasper setting on the exposure index for passengers under the proposed gasper operation strategy. According to the gasper setting distributions under the proposed operation strategy in Figure 5.4, we categorized all scenarios based on the source gasper setting for each source location, as shown in Table 5.1. One setting was that the source gasper was closed, and the other was that the source gasper was

open in accordance with the proposed strategy.

Table 5.1. Source gasper settings for all scenarios under the proposed operation strategy for each source location.

	Source in window seat 4A	Source in middle seat 4B	Source in aisle seat 4C
Source gasper closed	Scenarios 1, 5, 7	Scenarios 4, 6, 9	Scenarios 5, 7
Source gasper open in accordance with proposed strategy	Scenarios 0, 2, 3, 4, 6, 8, 9	Scenarios 0, 1, 2, 3, 5, 7, 8	Scenarios 0, 1, 2, 3, 4, 6, 8, 9

Next, we calculated the mean, maximum, and minimum of the mean exposure index values for all passengers (ε_{mean}) and the number of relatively high-risk passengers ($No_{\varepsilon>1}$) for each category. Figure 5.11(a) and (b) show ε_{mean} and $No_{\varepsilon>1}$ under the two source gasper settings for each source location. According to the results, when the source passenger was in the middle or aisle seat, opening the source gasper in accordance with the proposed strategy led to lower ε_{mean} and $No_{\varepsilon>1}$ than when the source gasper was closed. This is consistent with our previous findings, as the proposed gasper operation for the passenger in the middle or aisle seat was the same as the recommended gasper setting for the source passenger in our previous study [54]. When the source passenger was in the window seat, opening the source gasper as proposed unexpectedly led to both higher ε_{mean} and higher $No_{\varepsilon>1}$. This was due to the fact that for passengers in window seats, the proposed gasper setting was different from the recommended gasper setting for the source passenger in our previous study [54].

Overall, when the source passenger was in the window seat, opening the source gasper in accordance with the proposed strategy was not effective in controlling contaminant transmission. Meanwhile, when the source passenger was in the middle or aisle seat, opening the source gasper as proposed was more effective than keeping this gasper closed. Furthermore, the above results emphasize the importance of determining whether a window-seat passenger is a source or a receptor passenger.

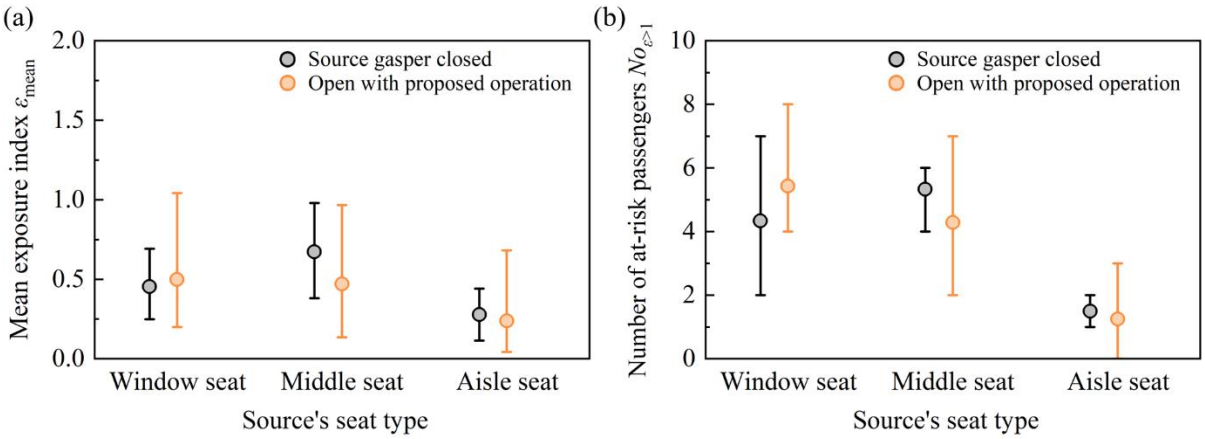

Figure 5.11. Comparison of (a) the mean exposure index value for all passengers and (b) the number of relatively high-risk passengers with different source gasper settings for each source location.

5.3 Discussion

In this study, the performance of the proposed gasper operation strategy was evaluated by comparing it with random gasper operation. However, several limitations must still be addressed. First, our study determined that the source location has a significant impact on the performance of a gasper operation strategy. However, we only considered the case with one source passenger in the aircraft cabin. More complicated situations with multiple source passengers are worth investigating. Second, this study assumed that the cabin was fully occupied, which is generally true. However, the main airflow would exhibit a more complex asymmetrical phenomenon if the cabin was not fully occupied. It would be worthwhile to evaluate the concurrent operation of gaspers under this scenario. Third, this study focused on single-aisle, economy-class aircraft cabins. For twin-aisle or business-class aircraft cabins, the interactions between gasper-induced flow, main ventilation and thermal plumes may differ [34]. Therefore, practical concurrent gasper-operation strategy for other cabins should be further investigated.

Additionally, more efforts should be made to facilitate the practical application of the current work. First, although the proposed operation strategy was expected to reduce the exposure risk, its effectiveness was sensitive to the seat type of the source and the locations of the passengers. As explained in Chapter 5.2.1 and 5.2.2, the use of the proposed operation strategy may be counterproductive for passengers in front of the source, and on the same side of the aisle as the source passenger. It would be very challenging for passengers to adjust their gaspers manually

in accordance with a specific strategy, as the passengers would need to determine the seat type of the source passenger and their positions in relation to the source passenger. Second, the operation strategy proposed in this study may not be beneficial to every passenger in the cabin, especially when the source passenger is in an aisle seat. Therefore, advanced optimization strategies should be developed to enable automated control of gaspers, thereby minimizing the exposure risk for all passengers in the cabin. Third, this study emphasized the importance of the source passenger's location in determining the appropriate gasper operation strategy for the cabin. Therefore, advanced technologies should be developed to identify the location of the source passenger.

5.4 Summary

This study aimed to identify an executable gasper operation strategy by which passengers might control airborne disease transmission in an aircraft cabin. A seven-row section of a single-aisle, fully occupied, economy-class aircraft cabin with personalized displacement ventilation was used for numerical investigation. First, a seat-type-dependent gasper operation strategy was proposed: for passengers in the window seat, the gasper setting was fully open towards the upper body, and for passengers in the middle or aisle seat, the gasper setting was half-open towards the upper body. Next, random gasper operation under realistic conditions was used as the benchmark to evaluate the performance of the proposed gasper operation strategy. Within the scope of this study, the following conclusions were drawn.

- When the source passenger was in the window or middle seat, the proposed operation strategy increased the mean exposure risk for passengers in front of the source, and on the same side of the aisle as the source passenger. Meanwhile, for passengers in other seats, opening the gaspers in accordance with the proposed strategy was effective in controlling contaminant transmission.

- When the source passenger was in the aisle seat, there was no significant difference between the proposed operation strategy and random operation in controlling contaminant transmission.

- The effectiveness of opening the source gasper in accordance with the proposed

operation strategy depended on the source passenger's seat type. Specifically, for source passenger in the window seat, it tended to increase the mean exposure index for all passengers, whereas for source passenger in the middle or aisle seat, it was effective in controlling contaminant transmission.

CHAPTER 6 THE CENTRALIZED CONTROL MODE OF THE GASPER SYSTEM

This chapter proposed two centralized control modes of the gasper system: full control of engaged gaspers and partial control of engaged gaspers, where engaged gaspers refer to those gaspers that had already turned on by passengers. In the full-control mode, all engaged gaspers were controlled to minimize airborne contaminant transmission. In the partial-control mode, only a small number of engaged gaspers were controlled, while most passengers could adjust their gaspers freely to satisfy individual comfort preference. To evaluate the effectiveness of the proposed centralized control modes, a no-control mode was used as the benchmark. In the no-control mode, all passengers freely adjusted their gaspers without external intervention, representing a realistic scenario in which passengers' comfort preferences are maximally satisfied. The above three gasper control modes were applied in a seven-row section of a single-aisle, fully occupied, economy-class aircraft cabin with personalized displacement ventilation for numerical investigation.

6.1 Methodology

The CFD simulation was employed to evaluate the proposed centralized control modes of the gasper system. For the controlled gaspers, the gasper operation was optimized using optimization method to minimize airborne contaminant transmission. The following sections describe in detail the CFD modeling, and optimization approach.

6.1.1 Numerical Models

CFD simulations were conducted to predict the airflow field and airborne disease transmission in the aircraft cabin. A commercial CFD code, ANSYS Fluent, was employed [77]. The airflow field in the aircraft cabin was calculated using the Shear-Stress Transport (SST) k-ω model [76], which has been shown to perform well in predicting gasper-induced jet flows [29, 32, 33]. In the SST k-ω model, the turbulence kinetic energy (k) and the specific dissipation rate (ω) are obtained from the following transport equations [77]:

$$\frac{\partial}{\partial t}(\rho k) + \frac{\partial}{\partial x_i}(\rho k U_i) = \frac{\partial}{\partial x_j}\left[\left(\mu + \frac{\mu_t}{\sigma_k}\right)\frac{\partial k}{\partial x_j}\right] + G_k - Y_k \quad (6.1)$$

$$\frac{\partial}{\partial t}(\rho \omega) + \frac{\partial}{\partial x_i}(\rho \omega U_i) = \frac{\partial}{\partial x_j}\left[\left(\mu + \frac{\mu_t}{\sigma_\omega}\right)\frac{\partial \omega}{\partial x_j}\right] + G_\omega - Y_\omega + D_\omega \quad (6.2)$$

where σ_k and σ_ω are the turbulent Prandtl number for k and ω, respectively. Meanwhile, G_k represents the generation of k due to mean velocity gradients; G_ω represents the generation of ω; Y_k and Y_ω represent the dissipation of k and ω, respectively, due to turbulence; and D_ω is the cross-diffusion term.

The exhaled air contaminant was assumed as gas contaminants [86]. Accordingly, the contaminant transport in the aircraft cabin was simulated using the Eulerian method [87], which has been widely applied to predict airborne disease transmission in enclosed environments [12, 33, 34, 79]:

$$\frac{\partial \rho \phi}{\partial t} + \frac{\partial}{\partial x_i}\left(\rho \phi U_i - \Gamma_\phi \frac{\partial \phi}{\partial x_i}\right) = S_\phi \quad (6.3)$$

where ϕ is contaminant concentration, t is time, ρ is density, U_i is air velocity, Γ_ϕ is the diffusion coefficient, and S_ϕ is the source term, defined as the mass flow rate of contaminant source per unit volume.

6.1.2 Optimization Method

The Bayesian optimization algorithm [103] was adopted to optimize gasper operations such that exposure risks for passengers were minimized. The exposure risk was quantified by the exposure index (ε), defined as the ratio of the contaminant concentration in a passenger's breathing zone to that in the return air [94]. This index has been widely used in previous studies [24, 33, 95-97]. The contaminant concentrations were calculated by CFD simulations. For the sake of simplicity, this study focused on the relatively high-risk passengers with ε>1 [54, 101], indicating that the contaminant concentrations in these passengers' breathing zone are higher than the average level under well-mixed condition. Considering uncertainties in numerical simulations, passengers with $\varepsilon > 0.95$ were assumed as relatively high-risk passengers in this

study, reserving a 5% buffer [101].

The objective function $f(s)$ was defined as the number of the relatively high-risk passengers, excluding the source passenger. The optimization variable (s) is the gasper operation, including open ratio and flow direction. The open ratio $r \in [0,1]$, r=0 signifies that the gasper is closed, while r=1 signifies that the gasper is fully open. The direction of gaspers was assumed adjustable within the range of the corresponding passenger's body. The range of the flow direction in x-y plane (φ) and y-z plane (θ) is shown in Figure 6.1.

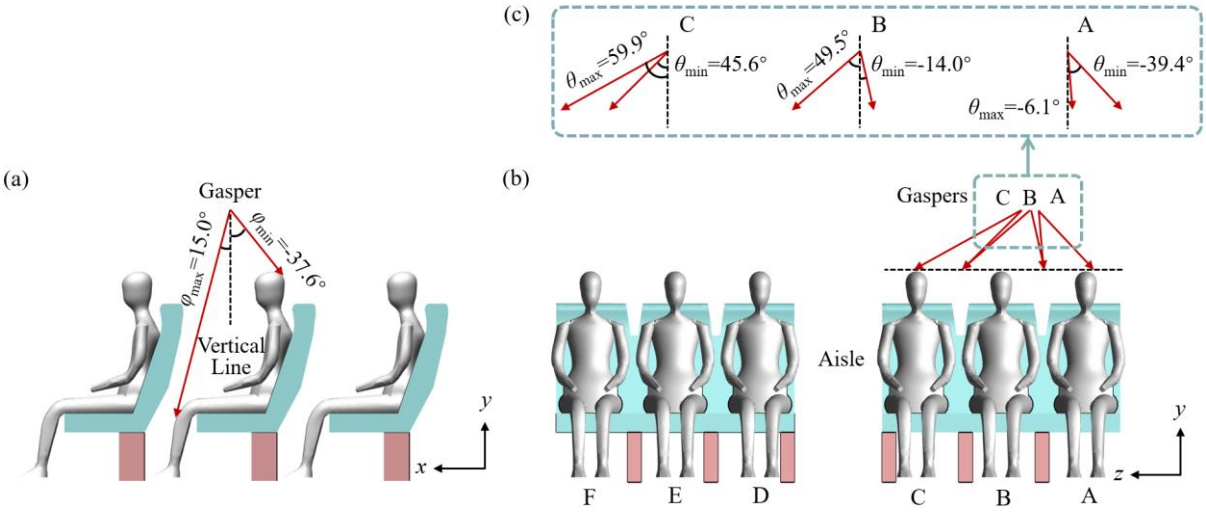

Figure 6.1. (a) The range of the flow direction in the single-aisle aircraft cabin: (a) direction in x-y plane, φ; (b-c) direction in y-z plane, θ.

The Bayesian optimization was based on CFD simulation to identify the globally optimal operation of gaspers, s^*, such that the objective function $f(s)$ was minimized. In each optimization trial, the CFD simulation was performed to calculate the value of the objective function based on a potential global optimum. The calculated function value would then be used to update the prior distribution through a Gaussian process [104]. The next potential global optimum would then be suggested by the acquisition function and evaluated by CFD simulation. The algorithm was realized by an open-source python code [105], and the optimization process was repeated to find the optimal gasper operations. The maximum number of trials in this study was set to 20, considering the limitation of computing resources. The ideal global optimum is $f(s^*)$=0, indicating that there are no relatively high-risk passengers and the optimization process would be stopped.

6.2 Case Setup

Numerical investigations were performed in a seven-row, single-aisle, fully occupied, economy-class aircraft cabin with a personalized displacement ventilation system, as shown in Figure 6.2(a). Fresh air was supplied through the individual diffusers (30 cm in height and 8 cm in width) under each seat, while the cabin air was exhausted through two slots (4mm in width) along the ceiling center. A total of 42 overhead gaspers were installed above passengers. To simplify the gasper geometry, each gasper was modelled as a round nozzle with a radius of 5 mm [33]. The maximum flow rate of the gasper was set as 1.32 L/s [31]. The supply air temperature from diffusers and gaspers was set as 19.3 ℃ [21]. Note that each time when the airflow rate of gaspers was adjusted, the total flow rate for the aircraft cabin kept constant at 320.46 L/s [24], corresponding to an air change rate of 39.7 ACH. The surface temperatures of the floor, sidewalls, ceiling, and passengers were set as 23.8 ℃, 24.5 ℃, 25.0 ℃, and 31.0 ℃, respectively [21]. Additional boundary condition details can be found in the reference literature [54].

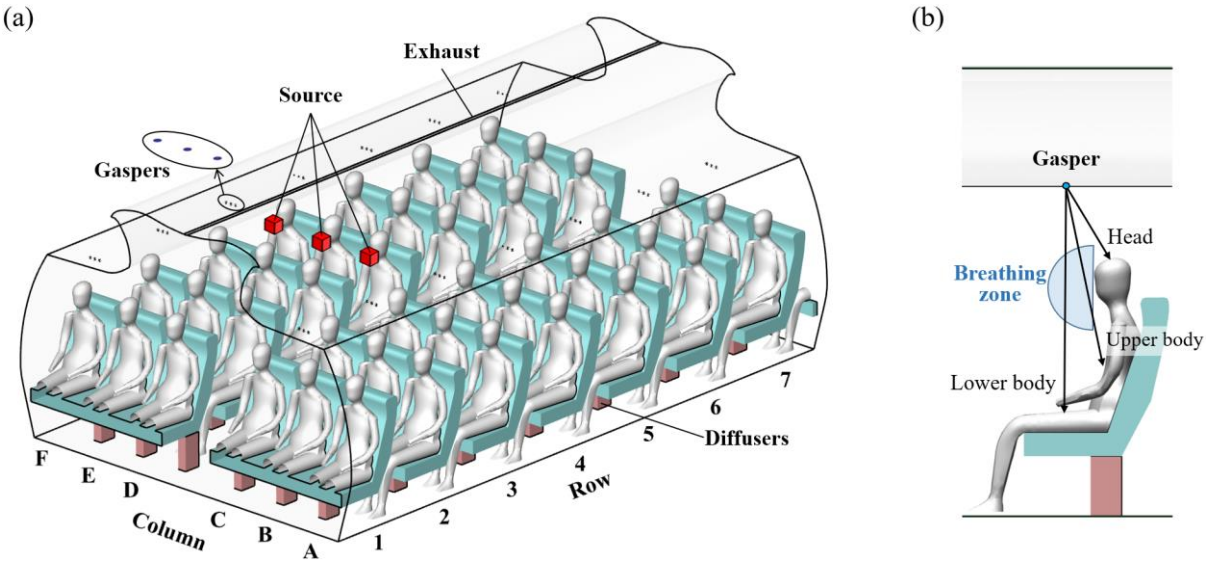

Figure 6.2. (a) Schematic of a seven-row section of a single-aisle, fully occupied, economy-class aircraft cabin and (b) side view of gasper directions and the breathing zone redrawn from [54].

Three gasper control modes were considered in this study: no-control mode, full control of engaged gaspers, and partial control of engaged gaspers, where engaged gaspers refer to those gaspers that had already been opened by passengers. Under the no-control mode, all passengers

freely adjusted their gaspers without external intervention, representing a real-life condition in which passengers' comfort preferences were maximally satisfied. This mode was used as the benchmark case to evaluate the other two centralized control modes. Under full control of engaged gaspers, all engaged gaspers were controlled to minimize airborne contaminant transmission, while the other gaspers remained off. Under partial control of engaged gaspers, only a small number of engaged gaspers were controlled, and most passengers could adjust their gaspers freely to satisfy individual comfort preference. Details of the gasper operations under the three modes are described in Sections 6.2.1, 6.2.2, and 6.2.3, respectively.

Three source locations were considered according to symmetry: the source passenger seated at 4A (window seat), at 4B (middle seat), and at 4C (aisle seat). Contaminants were released continuously with zero momentum from a cube in front of the mouth of the source passenger [54], as shown in Figure 6.2(a). The breathing zone was defined as a hemisphere with a radius of 20 cm in front of the mouth [106], as shown in Figure 6.2(b). The total number of cells for this seven-row section of an aircraft cabin was 8.36 million. Details of the detailed grid size, distribution, and independence test can be found in the reference literature [54].

6.2.1 No-Control Mode

The no-control mode represented a real-life situation in which passengers' comfort preferences were maximally satisfied. In this mode, all passengers freely adjusted their gaspers, including the flow rate and flow direction, without external intervention. According to the field survey conducted by Fang et al. [55], gasper usage behaviors under the no-control mode could be categorized into seven types, with the occurrence probability of each type specified. However, there are a vast number of possible gasper operation distributions throughout the cabin. To address this, a quasi-random sampling method [102] was applied to identify representative distributions. As described in Section 5.1.1, a total of 15 representative scenarios were finally determined, as shown in Figure 6.3. Considering three source locations, the total number of cases was 45 under the no-control mode.

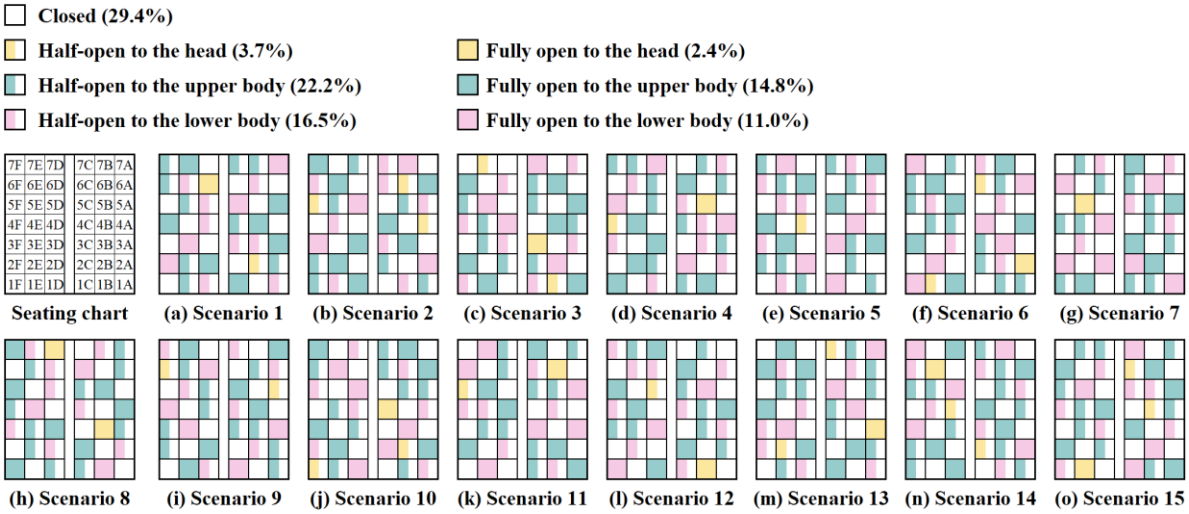

Figure 6.3. Representative gasper operation distributions under the no-control mode.

6.2.2 Full Control of Engaged Gaspers

Engaged gaspers are defined as those gaspers that were turned on by passengers under the no-control mode, regardless of whether they are half-open or fully open. As illustrated in Figure 6.3, coloured cells represent engaged gaspers, while white cells correspond to disengaged gaspers. Under the full-control mode, all engaged gaspers were controlled to minimize airborne contaminant transmission, while disengaged gaspers were kept closed. The optimization variables were open ratios and flow directions of engaged gaspers. An open ratio was defined as the actual flow rate divided by the total flow rate of the gasper. Considering three source locations, the total number of cases was 45 under this mode.

6.2.3 Partial Control of Engaged Gaspers

To simultaneously address airborne infection mitigation and comfort preferences maintenance, a mode was proposed under which engaged gaspers were partially controlled. Zhou et al. [101] found that with optimal operation of 9 gaspers near a source passenger, the number of relatively high-risk passengers was effectively reduced by at least 67% compared with the number of cases when all the gaspers were turned off. This finding highlights the critical role of near-source gaspers in controlling inter-passenger air contaminant transport. Accordingly, in the present study, under partial control of engaged gaspers, only those near-source gaspers that were engaged were controlled. Since the three source passengers considered in the present study were located in seats 4A, 4B, and 4C, the controlled gaspers in this mode were

accordingly clustered in rows 3–5 of columns A–C, as shown in in Figure 6.4. For example, for scenario 1 in Figure 6.4(a), the gaspers of passengers 3A–C, passengers 4B and 4C, and passengers 5A and 5C were controlled for optimization. Meanwhile, in scenario 2 in Figure 6.4(b), the controlled gaspers included those of passengers 3B and 3C, passengers 4A and 4C, and passengers 5A and 5B. Apart from the controlled gaspers, all remaining gaspers retained their original operations as under the no-control mode.

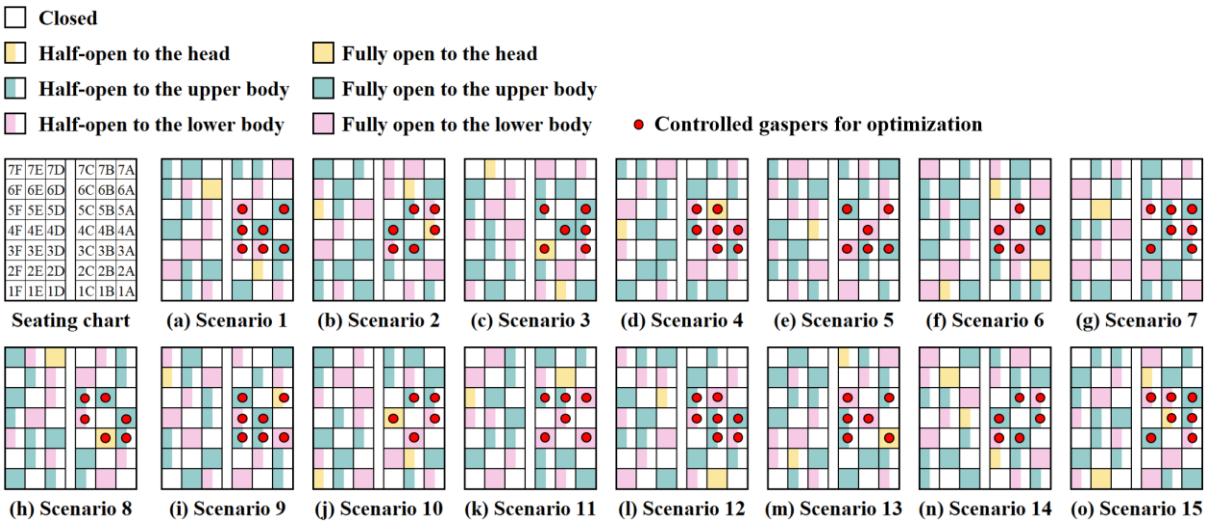

Figure 6.4. Locations of controlled gaspers and operations of uncontrolled gaspers under the partial-control mode.

6.3 Performance of Different Gasper Control Modes

The performance of the modes with full control and partial control of engaged gaspers was evaluated, and the no-control mode was used as the benchmark. We first compared the number of relatively high-risk passengers in each scenario to assess the modes' effectiveness in reducing exposure risk. Next, the airflow patterns and contaminant concentration distributions were analysed to determine the working mechanism of different modes. Finally, the distributions of open ratio and flow direction after optimization were compared with those under the no-control mode to evaluate the ability to maintain individual comfort preference.

6.3.1 Full Control of Engaged Gaspers

Figure 6.5(a)-(c) compare the number of relatively high-risk passengers in each scenario under the no-control mode and under full control of engaged gaspers, with the source passenger

located in window seat 4A, middle seat 4B, and aisle seat 4C, respectively. Under the full-control mode, the number of relatively high-risk passengers refers to the minimum value achieved within 20 optimization trials. The results showed that regardless of the seat type of the source passenger, the full-control mode effectively reduced or even completely eliminated the number of relatively high-risk passengers by optimizing all engaged gaspers. Specifically, under the full-control mode, the number of relatively high-risk passengers was effectively reduced by 83%, 79% and 97% when the source passenger was in the window seat, middle seat, and aisle seat, respectively, compared with the cases under the no-control mode.

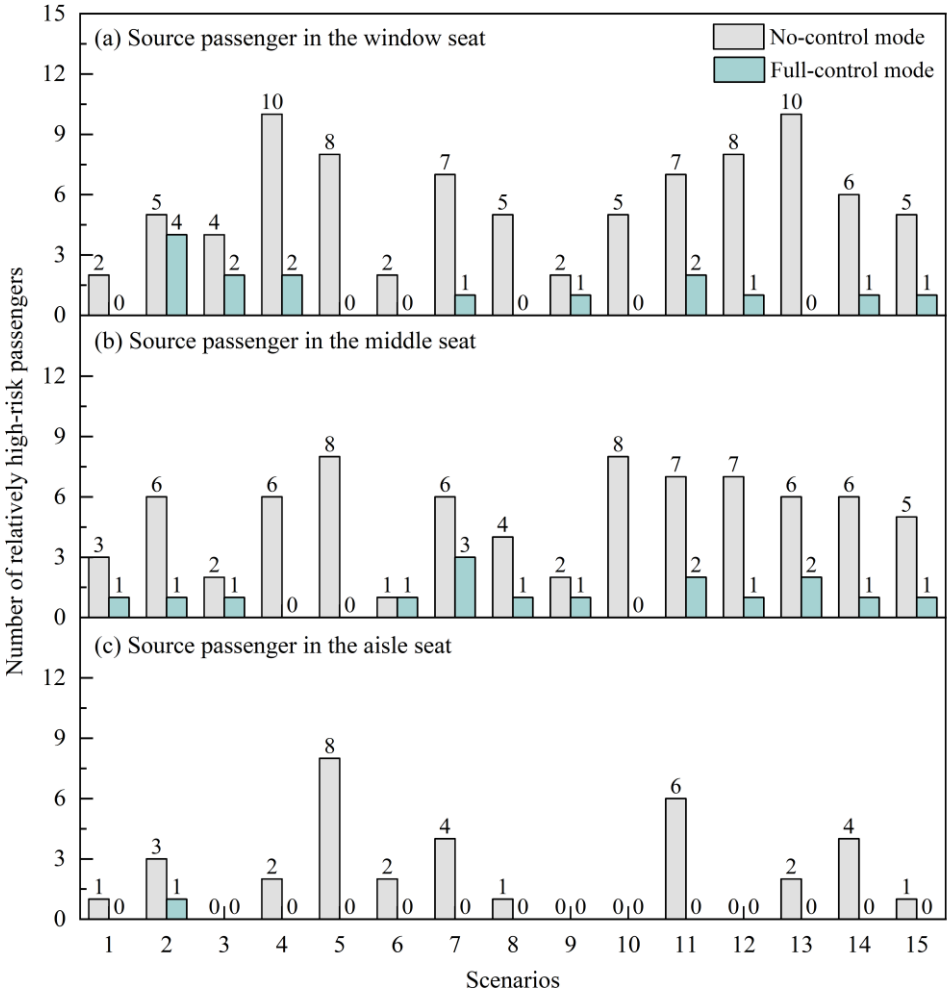

Figure 6.5. Comparison of the number of relatively high-risk passengers for each scenario under the no-control mode and under full control of engaged gaspers, with the source passenger located in (a) window seat 4A, (b) middle seat 4B, and (c) aisle seat 4C.

To explain the results, we analysed the airflow pattern and the dimensionless contaminant concentration C^* (normalized by the contaminant concentration in the return air) distributions

in the cross section located 0.05 m in front of the mouth of the source passenger (CS4) and the horizontal section at breathing level (HS), as shown in Figure 6.6(a) and (b). The exposure index distributions were also compared. For the sake of conciseness, only the results for Scenario 13 with the source passenger in window seat 4A are presented here; this scenario exhibited a larger number of relatively high-risk passengers under the no-control mode. It can be seen from Figure 6.6(a) that, under the no-control mode, the contaminants exhaled by source passenger 4A were entrained by the gasper jets of neighboring passengers 4B and 4C to the side of the source passenger, and were then transported to the rows in front of and behind the source passenger due to the main airflow and other gasper jets. Therefore, the exposure index for neighbouring passengers was relatively high. Meanwhile, under full control of engaged gaspers, the gaspers surrounding the source passenger were mostly closed, and the gasper of passenger 4D on the opposite side of the aisle was fully open. Therefore, the jet flow induced by the gasper of passenger 4D altered the airflow pattern near the source passengers, and the contaminants exhaled by source passenger 4A were contained in a localized area and then directly removed through the exhausts, resulting in a relatively low contaminant concentration throughout the cabin. In addition, the above results showed that the contaminant transmission was primarily influenced by the operation of gaspers near the source passenger.

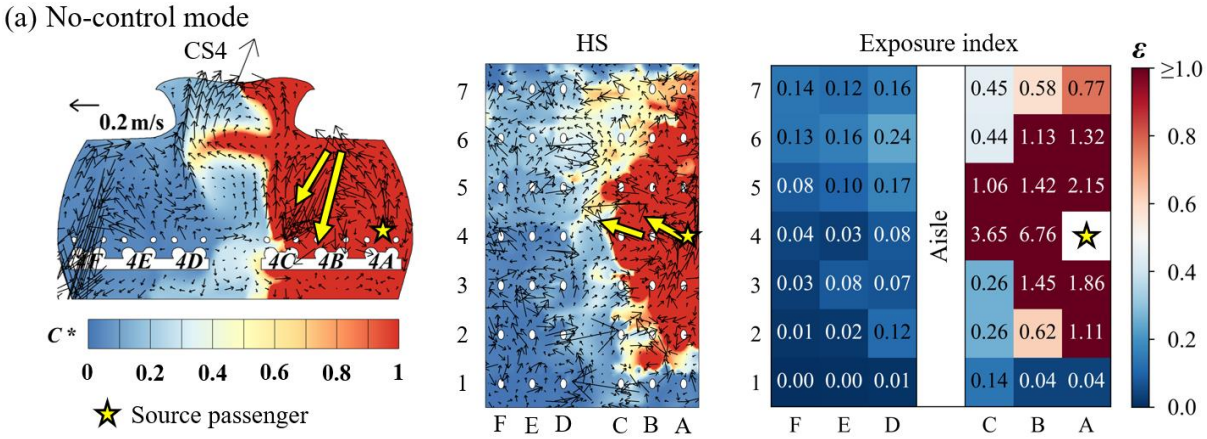

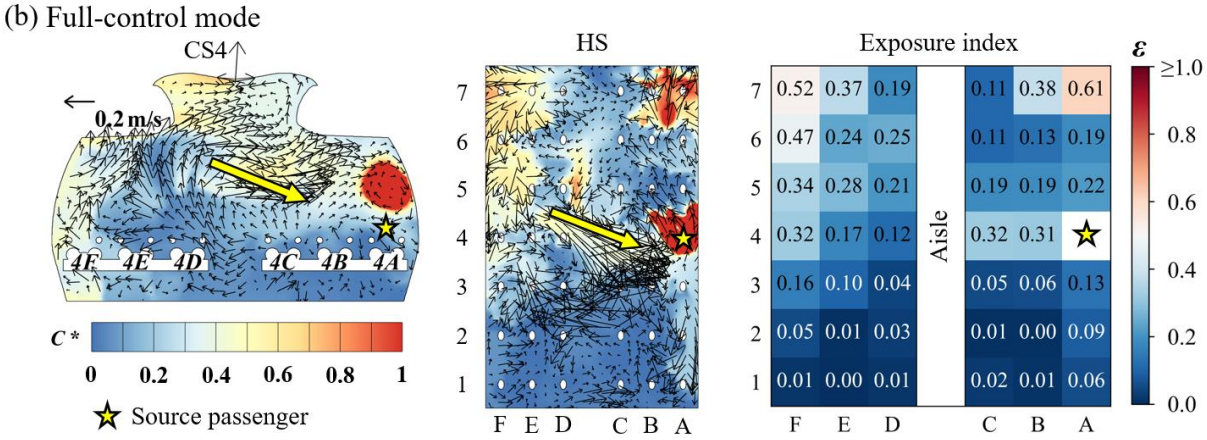

Figure 6.6. The airflow pattern and C^* distribution at CS4 and HS and the exposure index distribution under (a) the no-control mode and (b) full control of engaged gaspers for scenario 13, when the source passenger was seated at 4A.

To evaluate the performance of full control mode for passengers' comfort preferences, we next compared the gasper operation of each passenger under the no-control mode and under full control of engaged gaspers, as shown in Figure 6.7. For the full-control mode, the gasper operation refers to the optimized operation, i.e., the operation that achieved the minimum number of relatively high-risk passengers within 20 optimization trials. Note that only the results for scenario 13 with source passenger in the window seat 4A are presented here for the sake of conciseness. It can be seen in Figure 6.7(a) and (b) that the open ratio of the individual gaper under the full-control mode differed significantly from that under the no-control mode. Specifically, for gaspers near the source passenger (gaspers 3A–C, 4A–C, and 5A–C), the number of closed or nearly closed gaspers increased from 3 under the no-control mode to 9 under the full-control mode. For the remaining seats, most of the gaspers under the no-control mode were either fully open or closed, and only two passengers' gaspers were half-open, as shown in Figure 6.7(b). In contrast, under the full-control mode, more than 40% of passengers' gaspers were half-open. As for flow direction (Figure 6.7(c) and (d)), under the full-control mode, the flow direction deviated significantly from that under the no-control mode, such as for gaspers 2B, 3E, and 6B, as shown in the green rectangular boxes in Figure 6.7(d). Overall, gasper operations under the full-control mode were effective in reducing exposure risk. However, the open ratio and flow direction distributions significantly differed from those under the no-control mode, potentially compromising passengers' comfort preferences.

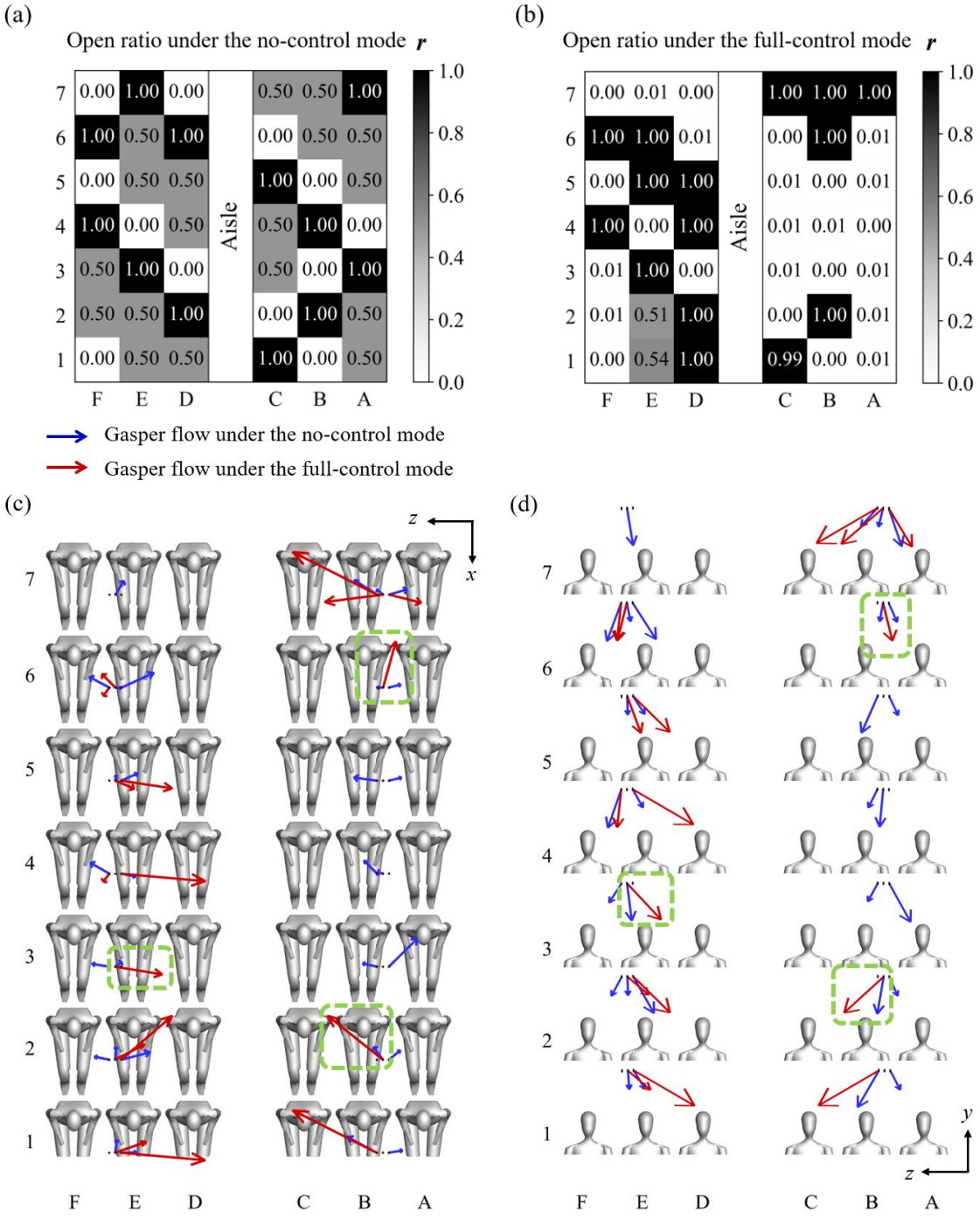

Figure 6.7. The open ratio of gaspers (a) under no-control mode and (b) under full-control mode that achieved the minimum number of relatively high-risk passengers, and the gasper flow from each gasper under no-control mode and under full-control mode in (c) top view and (d) front view.

6.3.1 Partial Control of Engaged Gaspers

Figure 6.8(a)-(c) compare the number of relatively high-risk passengers in each scenario under the no-control mode and under partial control of engaged gaspers, with the source passenger

located in window seat 4A, middle seat 4B, and aisle seat 4C, respectively. The results showed that regardless of the seat type of the source passenger, gasper operations under the partial-control mode effectively reduced or even completely eliminated the number of relatively high-risk passengers through the control of only a small number of engaged gaspers near the source passenger. Specifically, under the partial-control mode, the number of relatively high-risk passengers was effectively reduced by 81%, 66% and 88% when the source passenger was in the window seat, middle seat, and aisle seat, respectively, compared with the number of cases under the no-control mode.

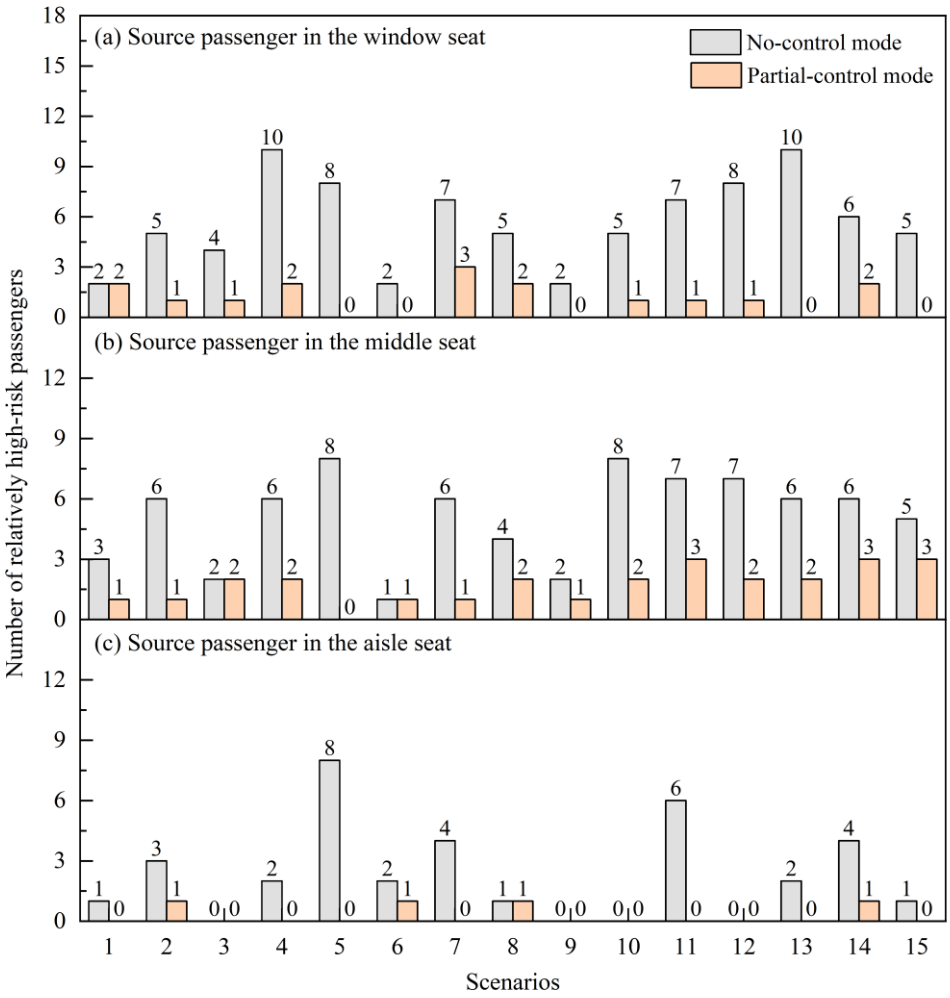

Figure 6.8. Comparison of the number of relatively high-risk passengers in each scenario under the no-control mode and under partial control of engaged gaspers, with the source passenger located in (a) window seat 4A, (b) middle seat 4B, and (c) aisle seat 4C.

To explain the results, we analysed the airflow pattern and the dimensionless contaminant concentration C^* distributions in the cross section located 0.05 m in front of the mouth of the

source passenger (CS4) and the horizontal section at breathing level (HS), as shown in Figure 6.9(a) and (b). The exposure index distributions were also compared. For the sake of conciseness, we have taken scenario 13 with source passenger in window seat 4A as an example here. It can be seen from Figure 6.9(b) that, under the partial-control mode, the open ratio of gaspers 4B and 4C near the source passenger was relatively small. Therefore, the contaminant exhaled by the source passenger was mainly transported upwards due to the airflow from the diffuser and thermal plume, and was then discharged along the sidewall from ceiling center. This resulted in a quite low exposure index for passengers compared to the no-control mode (Figure 6.9(a)).

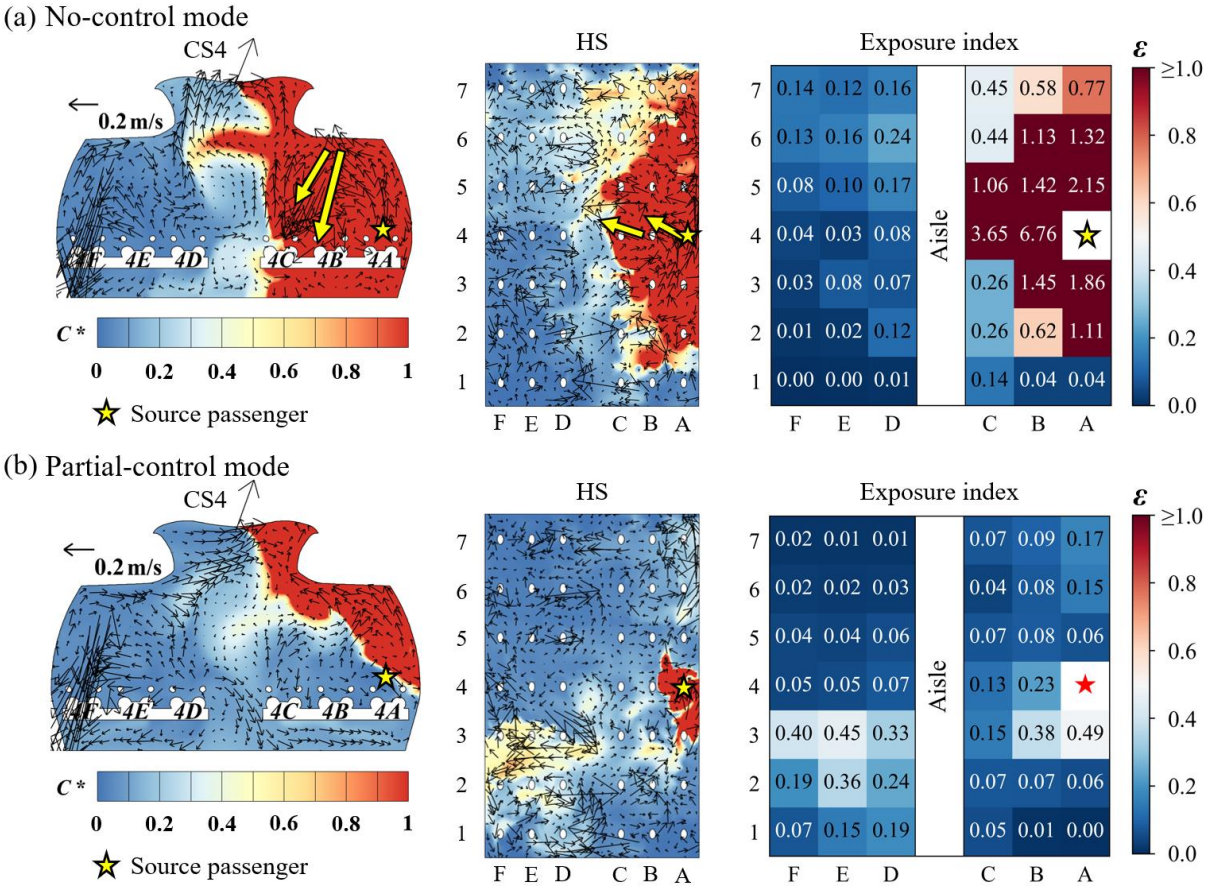

Figure 6.9. The airflow pattern and C^* distribution at CS4 and HS and the exposure index distribution under (a) the no-control mode and (b) the partial-control mode with scenario 13, when the source passenger was seated at 4A.

Additionally, we compared gasper operations under the no-control mode with the operations under the partial-control mode that achieved the minimum number of relatively high-risk passengers, as shown in Figure 6.10. For the sake of conciseness, only the results for scenario 13 with source passenger in the window seat 4A are presented here. As illustrated in Figure

6.10, differences in gasper operation between the two modes were observed only for gaspers near the source passengers, while other passengers retained their preferred gasper operations. This indicates that the partial-control mode can effectively reduce exposure risks in the cabin and ensure comfort preferences for most passengers.

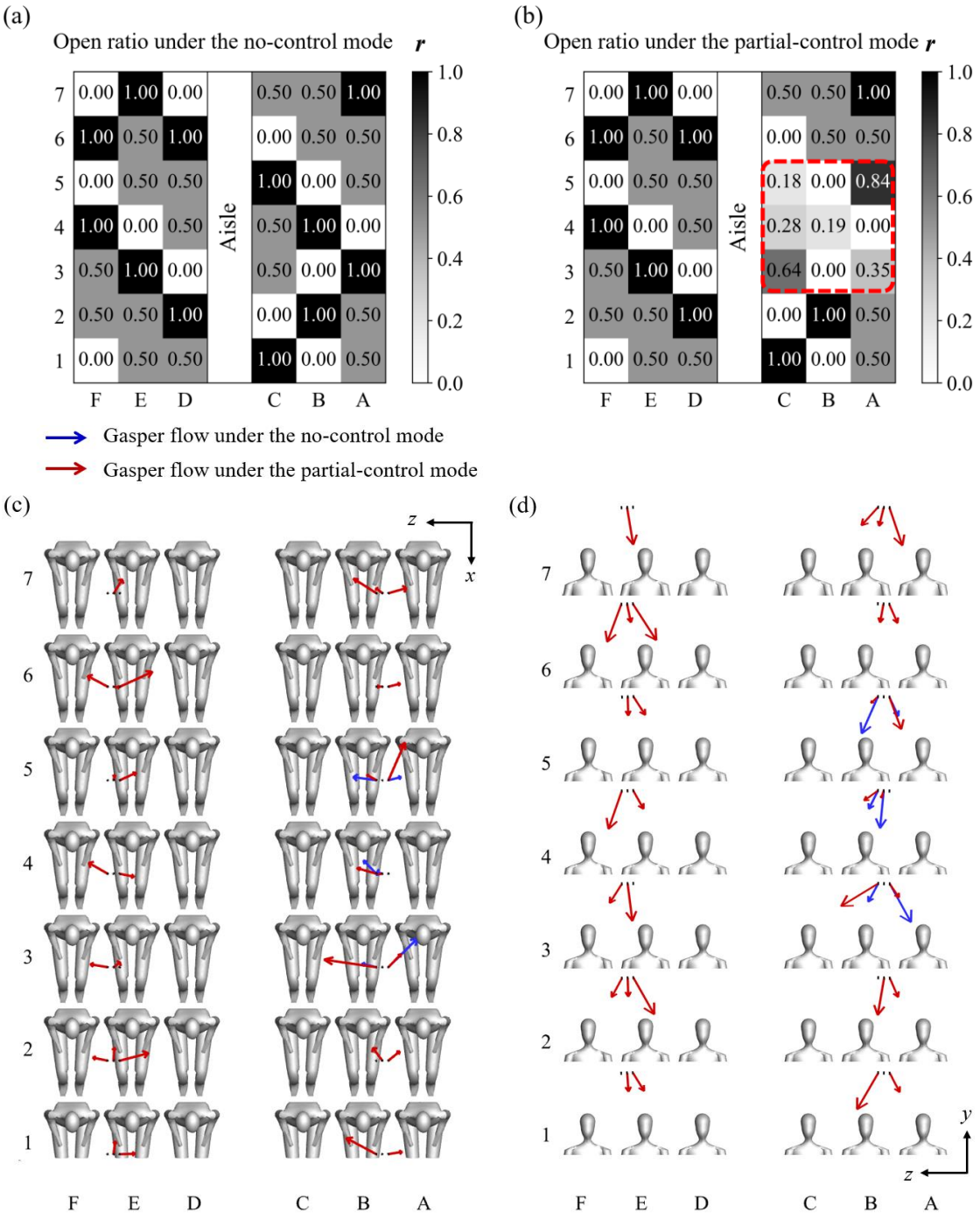

Figure 6.10. The open ratio of gaspers (a) under the no-control mode and (b) under the partial-control mode that achieved the minimum number of relatively high-risk passengers, and the flow from each gasper under the no-control mode and under the partial-control mode in (c) top view and (d) front view.

6.4 Discussion

This study proposed and evaluated different centralized control modes for the gasper system. Several limitations need to be addressed to facilitate the practical application of the current work. First, this study focused on the case with a single source passenger seated in the aircraft cabin. The effectiveness of partial control of engaged gaspers in more complicated situations, such as the presence of multiple source passengers at the same time requires further investigation. Second, this study assumed three seat types for the source location. However, in real scenarios, the exact position of an infectious source passenger is typically unknown during flight. To enhance practical applicability, advanced techniques such as real-time occupant monitoring systems should be integrated into future studies to identify the source location. Third, partial control of engaged gaspers may not be beneficial to every individual passenger, as this study only focused on minimizing overall exposure risks, and the effectiveness was evaluated based on the number of relatively high-risk passengers. Therefore, advanced optimization algorithms should be developed in the future to reduce exposure risks at the individual passenger level. Fourth, this study demonstrated the feasibility of partially controlling gaspers to minimize exposure risk in the cabin while ensuring comfort preferences for most passengers. Future research should focus on identifying the key gasper locations that influence contaminant transport and determining the minimum number of gaspers that need to be controlled.

6.5 Summary

This study aimed to evaluate different centralized control mode of the gasper system in mitigating airborne infection risk and maintaining comfort preferences in aircraft cabins with personalized displacement ventilation. The CFD simulation was employed to simulate different gasper control modes in a seven-row section of a single-aisle, fully occupied, economy-class aircraft cabin with personalized displacement ventilation. We proposed two centralized control modes: full control of engaged gaspers and partial control of engaged gaspers, where engaged gaspers refer to those gaspers that had already turned on by passengers. To evaluate the effectiveness of the proposed centralized control modes, a no-control mode was used as the benchmark. Within the scope of this study, the following conclusions can be made:

- Under full control of engaged gaspers, the number of relatively high-risk passengers was effectively reduced by 83%, 79% and 97% when the source passenger was in the window, middle, and aisle seat, respectively, compared with the number of cases under the no-control mode. However, the gasper open ratio and flow direction distributions significantly differed from those under the no-control mode.

- Under partial control of engaged gaspers, the number of relatively high-risk passengers was effectively reduced by 81%, 66% and 88% when the source passenger was in the window, middle, and aisle seat, respectively, compared with the cases under the no-control mode. Meanwhile, passengers' comfort preferences were maintained for the majority of passengers.

CHAPTER 7 CONCLUSIONS AND FUTURE WORK

This chapter summarizes the important conclusions and limitations of this study, and then discuss the future work.

7.1 Conclusions

To validate the performance of the CFD model on predicting airflow patterns and contaminant concentration distributions in aircraft cabins, it is important to obtain reliable and high-quality data. This study first carried out experimental measurements in a simplified three-row, single-aisle aircraft cabin mock-up with personalized displacement ventilation and a single gasper, as presented in Chapter 3. Then, the measured distributions of air velocity and contaminant concentration with gasper off and on were analysed. Finally, the obtained experimental data were compared with simulated results for CFD model validation. The experimental data demonstrated that the gasper-induced flow altered the cabin airflow field and consequently influenced the transport of airborne contaminants. Additionally, the simulation results showed that the RANS SST k-ω turbulence model combined with the Eulerian method could accurately predict both airflow patterns and contaminant concentration distributions.

The validated CFD model in chapter 3 was used to investigate the impact of source and receptor gaspers on airborne disease transmission in a seven-row, single-aisle, fully occupied, economy-class aircraft cabin with a personalized displacement ventilation system, as presented in chapter 4. We first investigated the impact of source gasper direction and flow rate on the airborne transmission near the contaminant source. We then investigated the protective effect of the receptor's gasper. For a source passenger's gasper, the direction and flow rate of the gasper flow either increased or decreased the air contaminant transmission to other passengers. Directing the source gasper to the abdomen with a medium flow rate performed best by reducing the receptors' mean exposure index by at least 45%, as this approach minimized the contaminant circulation in the cabin. Turning on a receptor passenger's gasper could be an effective strategy to protect the receptor, and the working mechanism was revealed. The gasper-induced jet flow entrained the surrounding air into the jet region, and the protective effect was related to the contaminant concentration at ceiling level. With a suitable gasper direction and flow rate, the gasper jet formed a virtual barrier between the source passenger and the receptor. When the

contaminants were transported upwards to a receptor's breathing zone, turning on the receptor's gasper reduced the contaminant concentration, since the downward gasper jet altered the airflow pattern in front of the receptor.

In practice, multiple gaspers are operated simultaneously by passengers, and their interaction with the main airflow significantly complicates the contaminant transport in the cabin. Chapter 5 aims to identify and evaluate an executable gasper operation strategy for passengers to control the transmission of airborne diseases. We first proposed a seat-type-dependent gasper operation strategy based on the working mechanism of a single gasper from our previous study. Random gasper operation under realistic conditions was innovatively used as the benchmark. The two operation strategies were then applied in a seven-row section of a single-aisle, fully occupied, economy-class aircraft cabin with a personalized displacement ventilation system for numerical simulations. The results showed that when the source passenger was in the window seat or middle seat, the proposed operation strategy with full utilization reduced the mean exposure index by at least 25.4% for most passengers, except those seated directly in front of the source passenger. When the source passenger was in the aisle seat, there was no significant difference between the proposed strategy and random operation in controlling the transmission. These findings suggest that it would be challenging for passengers to adjust their gaspers manually from a self-protection perspective.

Maintaining both passengers' comfort preferences and air quality in aircraft cabins is essential for air passengers and crew members. Therefore, Chapter 6 aims to investigate whether a centralized control mode of the gasper system is feasible to simultaneously mitigate airborne infection risk while maintaining passengers' comfort preferences. The verified CFD model in Chapter 3 was employed to simulate different gasper control modes in a seven-row section of a single-aisle, fully occupied, economy-class aircraft cabin with personalized displacement ventilation. Three gasper control modes were considered, no-control mode, full control of engaged gaspers, and partial control of engaged gaspers, respectively. The results show that under full control of engaged gaspers, the number of relatively high-risk passengers was reduced by at least 79% compared to the no-control mode. However, the gasper setting distributions significantly differed from those under the no-control mode. Partial control of engaged gaspers achieved slightly lower risk reduction but maintained comfort preferences for most passengers. These findings demonstrate the feasibility of the partial-control mode to

achieve both airborne infection mitigation and comfort preference maintenance in real-life cabin environments.

7.2 Limitations

This study systematically investigated the operation of gaspers for reducing airborne disease transmission in commercial airliners with personalized displacement ventilation system. However, several limitations remain.

The present study only considered the case with one source passenger in the aircraft cabin. This assumption simplifies the problem and allows for a systematic evaluation of airflow and contaminant transport patterns. However, under more complicated situations with multiple source passengers, whether the partial control mode proposed in Chapter 6 is still feasible to simultaneously mitigate airborne infection risk while maintaining passengers' comfort preferences remains unclear.

The evaluation of contaminant exposure was primarily based on exposure index within the breathing zone, and only overall exposure risk was focused. Therefore, the proposed control mode may not be beneficial to every individual passenger. Additionally, other important aspects, such as infection probability under different pathogen characteristics, were beyond the scope of this work. As a result, the exposure risk assessment remains preliminary.

Numerical investigations were conducted in a single-aisle, fully-occupied, economy-class aircraft cabin. However, airflow structures and contaminant transmission patterns may differ significantly in cabins of different layouts [34] (e.g., twin-aisle or business class cabins) or under varying occupancy levels. Therefore, the conclusions drawn from the single-aisle model in this study are not applicable to other aircraft cabins.

7.3 Future Work

Building upon the findings and limitations of this study, future work can proceed along the following directions to further improve cabin environments.

(1) Cabin environments

The partial centralized control mode proposed in this thesis was able to maintain the comfort preferences for most passengers. However, a small number of passengers still experienced deviations from their preferred gasper operations. Future studies should therefore focus on developing more advanced optimization algorithms, integrating thermal comfort evaluation indices, and achieving infection risk mitigation and passengers' thermal comfort maintenance at the individual level.

In addition, the current study considered only a single source passenger. Further investigations should evaluate the performance of the proposed centralized control strategy under multiple-source and more complex transmission scenarios, which better reflect realistic inflight conditions.

(3) Other indoor environments

The concept of personalized ventilation in this thesis has the potential to be extended beyond aircraft cabins. Future studies may explore its applicability in high-risk indoor environments, such as hospital wards, where airborne transmission is a major concern. Moreover, enclosed and densely occupied environments, such as movie theaters, may also benefit from occupant-oriented ventilation strategy. Investigating these broader applications would help establish generalized design principles for personalized ventilation systems in various built environments.

APPENDIX

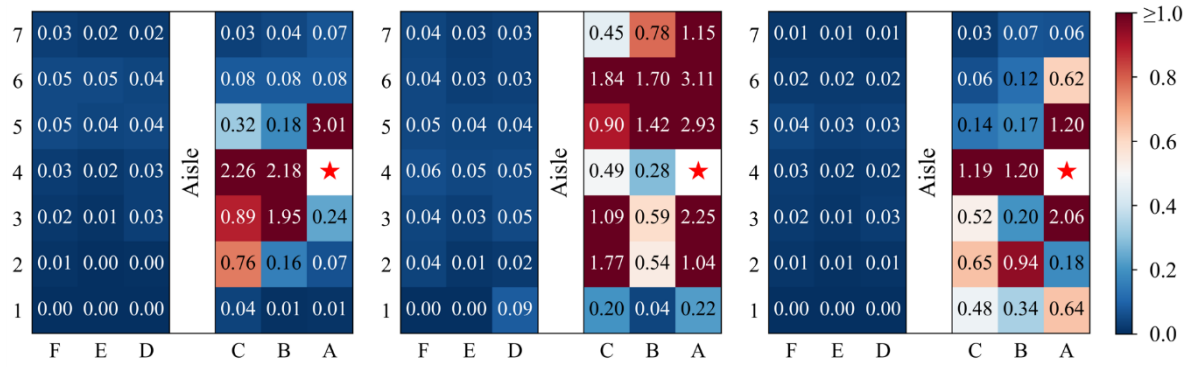

(a) Half-open to the head (b) Fully open to the head (c) Fully open to the abdomen

Figure. A. 1. Exposure index under different gasper settings with the source passenger seated in the window seat 4A.

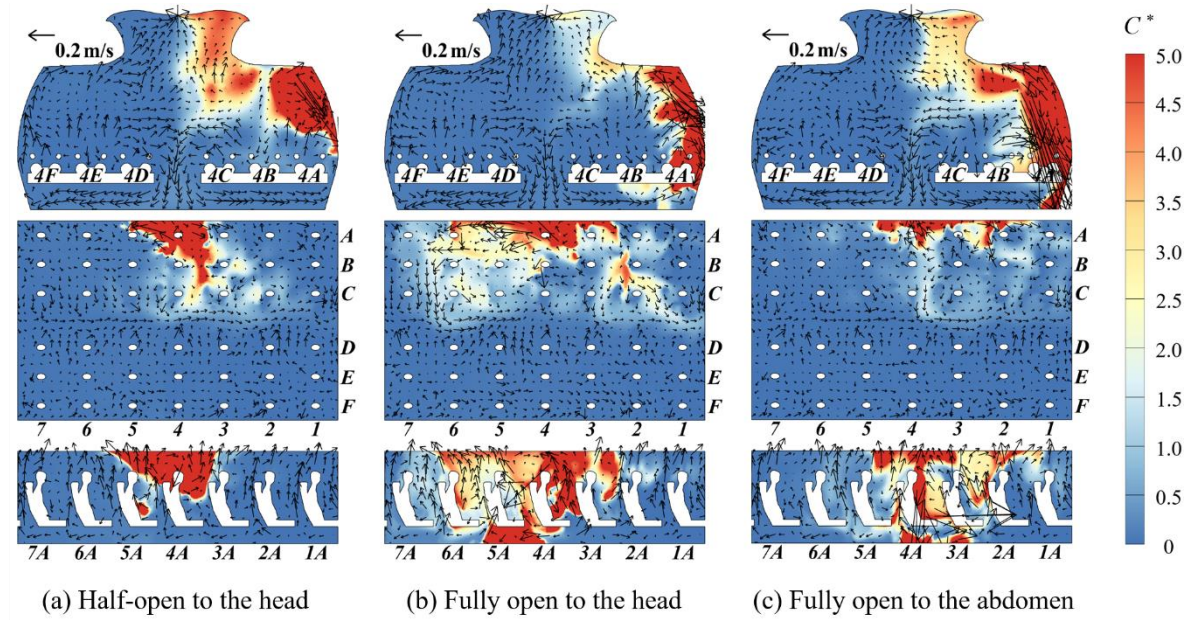

(a) Half-open to the head (b) Fully open to the head (c) Fully open to the abdomen

Figure. A. 2. The airflow patterns and C^* distributions at CS4, HS, and LSA under different gasper settings with the source passenger seated in the window seat 4A.

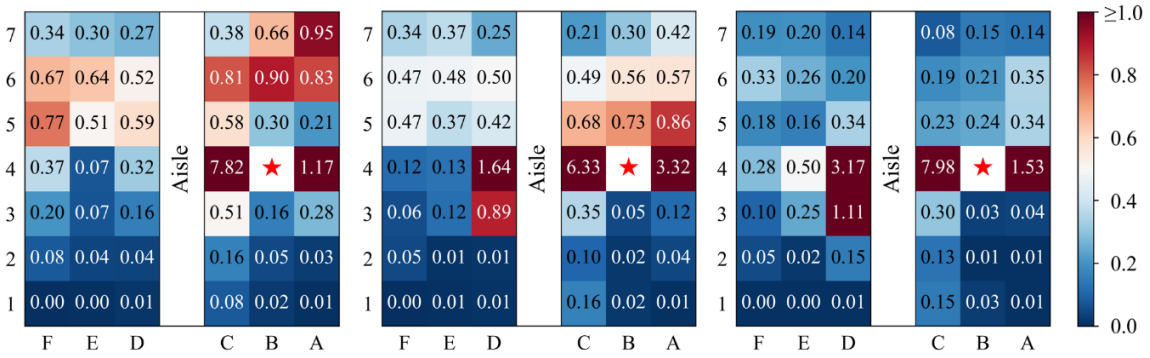

(a) Half-open to the mouth (b) Fully open to the mouth (c) Fully open to the abdomen

Figure. A. 3. Exposure index under different gasper settings with the source passenger seated in the middle seat 4B.

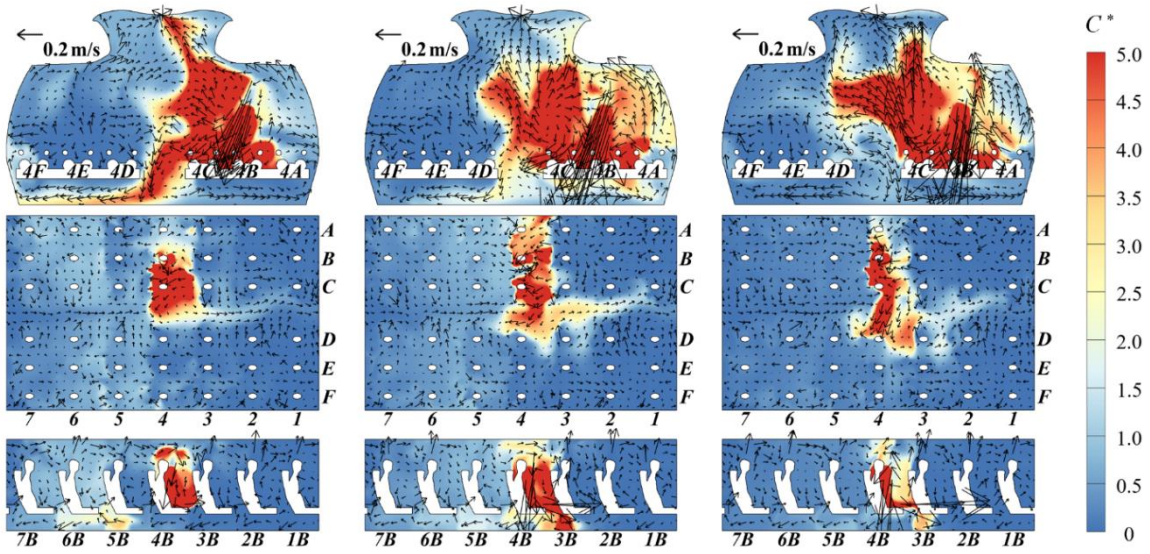

(a) Half-open to the mouth (b) Fully open to the mouth (c) Fully open to the abdomen

Figure. A. 4. The airflow patterns and C^* distributions at CS4, HS, and LSB under different gasper settings with the source passenger seated in the middle seat 4B.

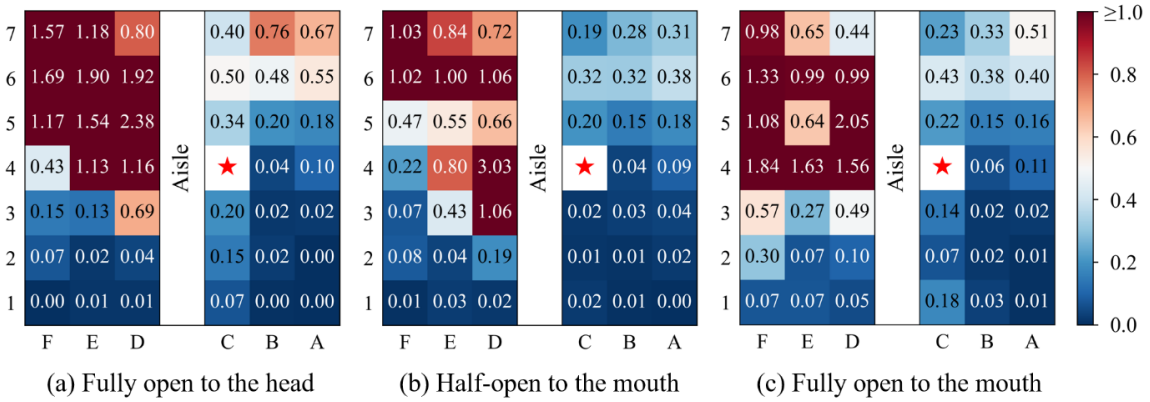

(a) Fully open to the head (b) Half-open to the mouth (c) Fully open to the mouth

Figure. A. 5. Exposure index under different gasper settings with the source passenger seated in the aisle seat 4C.

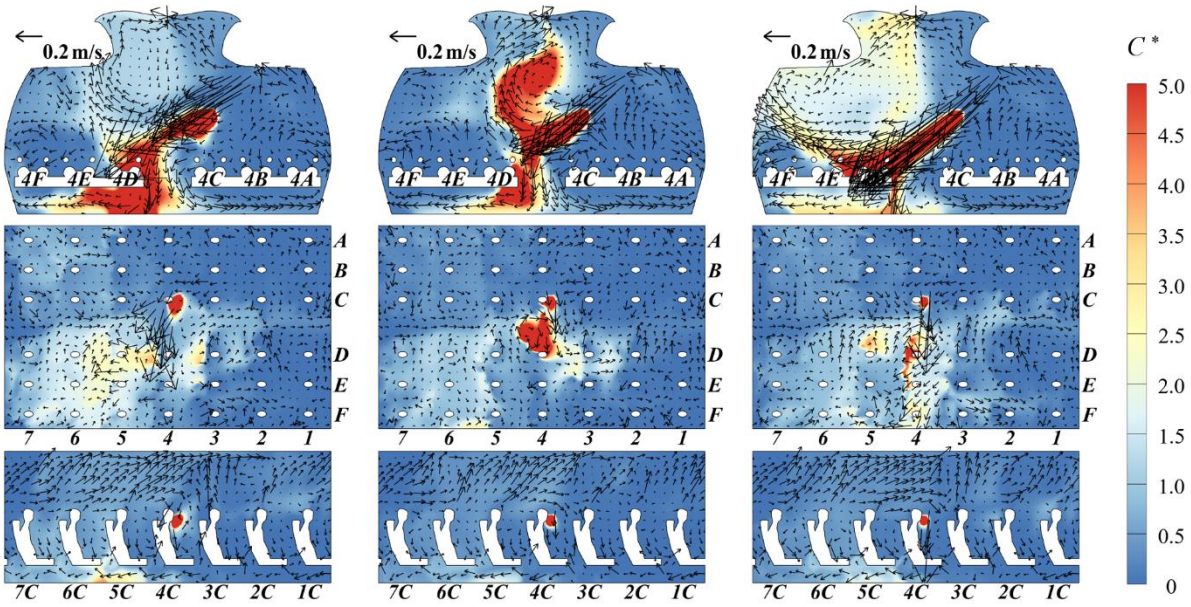

(a) Fully open to the head (b) Half-open to the mouth (c) Fully open to the mouth

Figure. A. 6. The airflow patterns and C^* distributions at CS4, HS, and LSC under different gasper settings with the source passenger seated in the aisle seat 4C.

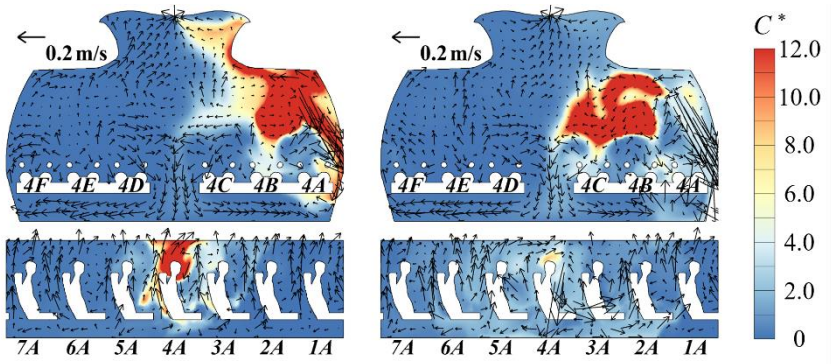

(a) Half-open to the mouth (b) Fully open to the mouth

Figure. A. 7. The airflow patterns and C^* distributions at CS4 and LSA under different gasper settings with the receptor seated in the window seat 4A.

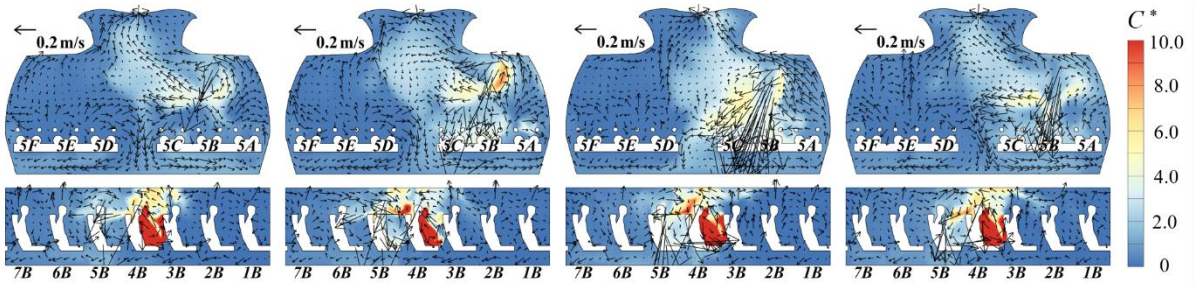

(a) Half-open to the head (b) Fully open to the head (c) Fully open to the mouth (d) Half-open to the abdomen

Figure. A. 8. The airflow patterns and C^* distributions at CS5 and LSB under different gasper settings with the receptor seated in the middle seat 5B.

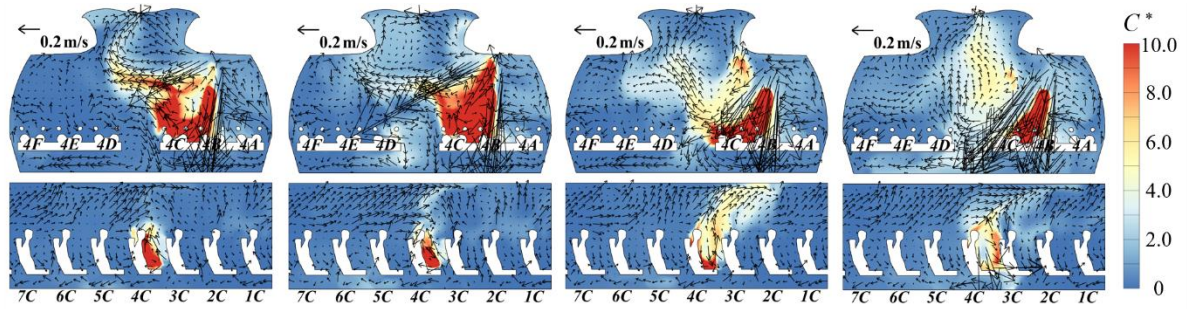

(a) Half-open to the head (b) Fully open to the head (c) Half-open to the abdomen (d) Fully open to the abdomen

Figure. A. 9. The airflow patterns and C^* distributions at CS4 and LSC under different gasper settings with the receptor seated in the aisle seat 4C.

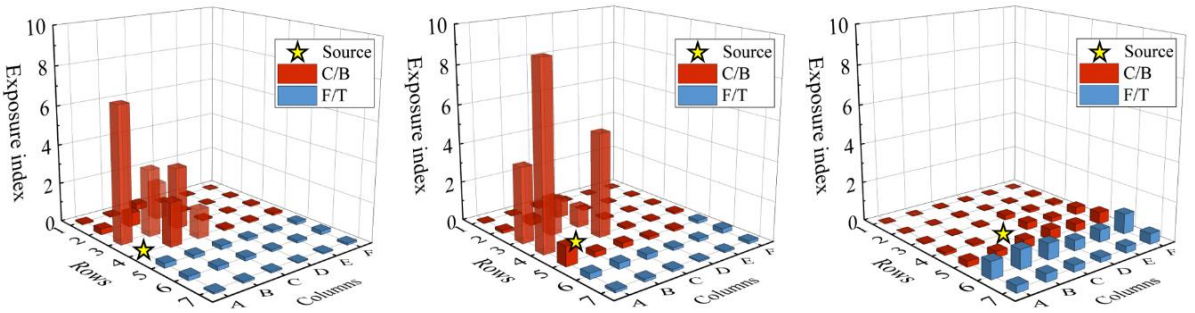

(a) Source 4A with gasper off (b) Source 4B with gasper off (c) Source 4C with gasper off

Figure. A. 10. Distribution of scenarios for all receptors when the gasper of the source passenger was off.

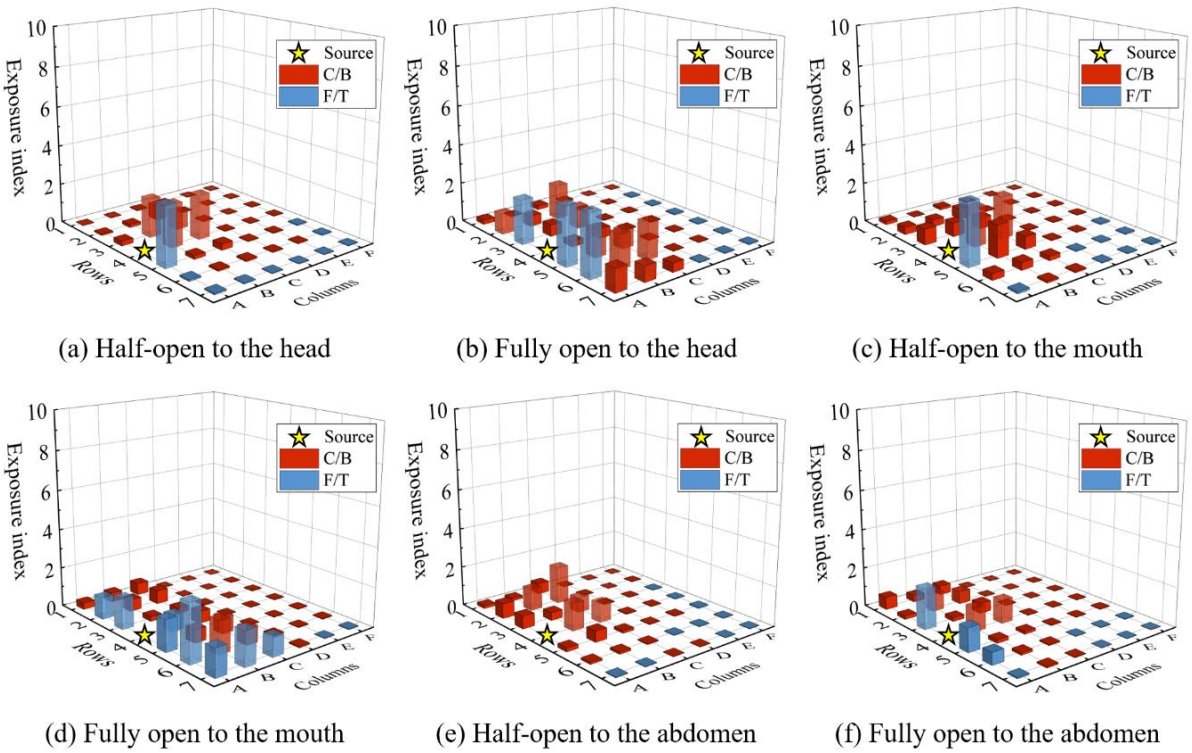

Figure. A. 11. Distribution of scenarios for all receptors when the gasper of the source passenger 4A was on.

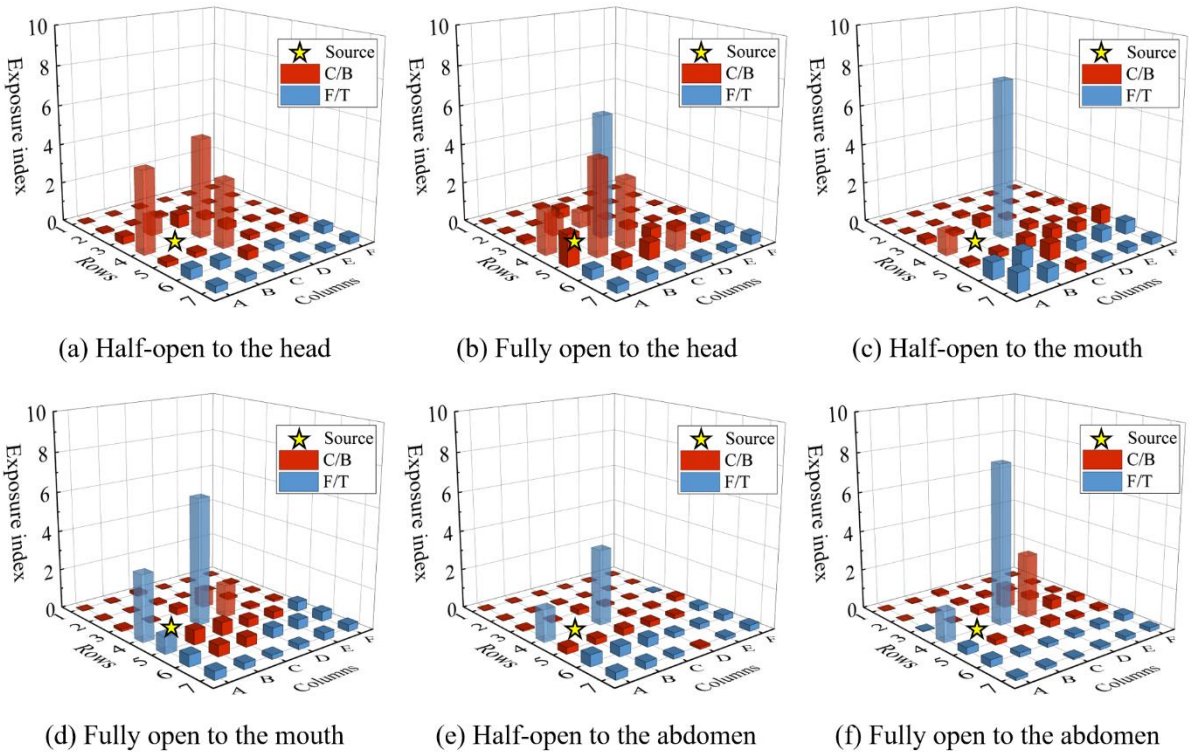

Figure. A. 12. Distribution of scenarios for all receptors when the gasper of the source passenger 4B was on.

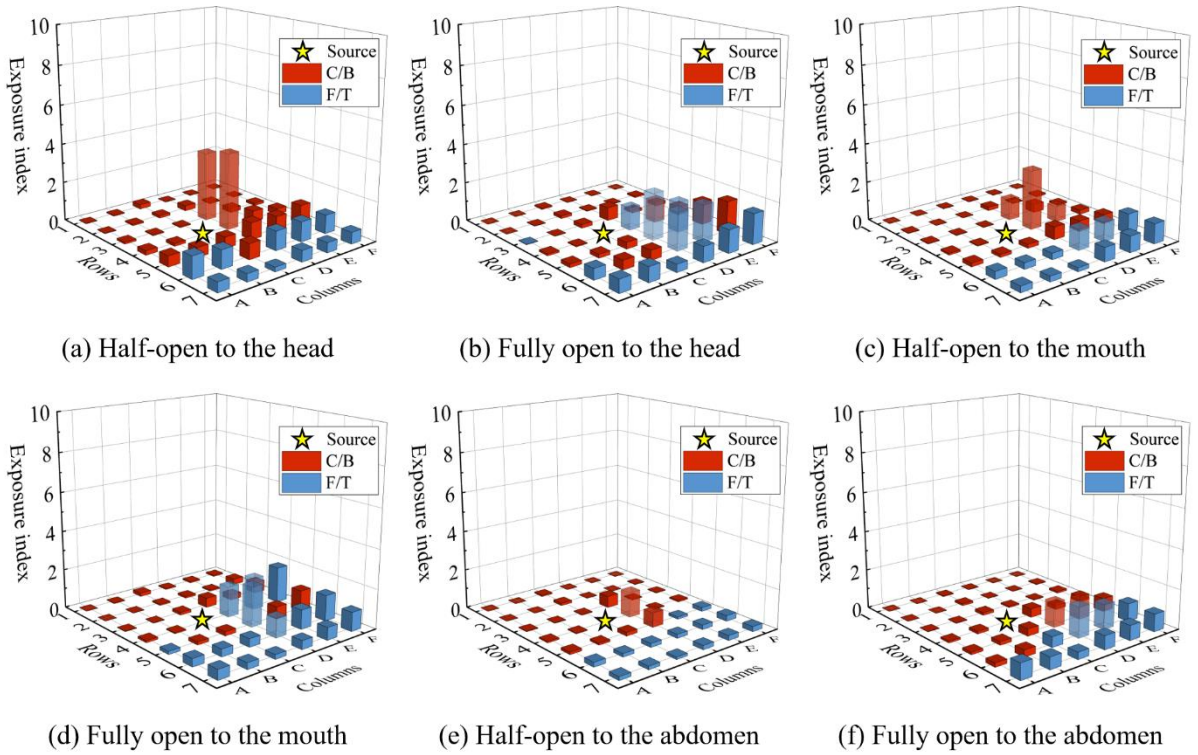

Figure. A. 13. Distribution of scenarios for all receptors when the gasper of the source passenger 4C was on.

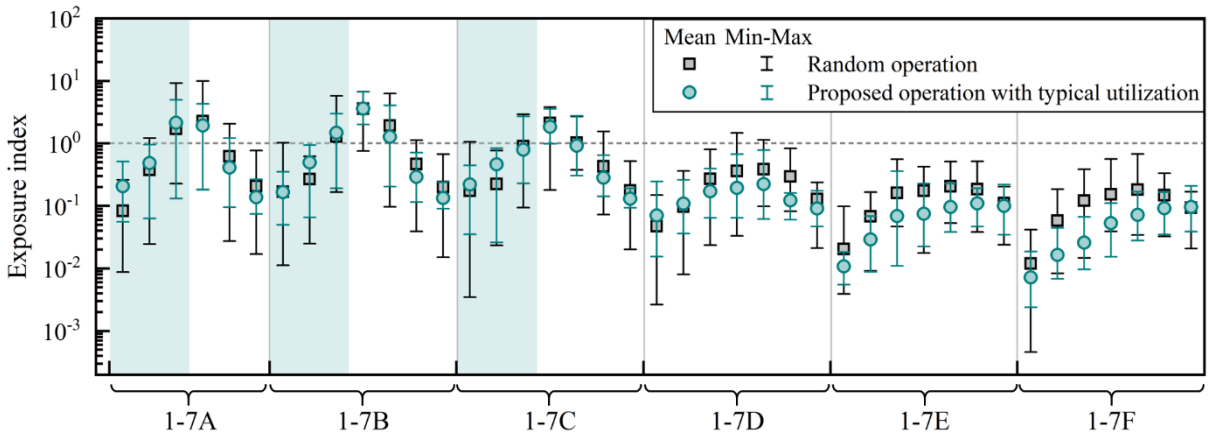

Figure. A. 14. Comparison of the exposure index for each passenger under the random operation and the proposed operation strategy with typical utilization, with the source passenger located in window seat 4A.

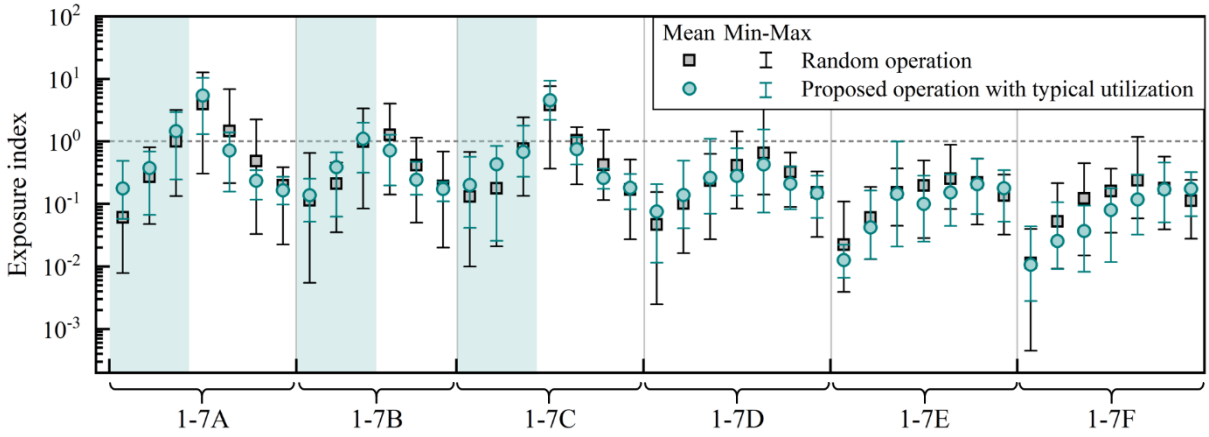

Figure. A. 15. Comparison of the exposure index for each passenger under the random operation and the proposed operation strategy with typical utilization, with the source passenger located in middle seat 4B.

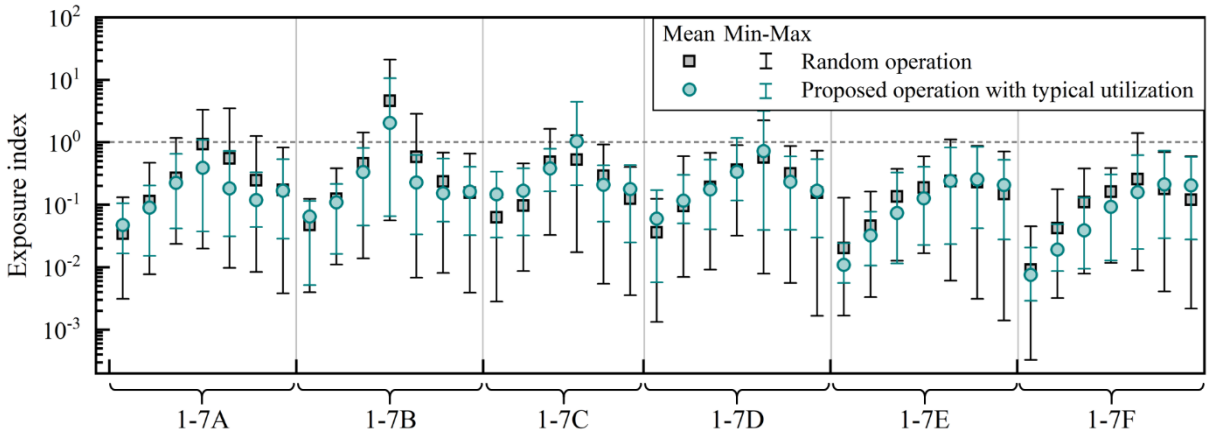

Figure. A. 16. Comparison of the exposure index for each passenger under the random operation and the proposed operation strategy with typical utilization, with the source passenger located in aisle seat 4C.

REFERENCES

[1] IATA. https://www.statista.com/statistics/564717/airline-industry-passenger-traffic-globally/. (Accessed 3 september 2024).

[2] W. Cui, Q. Ouyang, Y. Zhu, Field study of thermal environment spatial distribution and passenger local thermal comfort in aircraft cabin, Build. Environ. 80 (2014) 213-220. https://doi.org/10.1016/j.buildenv.2014.06.004.

[3] W. Cui, T. Wu, Q. Ouyang, Y. Zhu, Passenger thermal comfort and behavior: a field investigation in commercial aircraft cabins, Indoor air 27(1) (2017) 94-103. https://doi.org/10.1111/ina.12294.

[4] F. Haghighat, F. Allard, A.C. Megri, P. Blondeau, R. Shimotakahara, Measurement of thermal comfort and indoor air quality aboard 43 flights on commercial airlines, Indoor and Built Environ. 8(1) (1999) 58-66. https://doi.org/10.1159/000024610.

[5] C. Weisel, C.J. Weschler, K. Mohan, J. Vallarino, J.D. Spengler, Ozone and ozone byproducts in the cabins of commercial aircraft, Environ. Sci. Technol. 47(9) (2013) 4711-4717. https://doi.org/10.1021/es3046795.

[6] M.R. Moser, T.R. Bender, H.S. Margolis, G.R. Noble, A.P. Kendal, D.G. Ritter, An outbreak of influenza aboard a commercial airliner, American journal of epidemiology 110(1) (1979) 1-6. https://doi.org/10.1093/oxfordjournals.aje.a112781.

[7] S.J. Olsen, H.-L. Chang, T.Y.-Y. Cheung, A.F.-Y. Tang, T.L. Fisk, S.P.-L. Ooi, H.-W. Kuo, D.D.-S. Jiang, K.-T. Chen, J. Lando, Transmission of the severe acute respiratory syndrome on aircraft, New England Journal of Medicine 349(25) (2003) 2416-2422. https://doi.org/10.1056/NEJMoa031349.

[8] A. Mangili, M.A. Gendreau, Transmission of infectious diseases during commercial air travel, The Lancet 365(9463) (2005) 989-996. https://doi.org/10.1016/S0140-6736(05)71089-8.

[9] J.K. Gupta, C.H. Lin, Q. Chen, Risk assessment of airborne infectious diseases in aircraft cabins, Indoor air 22(5) (2012) 388-395. https://doi.org/10.1111/j.1600-0668.2012.00773.x.

[10] N.C. Khanh, P.Q. Thai, H.-L. Quach, N.-A.H. Thi, P.C. Dinh, T.N. Duong, N.D. Nghia, T.A. Tu, T. Dai Quang, T.-T. Nguyen, Transmission of SARS-CoV 2 during long-haul flight, Emerging infectious diseases 26(11) (2020) 2617. https://doi.org/10.3201/eid2611.203299.

[11] M. Bielecki, D. Patel, J. Hinkelbein, M. Komorowski, J. Kester, S. Ebrahim, A.J. Rodriguez-Morales, Z.A. Memish, P. Schlagenhauf, Reprint of: Air travel and COVID-19 prevention in the pandemic and peri-pandemic period: A narrative review, Travel medicine and infectious disease 38 (2020) 101939. https://doi.org/10.1016/j.tmaid.2020.101939.

[12] X. Zhao, S. Liu, Y. Yin, T. Zhang, Q. Chen, Airborne transmission of COVID-19 virus in enclosed spaces: an overview of research methods, Indoor air 32(6) (2022) e13056. https://doi.org/10.1111/ina.13056.

[13] S.H. Bae, H. Shin, H.-Y. Koo, S.W. Lee, J.M. Yang, D.K. Yon, Asymptomatic transmission of SARS-CoV-2 on evacuation flight, Emerging infectious diseases 26(11) (2020) 2705. https://doi.org/10.3201/eid2611.203353.

[14] T.A. Kenyon, S.E. Valway, W.W. Ihle, I.M. Onorato, K.G. Castro, Transmission of multidrug-resistant Mycobacterium tuberculosis during a long airplane flight, New England Journal of Medicine 334(15) (1996) 933-938. https://doi.org/ 10.1056/NEJM199604113341501.

[15] Y. Li, G.M. Leung, J. Tang, X. Yang, C. Chao, J.Z. Lin, J. Lu, P.V. Nielsen, J. Niu, H. Qian, Role of ventilation in airborne transmission of infectious agents in the built environment-a multidisciplinary systematic review, Indoor air 17(1) (2007) 2-18. https://doi.org/10.1111/j.1600-0668.2006.00445.x.

[16] N. Gao, J. Niu, Personalized ventilation for commercial aircraft cabins, Journal of aircraft 45(2) (2008) 508-512. https://doi.org/10.2514/1.30272.

[17] J. Fišer, M. Jícha, Impact of air distribution system on quality of ventilation in small aircraft cabin, Building and Environment 69 (2013) 171-182. https://doi.org/10.1016/j.buildenv.2013.08.007.

[18] F. Wang, R. You, T. Zhang, Q. Chen, Recent progress on studies of airborne infectious disease transmission, air quality, and thermal comfort in the airliner cabin air environment, Indoor air 32(4) (2022) e13032. https://doi.org/10.1111/ina.13032.

[19] Y. Zhang, J. Liu, J. Pei, J. Li, C. Wang, Performance evaluation of different air distribution systems in an aircraft cabin mockup, Aerospace science and technology 70 (2017) 359-366. https://doi.org/10.1016/j.ast.2017.08.009.

[20] Z. Zhang, X. Chen, S. Mazumdar, T. Zhang, Q. Chen, Experimental and numerical investigation of airflow and contaminant transport in an airliner cabin mockup, Building and Environment 44(1) (2009) 85-94. https://doi.org/10.1016/j.buildenv.2008.01.012.

[21] R. You, C.H. Lin, D. Wei, Q. Chen, Evaluating the commercial airliner cabin environment with different air distribution systems, Indoor Air 29(5) (2019) 840-853. https://doi.org/10.1111/ina.12578.

[22] M. Liu, J. Liu, Q. Cao, X. Li, S. Liu, S. Ji, C.-H. Lin, D. Wei, X. Shen, Z. Long, Evaluation of different air distribution systems in a commercial airliner cabin in terms of comfort and COVID-19 infection risk, Building and Environment 208 (2022) 108590. https://doi.org/10.1016/j.buildenv.2021.108590.

[23] M. Liu, D. Chang, J. Liu, S. Ji, C.-H. Lin, D. Wei, Z. Long, T. Zhang, X. Shen, Q. Cao, Experimental investigation of air distribution in an airliner cabin mockup with displacement ventilation, Building and Environment 191 (2021) 107577. https://doi.org/10.1016/j.buildenv.2020.107577.

[24] R. You, Y. Zhang, X. Zhao, C.-H. Lin, D. Wei, J. Liu, Q. Chen, An innovative personalized displacement ventilation system for airliner cabins, Building and environment 137 (2018) 41-50. https://doi.org/10.1016/j.buildenv.2018.03.057.

[25] T. Zhang, Q.Y. Chen, Novel air distribution systems for commercial aircraft cabins, Building and Environment 42(4) (2007) 1675-1684. https://doi.org/10.1016/j.buildenv.2006.02.014.

[26] P. Zítek, T. Vyhlídal, G. Simeunović, L. Nováková, J. Čížek, Novel personalized and humidified air supply for airliner passengers, Building and Environment 45(11) (2010) 2345-2353. https://doi.org/10.1016/j.buildenv.2010.04.005.

[27] T.T. Zhang, P. Li, S. Wang, A personal air distribution system with air terminals embedded in chair armrests on commercial airplanes, Building and Environment 47 (2012) 89-99. https://doi.org/10.1016/j.buildenv.2011.04.035.

[28] S. Dai, H. Sun, W. Liu, Y. Guo, N. Jiang, J. Liu, Experimental study on characteristics of the jet flow from an aircraft gasper, Building and Environment 93 (2015) 278-284. https://doi.org/10.1016/j.buildenv.2015.06.006.

[29] Z. Shi, J. Chen, R. You, C. Chen, Q. Chen, Modeling of gasper-induced jet flow and its impact on cabin air quality, Energy and Buildings 127 (2016) 700-713. https://doi.org/10.1016/j.enbuild.2016.06.038.

[30] J. Li, J. Liu, S. Dai, Y. Guo, N. Jiang, W. Yang, PIV experimental research on gasper jets interacting with the main ventilation in an aircraft cabin, Building and Environment 138 (2018) 149-159. https://doi.org/10.1016/j.buildenv.2018.04.023.

[31] B. Li, R. Duan, J. Li, Y. Huang, H. Yin, C.H. Lin, D. Wei, X. Shen, J. Liu, Q. Chen, Experimental studies of thermal environment and contaminant transport in a commercial aircraft cabin with gaspers on, Indoor air 26(5) (2016) 806-819. https://doi.org/10.1111/ina.12265.

[32] R. You, J. Chen, Z. Shi, W. Liu, C.-H. Lin, D. Wei, Q. Chen, Experimental and numerical study of airflow distribution in an aircraft cabin mock-up with a gasper on, Journal of

building performance simulation 9(5) (2016) 555-566. https://doi.org/10.1080/19401493.2015.1126762.

[33] R. You, W. Liu, J. Chen, C.-H. Lin, D. Wei, Q. Chen, Predicting airflow distribution and contaminant transport in aircraft cabins with a simplified gasper model, Journal of Building Performance Simulation 9(6) (2016) 699-708. https://doi.org/10.1080/19401493.2016.1196730.

[34] R. You, J. Chen, C.-H. Lin, D. Wei, Q. Chen, Investigating the impact of gaspers on cabin air quality in commercial airliners with a hybrid turbulence model, Building and Environment 111 (2017) 110-122. https://doi.org/10.1016/j.buildenv.2016.10.018.

[35] W. Liu, L. Liu, C. Xu, L. Fu, Y. Wang, P.V. Nielsen, C. Zhang, Exploring the potentials of personalized ventilation in mitigating airborne infection risk for two closely ranged occupants with different risk assessment models, Energy and Buildings 253 (2021) 111531. https://doi.org/10.1016/j.enbuild.2021.111531.

[36] Z. Tang, X. Cui, Y. Guo, N. Jiang, S. Dai, J. Liu, Near fields of gasper jet flows with wedged nozzle in aircraft cabin environment, Building and Environment 125 (2017) 99-110. https://doi.org/10.1016/j.buildenv.2017.08.047.

[37] Z. Fang, H. Liu, B. Li, A. Baldwin, J. Wang, K. Xia, Experimental investigation of personal air supply nozzle use in aircraft cabins, Applied ergonomics 47 (2015) 193-202. https://doi.org/10.1016/j.apergo.2014.09.011.

[38] A. ASHRAE, Standard 161–2007, air quality within commercial aircraft, American Society of Heating, Refrigerating and Air-Conditioning Engineers, Inc, Atlanta, 2007.

[39] J. Ren, Y. Wang, Q. Liu, Y. Liu, Numerical study of three ventilation strategies in a prefabricated COVID-19 inpatient ward, Building and Environment 188 (2021) 107467. https://doi.org/10.1016/j.buildenv.2020.107467.

[40] J.K. Gupta, C.H. Lin, Q. Chen, Transport of expiratory droplets in an aircraft cabin, Indoor air 21(1) (2011) 3-11. https://doi.org/10.1111/j.1600-0668.2010.00676.x.

[41] Z. Zhang, Q. Chen, Experimental measurements and numerical simulations of particle transport and distribution in ventilated rooms, Atmospheric environment 40(18) (2006) 3396-3408. https://doi.org/10.1016/j.atmosenv.2006.01.014.

[42] X. Yuan, Q. Chen, L.R. Glicksman, A critical review of displacement ventilation, (1998).

[43] H. Ahn, D. Rim, L.J. Lo, Ventilation and energy performance of partitioned indoor spaces under mixing and displacement ventilation, Building Simulation, Springer, 2018, pp. 561-574. https://doi.org/10.1007/s12273-017-0410-z.

[44] Q. Chen, L. Glicksman, System performance evaluation and design guidelines for displacement ventilation, ASHRAE, Altanta, GA (2003).

[45] F.S. Bauman, A. Daly. Underfloor air distribution (UFAD) design guide, Atlanta (2003).

[46] D. Al Assaad, C. Habchi, K. Ghali, N. Ghaddar, Simplified model for thermal comfort, IAQ and energy savings in rooms conditioned by displacement ventilation aided with transient personalized ventilation, Energy Conversion and Management 162 (2018) 203-217. https://doi.org/10.1016/j.enconman.2018.02.033.

[47] J. Wang, G. Smedje, T. Nordquist, D. Norbäck, Personal and demographic factors and change of subjective indoor air quality reported by school children in relation to exposure at Swedish schools: a 2-year longitudinal study, Science of the Total Environment 508 (2015) 288-296. https://doi.org/10.1016/j.scitotenv.2014.12.001.

[48] F. Berlanga, M.R. de Adana, I. Olmedo, J.M. Villafruela, J. San José, F. Castro, Experimental evaluation of thermal comfort, ventilation performance indices and exposure to airborne contaminant in an airborne infection isolation room equipped with a displacement air distribution system, Energy and buildings 158 (2018) 209-221. https://doi.org/10.1016/j.enbuild.2017.09.100.

[49] J. Bosbach, A. Heider, T. Dehne, M. Markwart, I. Gores, P. Bendfeldt, Evaluation of cabin displacement ventilation under flight conditions, ICAS2012, paper 304 (2012) 23-28.

[50] J. Maier, C. Marggraf-Micheel, T. Dehne, J. Bosbach, Thermal comfort of different displacement ventilation systems in an aircraft passenger cabin, Building and Environment 111 (2017) 256-264. https://doi.org/10.1016/j.buildenv.2016.11.017.

[51] J. Li, X. Cao, J. Liu, K. Mohanarangam, W. Yang, PIV measurement of human thermal convection flow in a simplified vehicle cabin, Building and Environment 144 (2018) 305-315. https://doi.org/10.1016/j.buildenv.2018.08.031.

[52] A.K. Melikov, V. Dzhartov, Advanced air distribution for minimizing airborne cross-infection in aircraft cabins, Hvac&R Research 19(8) (2013) 926-933. https://doi.org/10.1080/10789669.2013.818468.

[53] https://www.jiemian.com/article/1597477.html.

[54] Y. Hou, R. You, Investigating the impact of gaspers on airborne disease transmission in an economy-class aircraft cabin with personalized displacement ventilation, Building and Environment 245 (2023) 110963. https://doi.org/10.1016/j.buildenv.2023.110963.

[55] Z. Fang, H. Liu, B. Li, A. Baldwin, Investigation of thermal comfort and the nozzle usage behaviour in aircraft cabins, Indoor and built Environment 28(1) (2019) 118-131. https://doi.org/10.1177/1420326X17739446.

[56] W. Liu, S. Mazumdar, Z. Zhang, S.B. Poussou, J. Liu, C.-H. Lin, Q. Chen, State-of-the-art methods for studying air distributions in commercial airliner cabins, Building and Environment 47 (2012) 5-12. https://doi.org/10.1016/j.buildenv.2011.07.005.

[57] W. Liu, Q. Chen, Current studies on air distributions in commercial airliner cabins, Theoretical and Applied Mechanics Letters 3(6) (2013) 062001. https://doi.org/10.1063/2.1306201.

[58] H. Mo, M. Hosni, B. Jones, Application of particle image velocimetry for the measurement of the airflow characteristics in an aircraft cabin, ASHRAE Transactions 109 (2003) 101-110.

[59] W. Liu, J. Wen, J. Chao, W. Yin, C. Shen, D. Lai, C.-H. Lin, J. Liu, H. Sun, Q. Chen, Accurate and high-resolution boundary conditions and flow fields in the first-class cabin of an MD-82 commercial airliner, Atmospheric Environment 56 (2012) 33-44. https://doi.org/10.1016/j.atmosenv.2012.03.039.

[60] C. Wang, J. Zhang, H. Chen, J. Liu, Experimental study of thermo-fluid boundary conditions, airflow and temperature distributions in a single aisle aircraft cabin mockup, Indoor and Built Environment 30(8) (2021) 1185-1199. https://doi.org/10.1177/1420326X20932271.

[61] J. Li, X. Cao, J. Liu, C. Wang, Y. Zhang, Global airflow field distribution in a cabin mock-up measured via large-scale 2D-PIV, Building and Environment 93 (2015) 234-244. https://doi.org/10.1016/j.buildenv.2015.06.030.

[62] J. Bosbach, M. Kühn, C. Wagner, Large scale particle image velocimetry with helium filled soap bubbles, Experiments in fluids 46 (2009) 539-547. https://doi.org/10.1007/s00348-008-0579-0.

[63] Y. Sun, Y. Zhang, A. Wang, J.L. Topmiller, J.S. Bennet, Experimental Characterization of Airflows in Aircraft Cabins, Part I: Experimental System and Measurement Procedure, ASHRAE transactions 111(2) (2005).

[64] Y. Zhang, Y. Sun, A. Wang, J.L. Topmiller, J.S. Bennett, Experimental characterization of airflows in aircraft cabins, part II: results and research recommendations, ASHRAE transactions 111 (2005) 53-59.

[65] J. Li, J. Liu, C. Wang, N. Jiang, X. Cao, PIV methods for quantifying human thermal plumes in a cabin environment without ventilation, Journal of Visualization 20 (2017) 535-548. https://doi.org/10.1007/s12650-016-0404-4.

[66] J. Li, J. Liu, C. Wang, M. Wesseling, D. Mueller, PIV experimental study of the large-scale dynamic airflow structures in an aircraft cabin: Swing and oscillation, Building and Environment 125 (2017) 180-191. https://doi.org/10.1016/j.buildenv.2017.07.043.

[67] W. Yan, Y. Zhang, Y. Sun, D. Li, Experimental and CFD study of unsteady airborne pollutant transport within an aircraft cabin mock-up, Building and environment 44(1) (2009) 34-43. https://doi.org/10.1016/j.buildenv.2008.01.010.

[68] V. Yakhot, S.A. Orszag, Renormalization group analysis of turbulence. I. Basic theory, Journal of scientific computing 1(1) (1986) 3-51. https://doi.org/10.1007/BF01061452.

[69] C.-H.-. Lin, K. Dunn, R. Horstman, J. Topmiller, M. Ahlers, J. Bennett, L. Sedgwick, S. Wirogo, Numerical Simulation of Airflow and Airborne Pathogen Transport in Aircraft Cabins--Part I: Numerical Simulation of the Flow Field, ASHRAE transactions 111(1) (2005) 755-763.

[70] W. Liu, J. Wen, C.-H. Lin, J. Liu, Z. Long, Q. Chen, Evaluation of various categories of turbulence models for predicting air distribution in an airliner cabin, Building and Environment 65 (2013) 118-131. https://doi.org/10.1016/j.buildenv.2013.03.018.

[71] J. Smagorinsky, General circulation experiments with the primitive equations: I. The basic experiment, Monthly weather review 91(3) (1963) 99-164. https://doi.org/10.1175/1520-0493(1963)091<0099:GCEWTP>2.3.CO;2.

[72] J.W. Deardorff, A numerical study of three-dimensional turbulent channel flow at large Reynolds numbers, Journal of Fluid Mechanics 41(2) (1970) 453-480. https://doi.org/10.1017/S0022112070000691.

[73] P.R. Spalart, Comments on the Feasibility of LES for Wings and on the Hybrid RANS/LES Approach, Proceedings of the First AFOSR International Conference on DNS/LES, 1997, pp. 137-147.

[74] M. Shur, P. Spalart, M. Strelets, A. Travin, Detached-eddy simulation of an airfoil at high angle of attack, Engineering turbulence modelling and experiments 4, Elsevier1999, pp. 669-678. https://doi.org/10.1016/B978-008043328-8/50064-3.

[75] Z. Shi, J. Chen, Q. Chen, On the turbulence models and turbulent Schmidt number in simulating stratified flows, Journal of Building Performance Simulation 9(2) (2016) 134-148. https://doi.org/10.1080/19401493.2015.1004109.

[76] F.R. Menter, Two-equation eddy-viscosity turbulence models for engineering applications, AIAA journal 32(8) (1994) 1598-1605. https://doi.org/10.2514/3.12149.

[77] A. Fluent, Theory Guide 19.2, Ansys Inc, USA, 2018.

[78] Z. Liu, R. Li, Y. Wu, R. Ju, N. Gao, Numerical study on the effect of diner divider on the airborne transmission of diseases in canteens, Energy and Buildings 248 (2021) 111171. https://doi.org/10.1016/j.enbuild.2021.111171.

[79] Z. Zhang, Q. Chen, Prediction of particle deposition onto indoor surfaces by CFD with a modified Lagrangian method, Atmospheric Environment 43(2) (2009) 319-328. https://doi.org/10.1016/j.atmosenv.2008.09.041.

[80] C. Chen, W. Liu, C.-H. Lin, Q. Chen, Accelerating the Lagrangian method for modeling transient particle transport in indoor environments, Aerosol Science and Technology 49(5) (2015) 351-361. https://doi.org/10.1080/02786826.2015.1031724.

[81] F. Cui, X. Geng, O. Zervaki, D.D. Dionysiou, J. Katz, S.-J. Haig, M. Boufadel, Transport and fate of virus-laden particles in a supermarket: recommendations for risk reduction of COVID-19 spreading, Journal of environmental engineering 147(4) (2021) 04021007. https://doi.org/10.1061/(ASCE)EE.1943-7870.0001870.

[82] S. Liu, X. Zhao, S.R. Nichols, M.W. Bonilha, T. Derwinski, J.T. Auxier, Q. Chen, Evaluation of airborne particle exposure for riding elevators, Building and environment 207 (2022) 108543. https://doi.org/10.1016/j.buildenv.2021.108543.

[83] M. Ahmadzadeh, M. Shams, Passenger exposure to respiratory aerosols in a train cabin: Effects of window, injection source, output flow location, Sustainable Cities and Society 75 (2021) 103280. https://doi.org/10.1016/j.scs.2021.103280.

[84] M. Wang, C.-H. Lin, Q. Chen, Advanced turbulence models for predicting particle transport in enclosed environments, Building and Environment 47 (2012) 40-49. https://doi.org/10.1016/j.buildenv.2011.05.018.

[85] T. Mizine, M. Warfield, Development of three-dimensional thermal airflow analysis computer program and verification test, (1991).

[86] Y. Yin, W. Xu, J.K. Gupta, A. Guity, P. Marmion, A. Manning, B. Gulick, X. Zhang, Q. Chen, Experimental study on displacement and mixing ventilation systems for a patient ward, HVAC&R Research 15(6) (2009) 1175-1191. https://doi.org/10.1080/10789669.2009.10390885.

[87] Z. Zhang, Q. Chen, Comparison of the Eulerian and Lagrangian methods for predicting particle transport in enclosed spaces, Atmospheric environment 41(25) (2007) 5236-5248. https://doi.org/10.1016/j.atmosenv.2006.05.086.

[88] Y. Lu, M. Oladokun, Z. Lin, Reducing the exposure risk in hospital wards by applying stratum ventilation system, Building and Environment 183 (2020) 107204. https://doi.org/10.1016/j.buildenv.2020.107204.

[89] C.K. Ho, Modeling airborne pathogen transport and transmission risks of SARS-CoV-2, Applied Mathematical Modelling 95 (2021) 297-319. https://doi.org/10.1016/j.apm.2021.02.018.

[90] S. Srivastava, X. Zhao, A. Manay, Q. Chen, Effective ventilation and air disinfection system for reducing coronavirus disease 2019 (COVID-19) infection risk in office buildings, Sustainable Cities and Society 75 (2021) 103408. https://doi.org/10.1016/j.scs.2021.103408.

[91] D.D. Gray, A. Giorgini, The validity of the Boussinesq approximation for liquids and gases, International Journal of Heat and Mass Transfer 19(5) (1976) 545-551. https://doi.org/10.1016/0017-9310(76)90168-X.

[92] S.V. Patankar, Numerical heat transfer and fluid flow, Hemisphere Publ, 1980. https://doi.org/10.1201/9781482234213.

[93] SeatGuru. https://www.seatguru.com/findseatmap/findseatmap.php/. (Accessed 4 March 2023).

[94] H. Qian, Y. Li, Removal of exhaled particles by ventilation and deposition in a multibed airborne infection isolation room, Indoor air 20(4) (2010) 284-297. https://doi.org/10.1111/j.1600-0668.2010.00653.x.

[95] I. Olmedo, P.V. Nielsen, M. Ruiz de Adana, R.L. Jensen, P. Grzelecki, Distribution of exhaled contaminants and personal exposure in a room using three different air distribution strategies, Indoor air 22(1) (2012) 64-76. https://doi.org/10.1111/j.1600-0668.2011.00736.x.

[96] L. Liu, Y. Li, P.V. Nielsen, J. Wei, R.L. Jensen, Short-range airborne transmission of expiratory droplets between two people, Indoor air 27(2) (2017) 452-462. https://doi.org/10.1111/ina.12314.

[97] Z. Ai, T. Huang, A. Melikov, Airborne transmission of exhaled droplet nuclei between occupants in a room with horizontal air distribution, Building and Environment 163 (2019) 106328. https://doi.org/10.1016/j.buildenv.2019.106328.

[98] U.S.D.o. Labour, OSHA Technical Manual (OTM) - Section II: Chapter 1 | Occupational Safety and Health Administration. https://www.osha.gov/otm/section-2-health-hazards/chapter-1. (Accessed 24 March 2023).

[99] D. Frank, P. Linden, The effectiveness of an air curtain in the doorway of a ventilated building, Journal of Fluid Mechanics 756 (2014) 130-164. https://doi.org/10.1017/jfm.2014.433.

[100] D. Rim, A. Novoselac, Transport of particulate and gaseous pollutants in the vicinity of a human body, Building and Environment 44(9) (2009) 1840-1849. https://doi.org/10.1016/j.buildenv.2008.12.009.

[101] Y. Zhou, Y. Hou, C. Chen, R. You, Optimal operations of gaspers for minimizing the exposure risks of airborne disease transmission in an economy-class aircraft cabin, Indoor Environments 1(3) (2024) 100041. https://doi.org/10.1016/j.indenv.2024.100041.

[102] S.G. Nash, Quasi-Random Sampling, Encyclopedia of Statistical Sciences 10 (2004).

[103] B. Shahriari, K. Swersky, Z. Wang, R.P. Adams, N. De Freitas, Taking the human out of the loop: A review of Bayesian optimization, Proceedings of the IEEE 104(1) (2015) 148-175. https://doi.org/10.1109/JPROC.2015.2494218.

[104] C.E. Rasmussen, Gaussian processes in machine learning, Summer school on machine learning, Springer2003, pp. 63-71. https://doi.org/10.1007/978-3-540-28650-9_4.

[105] M.F. Nogueira, A Python implementation of global optimization with gaussian processes, 2014.

[106] United States Department of Labour, OSHA Technical Manual (OTM) - Section II: Chapter 1 | Occupational Safety and Health Administration. https://www.osha.gov/otm/section-2-health-hazards/chapter-1, (accessed 24 March 2023).